University of Louisville

ThinkIR: The University of Louisville's Institutional Repository

Electronic Theses and Dissertations

8-2021

Metabolic-epigenetic regulation of macrophage polarization.

Jordan T. Noe
University of Louisville

Follow this and additional works at: https://ir.library.louisville.edu/etd

Part of the Biological Phenomena, Cell Phenomena, and Immunity Commons

METABOLIC-EPIGENETIC REGULATION OF MACROPHAGE POLARIZATION

By

Jordan T. Noe
B.S., University of Utah 2013
M.S., University of Louisville 2018

A Dissertation
Submitted to the Faculty of the
School of Medicine at the University of Louisville
In Partial Fulfillment of the Requirements for the Degree of

Doctor of Philosophy in Biochemistry and Molecular Genetics

Department of Biochemistry and Molecular Genetics
University of Louisville
Louisville, Kentucky

August 2021

METABOLIC-EPIGENETIC REGULATION OF MACROPHAGE POLARIZATION

By

Jordan T. Noe
B.S. University of Utah 2013
M.S. University of Louisville 2018

A Dissertation Approved on

May 14, 2021

by the Following Dissertation Committee:

_____
Robert Mitchell, Ph.D

_____
Brian Clem, Ph.D

_____
Bradford Hill, Ph.D

_____
Alan Cheng, Ph.D

_____
Kavitha Yaddanapudi, Ph.D

DEDICATION

This dissertation is dedicated to my family. To my mother, Sheila, for the endless support and encouragement to push me to be the best version of myself, my father, David, for instilling in me a strong work ethic and sense of discipline to achieve my goals, and my siblings, Jonathan and Baylee, for keeping me sane through the ups and downs of graduate school.

ACKNOWLEDGEMENTS

ABSTRACT

METABOLIC-EPIGENETIC REGULATION OF MACROPHAGE POLARIZATION

Jordan T. Noe

May 14, 2021

Tumor-associated macrophages polarized to an M2 phenotype (M2-TAMs) promote neo-angiogenesis, tumor-stromal matrix remodeling, and immuno-evasion, which, collectively, contribute to immunotherapeutic resistance and reduced cancer patient survival. Highly glycolytic "Warburg" cancer cells produce lactate that independently drives naïve M0→immunosuppressive M2 (M0→M2) macrophage polarization, but the mechanisms have not been fully elucidated. The atypical cytokine macrophage migration inhibitory factor (MIF) is a fundamental underlying requirement for immunosuppressive M2 macrophage polarization. Still, it is unknown whether a molecular link exists between lactate-supported and MIF-dependent M2 macrophage polarization.

Using a combination of gene expression assays, chromatin immunoprecipitation, and metabolomic analyses, we identified that M2 macrophages incorporate exogenous lactate into the TCA cycle, with subsequent mitochondrial export as citrate and cleavage by ATP-citrate lyase (ACLY) to generate nucleo-cytosolic acetyl-CoA for histone acetylation. For the first time, our studies identify lactate as a *bona fide* mitochondrial metabolite in M2 macrophages

that supports metabolic reprogramming and macrophage-mediated immunosuppression. These results enhance the understanding of the metabolic interplay between lactate-producing "Warburg-like" tumors and immunosuppressive macrophage phenotypes and may help identify molecular targets for the development of TAM-directed immunotherapies.

Separately, we also identified that MIF is a critical determinant of metabolic reprogramming during M2 macrophage polarization by sustaining mitochondrial metabolism to support a metabolic-epigenetic link through α-ketoglutarate-dependent histone demethylation. Additionally, our data suggest that a CSN5/NRF2 pathway exists as an intermediary mechanistic link of MIF-dependent metabolic reprogramming during M2 macrophage polarization. These results suggest that small molecule MIF inhibition may be an efficacious immunotherapeutic strategy by targeting metabolic reprogramming during M2-TAM-mediated tumor progression.

Altogether, the work described in this dissertation expands our knowledge of the metabolic-epigenetic regulations of M2 macrophage polarization by identifying the contribution of mitochondrial lactate metabolism in ACLY-dependent histone acetylation and by determining the contribution of MIF in metabolic reprogramming-dependent histone demethylation.

TABLE OF CONTENTS

LIST OF FIGURES

CHAPTER 1: INTRODUCTION

Tumor-Associated Macrophages

De novo immune reactivity to malignant cells dictates tumor progression and, ultimately, patient survival (1,2). These tumor-immune responses are shaped and characterized by several factors, including mutational burden, inflammatory response, differential expression of cytokines and chemokines, and both tumoral and stromal immune-suppressive checkpoint ligands and receptors (3).

Tumor-associated macrophages (TAMs) are innate myeloid immune cells that regulate *de novo* anti-tumor immune response. Immature circulating monocytes (4,5), or monocytic myeloid-derived suppressor cells (MDSCs) (6), express chemokine trafficking receptors, such as CCR2, for extravasation out of the circulation and into the tumor-stromal matrix (7,8). Once in the tumor microenvironment (TME), monocytes recognize colony-stimulating factors, such as colony-stimulating factor 1 (i.e., macrophage colony-stimulating factor, M-CSF), that promotes intratumoral monocyte→TAM differentiation (9). While monocyte infiltration/TAM differentiation represents the predominant ontogeny of TAMs, some tumors exhibit *in situ* proliferation of tissue-resident macrophages (10,11).

Intratumorally, TAM polarization is dictated by the composition of tumor-derived *vs.* immune cell-derived cytokines (12,13), growth factors (9,14), oxygenation (15,16), and metabolic substrate composition (17,18), among many other factors. Altogether these factors govern whether TAMs are differentially polarized towards an "M1-" or "M2-" macrophage phenotype that has anti- or pro-tumor functions, respectively (Figure 1).
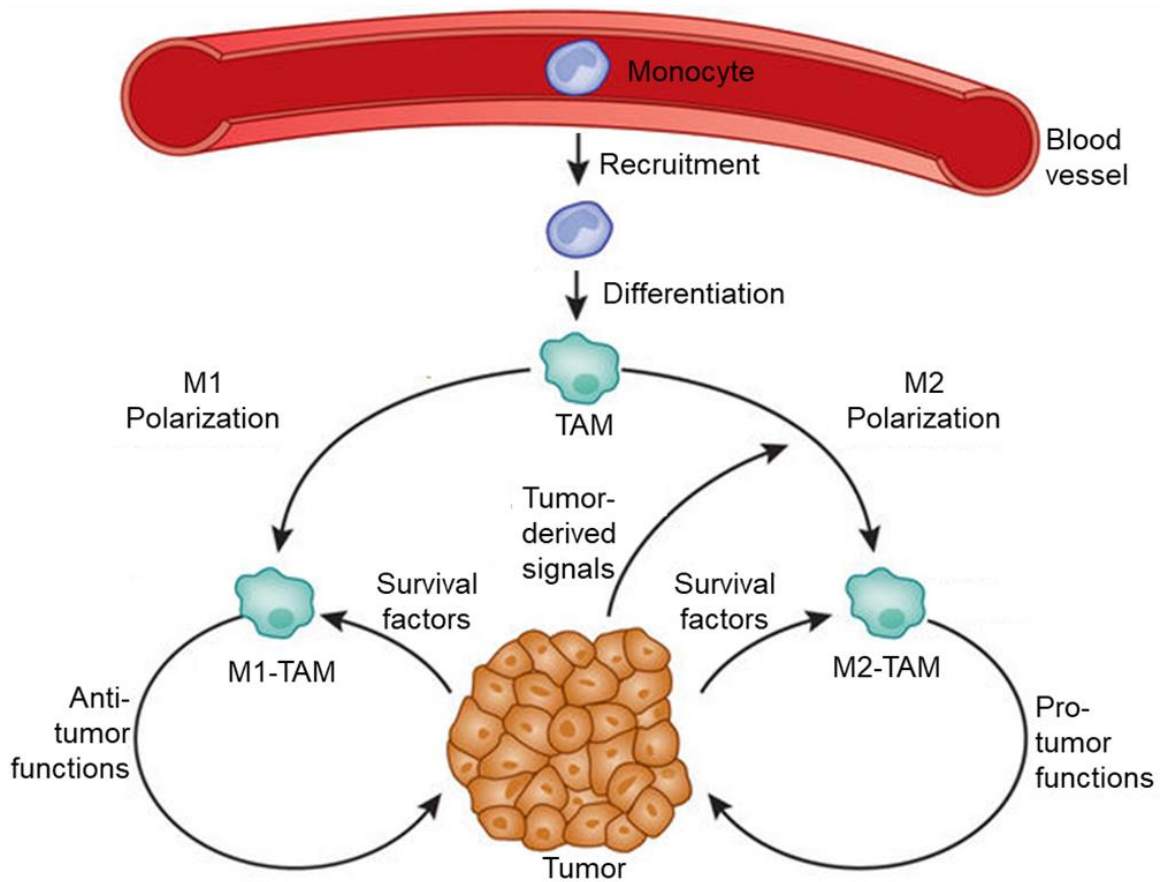
Figure 1. Schematic of tumor-associated macrophage polarization. Circulating monocytes are recruited to, and infiltrate into, the tumor stroma and undergo differentiation to tumor-associated macrophages (TAMs). Intratumoral TAMs are exposed to factors that stimulate anti-tumor M1 polarization or pro-tumor M2 polarization. Adapted with permission from MacMillan Publishers Ltd.: *"Understanding Local Macrophage Phenotypes in Disease: Modulating Macrophage Function to Treat Cancer."* Bronte V., Murray P.J... Springer Nature: Nature Medicine. Copyright 2015.

M1"-TAMs have an inflammatory/immunostimulatory phenotype that activates adaptive immune responses and produces inflammatory reactive oxygen and nitrogen species (19), prostaglandins (20), and cytokines (21). During cancer-related inflammation, early-stage dysplasia, and ensuing tumor initiation, M1-TAMs promote anti-tumor responses via tumor-cell phagocytosis (22-24), tumor-antigen presentation (25,26), and inflammatory biomolecules production (27,28).

Conversely, anti-inflammatory/immunosuppressive M2 macrophages promote wound healing and resolution of chronic inflammatory responses that would otherwise drive tumor initiation (29). However, in malignant settings of established tumors, this otherwise beneficial M2-TAM phenotype is co-opted and used to promote tumor progression through the evasion of anti-tumor immunity (30-36), *de novo* neoangiogenesis (37,38), and extracellular matrix remodeling (39) (Figure 2).

Investigators typically rely on various methodologies to define macrophage phenotypes, including morphological and functional characteristics, phenotype-associated expression of intracellular and cell-surface genes, and production of bioactive molecules (40,41). Morphologically, pro-inflammatory M1 macrophages are small and round with a "fried egg" appearance, while M2 macrophages are more prominent with irregular cell bodies and extensive elongated spindle-like projections (42). Functional assays to define macrophage phenotypes analyze the relative ability to phagocytose different particles or suppress T lymphocyte proliferation and cytokine production – the latter of which is a defining functional hallmark of immunosuppressive M2 macrophage (43-45).
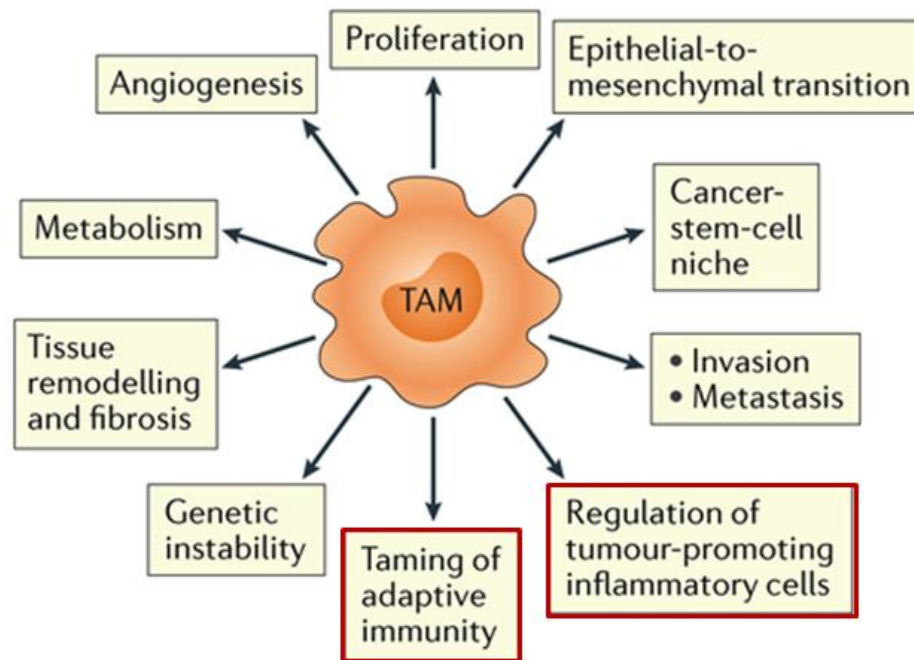
Figure 2. M2-TAM pro-tumor effector functions. M2 polarized tumor-associated macrophages promote tumor progression through several mechanisms, including regulating tumor-promoting inflammatory cells and taming of an anti-tumor adaptive immune response. Adapted with permission from MacMillan Publishers Ltd.: *"Tumor-Associated Macrophages as Treatment Targets in Oncology,"* Mantovani A., Allavena P., *et al.* Springer Nature: Nature Reviews Clinical Oncology. Copyright 2017.

Gene expression analyses also define M2 macrophages based on intracellular gene product markers (e.g., Resistin-like alpha – *Retnla*) (46,47) and cell-surface receptors, including CD163 (i.e., macrophage scavenger receptor) and CD206 (i.e., mannose receptor) (48). A defining hallmark of M2 macrophages is the production of the bioactive factor Arginase 1 (ARG1) that depletes extracellular arginine (19), resulting in metabolic immunosuppression of T cells that require this amino acid for anti-tumor activity (49). In addition to ARG1, M2 macrophages produce other bioactive factors, including vascular endothelial growth factor (VEGF – initiates *de novo* angiogenesis) (50), and matrix metalloproteases (MMPs – alter the tissue-stromal matrix) (51,52). M2 macrophages also express multifunctional immunoregulatory cytokines such as interleukin 10 (IL-10) and transforming growth factor-beta (TGF-β) (53,54), as well as several (C-C motif) chemokine ligands such as CCL17 and CCL22 (55,56).

In vitro polarization of macrophages can occur with multiple stimuli, often used alone or in combination, which adds another layer of complexity to succinctly describing polarization phenotypes. M1 macrophage polarization occurs with lipopolysaccharide (LPS), a pathogen-associated molecular pattern (PAMP) (57), or with interferon-gamma (IFN-γ), a Type II interferon (58-60). LPS binds to toll-like receptor 4 (TLR4) (61,62) and activates the nuclear factor kappa B (NF-κB) signaling pathway (63,64). In contrast, IFN-γ binds to the interferon-gamma receptor (IFNGR) and triggers a signaling cascade involving Janus family kinases 1 and 2 (JAK1 and JAK2) (60) and signal transducer and activator of transcription 1 (STAT1) (65).

M2 macrophage polarization is induced *in vitro* by the immunoregulatory Type II cytokine IL-4, with or without another Type II cytokine IL-13 (66). Polarizing macrophages with IL-4 by itself results in binding to the cognate IL-4Rα receptor that is in a heterodimeric complex with the common gamma (γC) receptor (67,68), whereas IL-4/IL-13-dependent M2 macrophage polarization occurs through an IL-4Rα/IL-13Rα heterodimeric receptor complex (67,69). While some divergent signaling pathways are activated depending on the heterodimeric complex (70), the predominant downstream effect is the activation of a JAK1/STAT6 signaling cascade. Briefly, IL-4 binding to the ectodomain of IL-4Rα induces a conformational change that activates the intracellular signaling domain (71), resulting in JAK1 auto- and cross-phosphorylation at tyrosine residues (72). JAK1 phosphorylation, in turn, promotes STAT6 recruitment to the receptor signaling domain that induces STAT6 phosphorylation (72), which causes STAT6 homodimerization, nuclear translocation, and STAT6-dependent transcription of IL-4 induced gene products (73-75).

IL-4 is critical for initiating and maintaining a Th2 immune response – early in this response, innate immune cells such as mast cells (76), γδ T cells (77), NKT cells (78,79), basophils (80), and eosinophils produce IL-4 that subsequently modulates adaptive and innate immunity. Adaptive T cells and B cells activated by IL-4 differentiate into Th2 helper T cells (81) and B effector 2 cells (82), respectively, that produce more IL-4 resulting in a positive feedback loop. IL-4 also regulates the innate immune system by promoting M2 macrophage polarization, differentiation of dendritic cells (83), and feedback activation of eosinophils (84).

IL-4 plays a significant role during several physiological and pathological processes. Physiologically, IL-4 provides immunity to parasitic helminths (e.g., flat worms, hook worms, round worms) (85,86) and during protozoal infections (e.g., malaria and leishmania) (87,88). Overproduction of IL-4 drives pathological allergic diseases by inducing the differentiation of B cells into plasma cells and immunoglobulin class-switching to IgE (75). Pathologically, several cancers, including colorectal carcinoma (89), non-small cell lung carcinoma (89), pancreatic adenocarcinoma (90), and others utilize IL-4/IL-4Rα signaling for pro-proliferative and anti-apoptotic effects. Importantly, in addition to these tumor cell-autonomous effects, IL-4's tumorigenic role is highly dependent on the IL-4-driven polarization of M2-TAMs and subsequent suppression of anti-tumor immunity (91).

Notably, even in tumors not driven by IL-4, M2-TAMs *in vivo* are strikingly similar in the genetic, phenotypic, and functional characteristics of *in vitro* IL-4 polarized M2 macrophages (92,93). Because of these close similarities, the polarization of macrophages with IL-4 is arguably the gold-standard method to currently model M2-TAMs (94). Investigators use these models to either identify molecular mechanisms leading to M2 polarization *in vitro* and then validate the phenotype with *in vivo* models or identify an M2-TAM phenotype *in vivo* and then investigate the underlying mechanisms using *in vitro* IL-4-polarized macrophages.

Nonetheless, defining macrophage phenotypes *in vivo* is still challenging due to the intratumoral heterogeneity of polarizing stimuli, metabolites, and immune cell composition (41,95). This heterogeneity leads to a broad spectrum of potential TAM activation/polarization profiles that evolve in a spatiotemporal

manner during tumor progression (93). For example, during chronic inflammation that leads to tumor initiation (96), infiltrating naïve M0 macrophages are polarized to a pro-inflammatory phenotype (M0→M1 polarization), but as these lesions progress to late-stage tumors, the intratumoral TAMs lose their inflammatory potential (21) and adopt an immunosuppressive phenotype (M1→M2 re-polarization) (97). In contrast, late-stage tumors that actively suppress anti-tumor immunity recruit naïve M0 macrophages to the tumor stroma with direct polarization to an immunosuppressive M2 phenotype (M0→M2 polarization) (98). Despite this spatiotemporal and phenotypic heterogeneity, immunogenomic analysis of 10,000 tumors across 33 tumor types revealed that an immunological landscape dominated by M2-TAMs is associated with reduced anti-tumor lymphocyte infiltration, enhanced tumor immune suppression, and worse patient survival outcomes (Figure 3) (99).

In addition to retrospective associative analyses, M2-TAMs are also significant forward-looking prognostic indicators of patient outcomes (100), metastatic potential (101), and neoadjuvant immunotherapeutic resistance (102). The result of enhanced M2-TAM infiltration in late-stage tumors is decreased efficacious and durable clinical responses to immunotherapies, increased primary tumor progression as well as secondary tumor formation, and, ultimately, increased mortality (103). Therefore, investigating the mechanisms that drive pro-tumorigenic M2-TAM effector functions may elucidate targetable pathways for developing novel therapies to enhance the efficacy of immunotherapies and extend the lives of patients diagnosed with late-stage cancers.
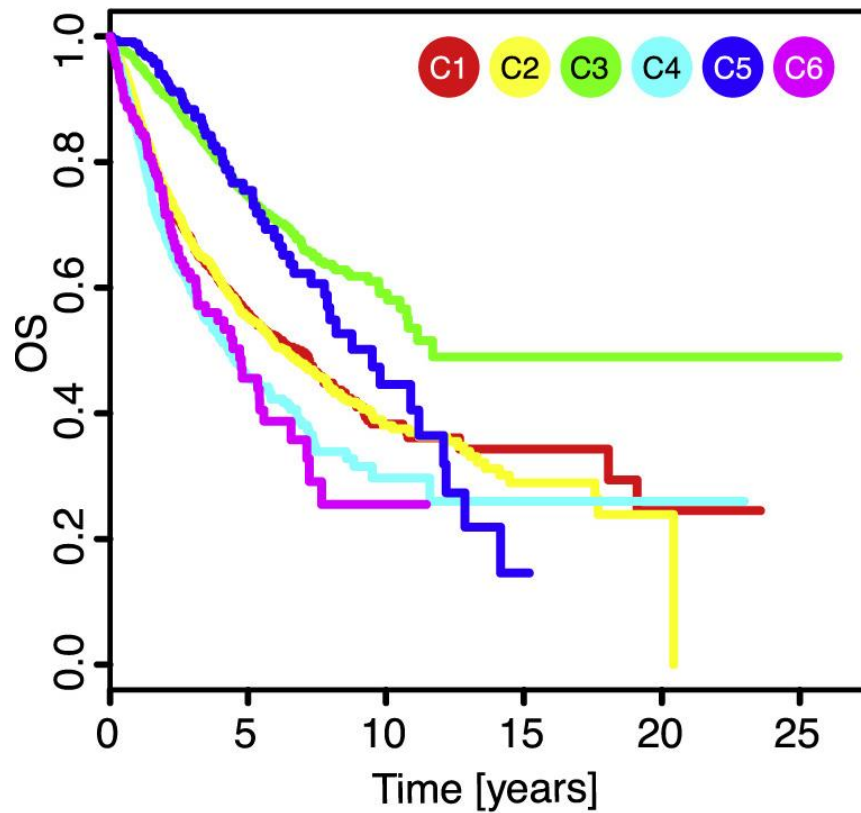
Figure 3. Intratumoral M2-TAM content reduces patient survival. Immune landscape C4 (teal) and C6 (magenta) subtypes conferred the worst prognosis and displayed an M2-TAM dominated, low lymphocytic infiltrate, immunosuppressed TME. Immune landscape C3 (green) subtype reveals an M1-TAM dominated, inflammatory TME associated with increased survival. Reprinted from Cell Press: Immunity. *"The Immune Landscape of Cancer."* Thorsson V., Shmulevich I., *et al.* Copyright 2018, with permission from Elsevier.

Metabolic Reprogramming during Macrophage Polarization

Macrophage polarization also induces metabolic reprogramming for differential utilization of metabolic pathways to support maximal activation of phenotypes and effector functions (104). M1 macrophages utilize glycolysis with terminal lactate secretion for adenosine triphosphate (ATP) production (105,106), whereas anti-inflammatory macrophages rely on oxidative phosphorylation (OXPHOS) in the mitochondria to obtain ATP (107,108). These metabolic differences are evident with extracellular flux analysis — M1 macrophages increase extracellular acidification rates (ECAR — indicative of glycolysis), whereas M2 macrophages have high oxygen consumption rates (OCR — indicative of mitochondrial metabolism) (109).

From a bioenergetic standpoint, differential utilization of metabolic pathways in macrophages makes sense. Pro-inflammatory macrophages quickly respond to pathogens, and glycolysis rapidly supports cellular bioenergetics and inflammasome activation (110,111). Following pathogen clearance, anti-inflammatory macrophages resolve the inflammatory response to prevent excess host tissue damage. A switch to mitochondrial OXPHOS ensures sustained cellular bioenergetics needed for tissue homeostasis and wound resolution (112-114).

Macrophage Polarization and the TCA cycle

The tricarboxylic acid (TCA) cycle – also known as the citric acid or Krebs cycle – is a series of enzyme-catalyzed reactions within the mitochondria that serves as the terminal metabolic pathway for the oxidation of several macronutrients (i.e., carbohydrates, amino acids, and fats) (115).

Pyruvate metabolism is a critical link between carbohydrate metabolism and the mitochondrial TCA cycle. Pyruvate is the end product of cytosolic glycolysis produced from the sequential catabolism of a six-carbon glucose molecule into two molecules of three-carbon pyruvate (116). Pyruvate is then either reduced to lactate within the cytosol or enters into the mitochondria (117). While molecules readily diffuse through the outer mitochondrial membrane into the intermembrane space, the inner mitochondrial membrane is impermeable to most metabolites (118). For transport into the mitochondrial matrix, pyruvate utilizes the mitochondrial pyruvate carrier 1 (MPC1) (119,120), a hetero-oligomeric carrier complex located in the inner mitochondrial membrane that is required for mitochondrial pyruvate uptake. Following import into the mitochondria, pyruvate undergoes oxidative decarboxylation by pyruvate dehydrogenase (PDH), resulting in the production of acetyl-CoA (Ac-CoA) and reduced nicotinamide adenine dinucleotide (NADH) (121).

Ac-CoA is a key anapleurotic metabolite for the TCA cycle. The two-carbon acetyl group of Ac-CoA condenses with the last metabolite in the TCA cycle (122), the four-carbon oxaloacetate, by the enzyme citrate synthase to form a six-carbon citrate molecule (123,124) – the first metabolite in the TCA cycle. With continuous TCA cycling, citrate is sequentially metabolized back to oxaloacetate with concomitant production of the electron carriers NADH and flavin adenine dinucleotide ($FADH_2$) (116). These electron carriers then serve as an electron source to fuel the electron transport chain (ETC), which governs mitochondrial OXPHOS-dependent ATP production (125)

Although the TCA cycle supports bioenergetics, the role of the TCA cycle in macrophage polarization is not limited to ATP production. Macrophage polarization can induce TCA cycle changes by regulating the activity of specific TCA cycle enzymes and the expression of genes responsible for trafficking these metabolites (126). This metabolic reprogramming allows for the dynamic ability for coordinated accumulation of TCA cycle metabolites within the mitochondria and specific distribution into different cellular compartments.

Combined metabolomics/transcriptomics provides compelling evidence that dynamic regulation of TCA cycle metabolites initiates and maintains specific macrophage effector functions (127). In particular, differential utilization of specific TCA cycle metabolites is increasingly becoming accepted as critically important control mechanisms governing macrophage transcriptional profiles and phenotypes (126,127). Mechanistically, TCA cycle metabolites alter transcriptional processes through several means, including influencing the stability of transcription factors (28), regulating the activity of epigenetic enzymes for chromatin remodeling (128), and serving as epigenetic modifications by direct addition onto nuclear histones (129,130).

ATP Citrate Lyase and Ac-CoA metabolism

ATP-Citrate Lyase (ACLY) is a nucleo-cytosolic transferase that serves as a metabolic-epigenetic link between TCA cycle-derived citrate, cytosolic Ac-CoA, and histone acetylation (130-132). Spatiotemporal control is acetyl-CoA metabolism is highly regulated as cytosolic Ac-CoA supports histone acetylation and *de novo* lipogenesis. However, while the TCA cycle produces Ac-CoA, a

mitochondrial carrier that exports Ac-CoA into the cytosol has not been identified (122,133). Therefore, to generate cytosolic Ac-CoA, macrophages export citrate out of the mitochondria through the mitochondrial citrate carrier (i.e., SLC25A1 or CIC), and then cytosolic TCA cycle-derived citrate is cleaved by ACLY to produce nucleo-cytoplasmic oxaloacetate and Ac-CoA (Figure 4) (132).

Initial studies evaluating citrate metabolism in macrophages revealed that citrate efflux from mitochondria supports pro-inflammatory macrophage effector functions. TNF-α and IFN-γ transcriptionally-induced CIC supports pro-inflammatory NO and prostaglandin E2 (PGE_2) production (134,135) through two separate mechanisms. CIC-mediated citrate export and subsequent ACLY-dependent Ac-CoA production provides biosynthetic requirements for PGE_2 production (132) and increased NADPH derived from ACLY-mediated oxaloacetate production contributes to NADPH-dependent inducible nitric oxide synthase (iNOS)-mediated NO production (136,137). Therefore, the trafficking of citrate from the mitochondria during infection supports pathogen clearance by macrophages through the production of pro-inflammatory mediators.

Recent studies have demonstrated that mitochondrial citrate export and subsequent ACLY-mediated cleavage are critically important in driving anti-inflammatory macrophage polarization through increased availability of nuclear Ac-CoA and subsequent histone acetylation (138). Histone acetylation is an epigenetic modification that regulates specific gene expression patterns and, through ACLY-dependent production of Ac-CoA, serves as a novel link between citrate metabolism/trafficking and M2 macrophage gene transcription (130,139).
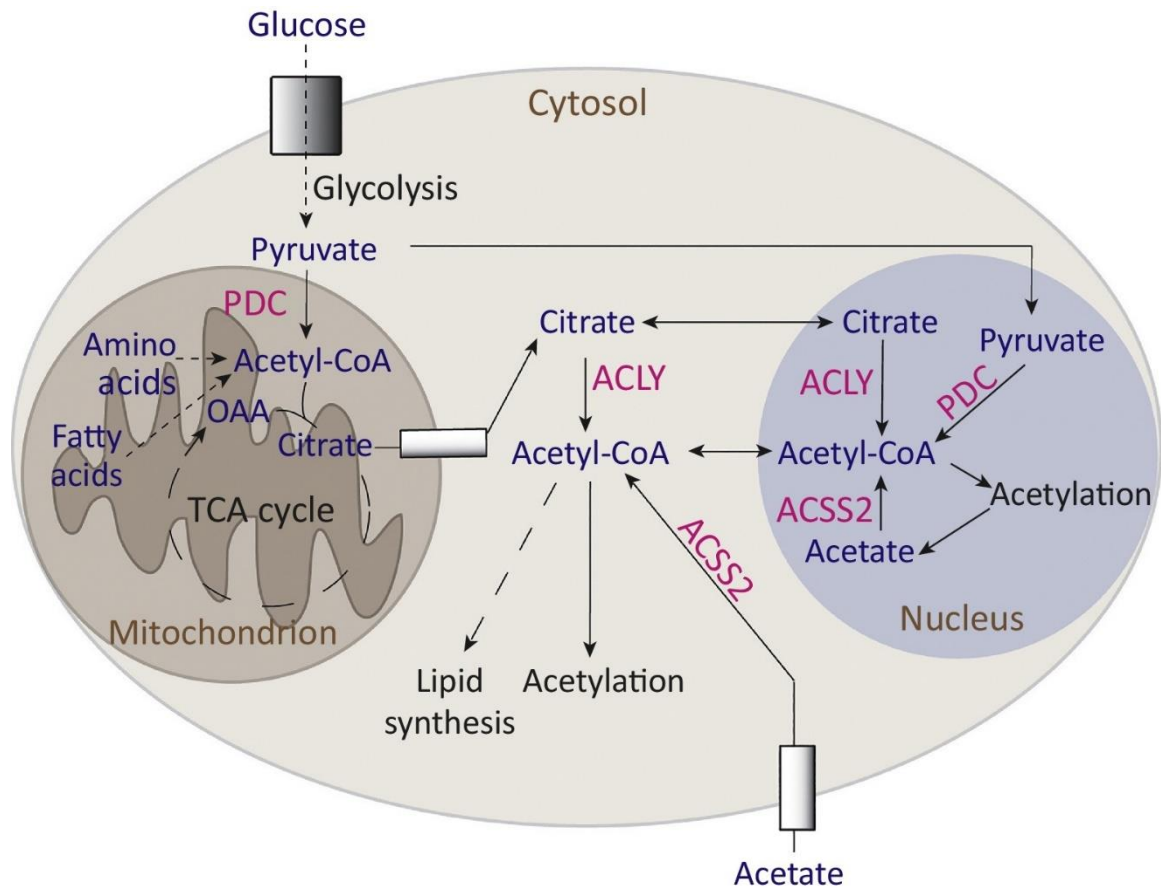
Trends in Biochemical Sciences

Figure 4. Summary of spatiotemporal control of acetyl-CoA metabolism. Cytosolic acetyl-CoA is produced following the mitochondrial export of TCA cycle-derived citrate with subsequent cleavage by ACLY or from synthesis using exogenous acetate by ACSS2. Cytosolic acetyl-CoA supports both lipid synthesis and protein/histone acetylation. Reprinted from Cell Press: Trends in Biochemical Sciences. *"Spatiotemporal Control of Acetyl-CoA Metabolism in Chromatin Regulation."* Sivanand S., Viney I., Wellen K.E... Copyright 2018, with permission from Elsevier.

14

Covarrubias and colleagues identified that IL-4 functionally initiates Akt/mTORC1 signaling cascades to increase ACLY phosphorylation/activation for nucleo-cytoplasmic Ac-CoA production and histone acetylation-dependent expression of anti-inflammatory gene products (140). Further supporting the role of ACLY-dependent histone acetylation in regulating anti-inflammatory macrophages was the finding that histone deacetylase 3 (HDAC3) – which decreases histone H3 acetylation – serves as an epigenetic brake that prevents M2 polarization (141). In this study, HDAC3 loss or inhibition increases the expression of IL-4-induced M2 macrophage-associated gene products. Notably, a recent study developed a macrophage-specific transgenic ACLY knockout model and identified that genetic deficiency of macrophage-derived ACLY impairs M2 macrophage phenotypic characteristics (142).

Altogether, whether citrate promotes pro- or anti-inflammatory macrophage phenotypes depends on the physiological context and differential trafficking of metabolites, which ultimately dictate the molecular pathways that are activated. Notably, recent studies identified that ACLY inhibitors have off-target effects that could alter the interpretation of earlier studies (143). Nonetheless, as IL-4 induces ACLY activation *in vitro* (140) and genetic ACLY deficiency impairs M2 polarization (142), ACLY-dependent Ac-CoA production and subsequent histone acetylation is likely a critical requirement of M2 polarization. Further studies are needed to determine the metabolic substrates utilized by M2 macrophages to support ACLY-dependent histone acetylation and also whether ACLY contributes to M2-TAM-dependent immunosuppression and tumor progression.

Tumor-Derived Lactate

Tumor-derived lactate serves as a potentially interesting link between M2-TAM polarization and altered cancer cell metabolism, a central hallmark of malignancy (144,145). Nearly a century ago, Otto Warburg discovered that some tumor types preferentially metabolize glucose to lactate despite sufficient oxygen levels, a term called aerobic glycolysis (146,147). Under physiological oxygen partial pressure, non-transformed cells usually engage in the oxidative metabolism of glucose through mitochondrial metabolism (148). Instead, these highly glycolytic "Warburg-like" cancer cells metabolize glucose through glycolysis with subsequent terminal lactate production and secretion (148). This metabolic phenotype fundamentally changes the metabolic landscape of the TME as the copious amounts of lactate produced result in significantly higher levels than in non-malignant, tumor-adjacent healthy tissues (149).

Since the initial discovery of "Warburg-like" cancer cells, the resultant lactate was thought to be a metabolic waste byproduct or used as an anabolic source by providing carbon-precursors for tumor growth (150). However, lactate is becoming recognized as a critical TME signal that regulates the effector functions of a variety of tumor-infiltrating immune cells (129,151,152). In addition to the tumor cell-autonomous anabolic effects, lactate also serves as a catabolic source in some tumor types – paradigm-shifting studies revealed that circulating lactate, derived from glycolysis and lactate secretion, can be actively metabolized in the mitochondrial tricarboxylic acid (TCA) (153,154).

Perhaps relatedly, tumor-derived lactate functionally regulates M2 macrophage polarization (17), although the metabolic mechanism(s) are not fully elucidated. In this study, Colegio and colleagues identified that tumor-derived lactate enhances M2 polarization of both TAMs *in vivo* and macrophages *in vitro* (17). They also found a critical requirement for the transcription factor hypoxia-inducible factor 1α (HIF-1α) in lactate-enhanced M2 macrophage polarization, but a specific mechanistic molecular link of how lactate facilitates HIF-1α-dependent transcription of M2 macrophage-associated gene products was not identified (Figure 5). Since M2 macrophages undergo metabolic programming towards enhanced mitochondrial TCA cycle activity (107,109), and M2-TAMs reside in the low glucose/high lactate TME (18), understanding if lactate is metabolized during M2 macrophage polarization and whether/how it regulates gene expression patterns will help to elucidate the mechanisms by which the TME influences tumor-infiltrating macrophage functions.

Recently, a pivotal study identified a metabolic-epigenetic link that directly utilizes lactate to induce a functional switch of macrophage phenotypes (129) – in an early polarization phase, inflammatory M1 macrophages engage their glycolytic capacity for *lactate anabolism* to generate an acyl-CoA source (i.e., lactyl-CoA) for histone modifications, termed lactylation, needed to eventually switch to an anti-inflammatory M2 macrophage phenotype (M1→M2 repolarization). This likely represents one of the mechanisms by which M1-TAMs in early-stage tumors eventually repolarize to immunosuppressive M2-TAMs in late-stage tumors.
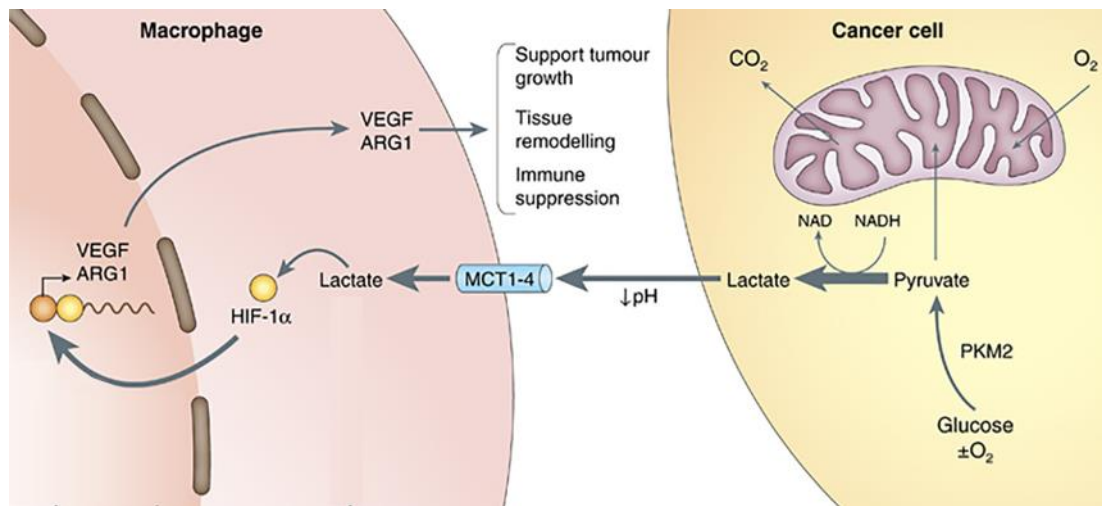
Figure 5: Metabolic cooperation between tumor-derived lactate and M2-TAMs. Glycolytic "Warburg-like" cancer cells secrete lactate into the TME, which is taken up by tumor-associated macrophages to mediate the expression of M2-TAM-associated gene products in a HIF-1α-dependent manner. Adapted with permission from: *"Tumor cells hijack macrophages via lactic acid."* Bronte V. Wiley and Sons: Immunology and Cell Biology. Copyright 2014.

In contrast to M1→M2 macrophage repolarization, direct polarization of naïve M0 macrophages to an M2 phenotype (M0→M2 polarization) initiates a metabolic reprogramming away from glycolysis. Instead, it enhances mitochondrial metabolism, tricarboxylic acid (TCA) cycle activity, and oxidative phosphorylation (OXPHOS) (155). Given the significant requirement of and regulation for acyl-CoA sources to modify histones for M2 polarization – coupled with the fact that M0→M2 macrophage polarization diverts away from lactate anabolism – this suggests that other metabolites serve as acyl-CoA sources for epigenetic modifications needed during direct M0→M2 macrophage polarization.

Macrophage Migration Inhibitory Factor (MIF)

Although IL-4 initiates metabolic reprogramming during direct M0→M2 macrophage polarization, additional regulators are needed to support and maintain maximal M2-TAM polarization. Previously, the Mitchell Laboratory identified that macrophage-derived expression of the atypical cytokine macrophage migration inhibitory factor (MIF) regulates M2-TAM polarization in metastatic melanoma (156) and oral squamous cell carcinoma (157). Elevated MIF levels are associated with worsened clinical outcomes during malignancies, including endometrial carcinoma (158), non-small cell lung carcinoma (159), hepatocellular carcinoma (160), colorectal carcinoma (161), and several other cancer types (162,163). Therefore, investigating the contribution of MIF in macrophage polarization may provide further rationale for therapeutic MIF inhibition with current cancer immunotherapies to enhance anti-tumor immunity.

Identified initially over 50 years ago as a secreted lymphocyte product associated with Type IV delayed-type hypersensitivity (164,165), MIF has become one of the most enigmatic regulators of innate and adaptive immune responses. Although the first description of a functional role for MIF was in adaptive immunity by facilitating T cell responses (166), further characterization studies identified MIF's expression in myeloid lineage cells (167,168) and discovered its functional importance in driving innate immune responses (169).

MIF expression/activity in macrophages contributes to the pathogenesis of numerous inflammatory conditions, including bacterial sepsis (170-173), rheumatoid arthritis (174,175), acute respiratory distress syndrome (ARDs) (176,177), and atherosclerosis (174,178). Consistent with these findings, MIF drives maximal inflammation-associated carcinogenesis and early-stage hyperplasia (179) – this is especially true for inflammatory colitis, a significant risk factor for colorectal adenoma development and adenocarcinoma progression (180).

Initial studies looking at the contribution of MIF in governing anti-inflammatory/immunosuppressive M2 macrophage activation determined that paracrine acting, tumor-derived MIF initiates monocyte/macrophage-dependent angiogenesis and ensuing tumor progression (181). Subsequent studies reported that macrophage-derived MIF drives the angiogenic contribution of bone marrow-derived macrophages (BMDMs) during teratoma formation, suggesting a dominant role for monocyte/macrophage-derived MIF in M2 macrophage effector functions (182).

These findings were later confirmed in the Mitchell Laboratory using mouse models of both primary and metastatic melanoma in $MIF^{+/+}$ and $MIF^{-/-}$ mice (156). In these studies, macrophage-derived MIF was necessary for maximal angiogenic growth factor expression and immune-suppressive activities of melanoma polarized TAMs. Notably, both MIF-deficient and MIF small molecule inhibitor 4-IPP-treated TAMs revert to an M1-like polarization profile spontaneously (156,157). These findings indicate that loss or inhibition of MIF efficiently repolarizes intratumoral TAMs from an immunosuppressive/angiogenic, pro-tumor phenotype to an immunostimulatory/non-angiogenic, anti-tumor phenotype with an ensuing reduction in tumor outgrowth (156).

Thus far, a unifying mechanism of how MIF contributes to these seemingly divergent M1 (inflammatory/immune-stimulatory) and M2 (anti-inflammatory/immune-suppressive) macrophage phenotypes is still lacking. One potential explanation could be that MIF provides an amplification or general activation phenotype in macrophages that acts to support generalized M1 or M2 gene expression patterns – this could be through promoting metabolic, transcriptional, and epigenetic pathways that broadly contribute to the general activation properties of infiltrating macrophages. It is also possible that differential expression of MIF receptors governed by microenvironmental polarization cues could explain the M1 *vs.* M2 effects of MIF. Nevertheless, it is becoming increasingly evident that MIF plays an essential regulatory role in governing TAM-dependent tumor initiation, progression, and metastatic potential.

MIF-dependent signaling mechanisms

MIF elicits bio-actions via both extracellular and intracellular mechanisms. Prototypical outside-in signaling occurs by extracellular MIF binding to receptor/co-receptor complexes on the cell surface. In contrast, intracellular MIF acts in a receptor-independent manner by interacting with various intracellular proteins and enzymes, thereby modifying their specific effector functions (Figure 6) (183).

MIF is upregulated and secreted in response to various activating ligands such as DAMPs (184), PAMPs (170,185), and environmental metabolic changes (183,186). Once secreted, MIF signals in either a paracrine or autocrine fashion by binding to transmembrane receptors, leading to intracellular transduction cascades (186,187). The Bucala group initially identified CD74, the invariant chain of the major histocompatibility complex II (MHCII), to be a primary cognate receptor for MIF (188). Extracellular binding of MIF to cell surface CD74 initiates signal transduction through the ERK MAP kinase cascade resulting in cellular proliferation and prostaglandin E2 (PGE_2) production (188).

As CD74 does not possess a cytoplasmic tail capable of instigating downstream signaling, CD74-dependent signaling requires the formation of a heterodimeric receptor complex (189). During canonical CD74 signaling cascade, CD74 forms a complex with CD44 that allows for activation of the ERK MAP kinase pathway (189). In addition to signaling through CD74/CD44 complexes, MIF has also been shown to be a non-cognate ligand for the chemokine receptors CXCR2, CXCR4, and CXCR7 and acts as a chemokine-like molecule resulting in monocyte activation of Gαi- and integrin-dependent adhesion and recruitment (190-192).
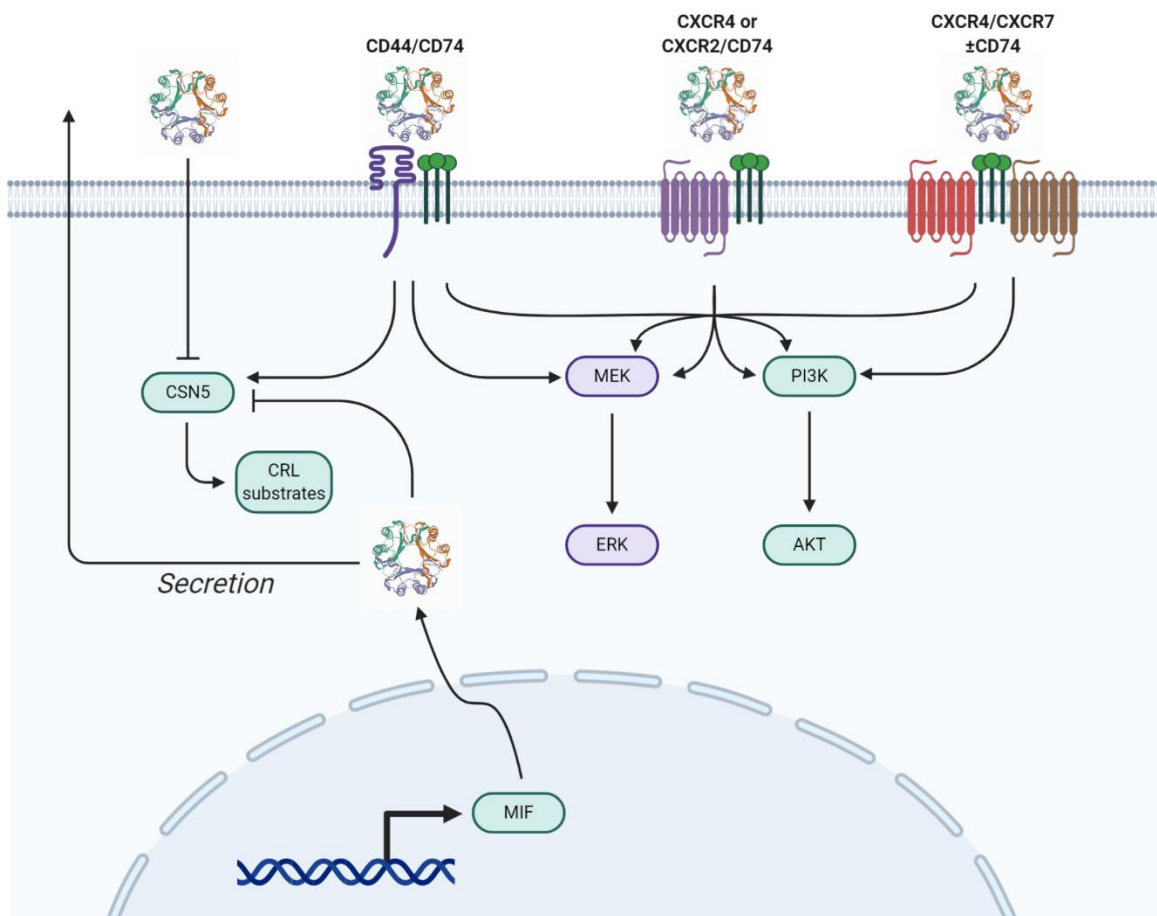
Figure 6. Schematic of MIF's intracellular and extracellular mechanisms of action. Intracellular MIF will either interact with CSN5 to regulate cullin RING ubiquitin ligase (CRL) substrates or undergo secretion out of the cell. Extracellular MIF can bind to 1) a CD44/CD74 heterodimer to regulate CSN5 activity and the MEK/ERK signaling pathway, 2) a CXCR2 or CXCR4/CD74 heterodimer to regulate the MEK/ERK and PI3K/AKT pathways, or 3) CXCR4/CXCR7 heterodimer or CXCR4/CXCR7/CD74 heterotrimer to regulate both the PI3K/AKT and MEK/ERK pathways. Created with BioRender.com.

Given that these receptors are variably expressed on numerous immune cell types implicated in tumor immune responses, the effector function(s) and biological activities elicited by extracellular MIF are likely highly dependent on signals stemming from the TME and immune landscape within the tumor stroma that control the relative expression of each receptor.

In addition to its extracellular receptor-dependent functions, cytosolic MIF binds to several different intracellular proteins to modulate their biological activities. The best characterized of these intracellular effectors is the COP9-signalosome subunit 5 (CSN5), which is an essential determinant of cullin-RING ligase (CRL)-dependent protein turnover (193,194). CSN5 can also dissociate from the CSN complex to facilitate transactivation of c-Jun transcription and, in this context, is also referred to as Jun-activation domain-binding protein (Jab1) (195). Bernhagen's group first identified that MIF negatively regulates the activity of cytosolic Jab1 on both steady-state and stimulus-induced AP-1-dependent transcription (196,197). Given that AP-1 is associated with the activation of pro-inflammatory responses in numerous immune cell types (198,199), an anti-inflammatory/immunosuppressive role for MIF might be expected when intracellular MIF concentrations are sufficient to inhibit Jab1/CSN5 functionally. That being said, extracellular MIF/CD74 interaction is shown to functionally activate c-Jun phosphorylation and increase AP-1-dependent transcription (200-202), so it is conceivable, if not likely, that the relative balance between extracellular and intracellular MIF levels in the TME or circulation at any given time dictates the ensuing MIF-associated phenotype.

Beyond MIF's activities regulating AP-1 through Jab1 binding, MIF also modulates CSN5-dependent ubiquitylation/proteasomal degradation of various proteins. These include p27^{Kip1} (196), Cdc25A (203), E2F family members (203), and, more recently, HIF-1α (204,205). In hypoxic tissues, such as the TME, there is a reciprocally synergistic relationship between MIF and HIF-1α; hypoxia-driven HIF-1α stabilization and subsequent transcriptional regulation promotes enhanced expression of MIF (206), and this ensuing increase in MIF expression amplifies the transcriptional response of HIF-1α (204). Given the critical role of HIF-1α in regulating the phenotypes and relative differentiation/maturation of multiple different immune cell types (207), intracellular MIF-mediated HIF-1α stabilization may be a centrally important mechanism of action responsible for several of the MIF-associated pro/anti-tumor immune phenotypes.

It is likely that MIF's site of action – either extracellular or intracellular – and which receptor/co-receptor or intracellular protein/enzyme that MIF interacts with is ultimately responsible for specific phenotypes elicited by MIF. Given both MIF's ability to regulate several types of tumor-infiltrating immune cells and its pleiotropic nature due to multiple potential signaling mechanisms, it will be imperative to characterize and define the relative contributions of the intermediary mechanism(s) required for MIF-dependent control of tumor immunity.

MIF and metabolic reprogramming

Interestingly, the Mitchell Laboratory previously identified that MIF might regulate mitochondrial metabolism (*unpublished*). Additionally, a recent investigation identified that down regulation of MIF results in significantly impaired

mitochondrial dynamics leading to mitochondrial membrane potential depolarization in cancer cell lines (208). Given that MIF is a critical requirement for M2 macrophage polarization and M2 polarization requires metabolic reprogramming towards mitochondrial metabolism, MIF may regulate M2 macrophage polarization by supporting mitochondrial metabolism.

Following mitochondrial damage, the electron transport chain becomes highly inefficient, leading to both the accumulation of partially reduced products and non-oxidized substrates (209). The ETC consists of five transmembrane protein complexes that oxidize substrates and then transfer the generated electrons within a ubiquinone pool to reduce oxygen into water (210). Interestingly, ETC Complex II (also known as Succinate Dehydrogenase – SDH) oxidizes the TCA cycle metabolite succinate; therefore, SDH serves as a direct link between the ETC and the TCA cycle (211). As mitochondria become damaged, the activity of the ETC complexes (i.e., SDH) decreases, resulting in succinate accumulation (209). Succinate is a highly pro-inflammatory metabolite that drives M1 macrophage polarization by interfering with the activity of several enzymes (212).

Alpha-ketoglutarate (αKG)-dependent dioxygenases (αKGDs) are a class of enzymes that use αKG as a cofactor with molecular oxygen as a substrate to add hydroxyl group modifications to proteins (213). In the process of hydroxylation, αKG becomes oxidized to succinate, which can then feedback-inhibit αKGDs by antagonizing their enzymatic activity (214). Therefore, the relative ratio of αKG to succinate concentrations regulates the activity of αKGDs (i.e., high αKG/succinate supports high αKGD activity).

Several αKGDs have been identified to regulate macrophage polarization, so the relative αKG/succinate ratio influences the ability of macrophages to obtain a specific phenotype (28,128,212). For example, a low αKG/succinate ratio supports M1 polarization by allowing for LPS-induced NF-κβ signal pathway activation (128). In this mechanism, high succinate levels block the activity of an αKGD (i.e., prolyl hydroxylase – PHD) that antagonizes NF-κβ activation by the hydroxylation and subsequent degradation of a critical NF-κβ cofactor.

Additionally, a high αKG/succinate ratio supports M2 polarization by activating histone lysine demethylase 6B (KDM6B; also known as Jumonji domain-containing 3, histone lysine demethylase – JMJD3) (128,215). The interaction between JMJD3 and αKG serves as a metabolic-epigenetic link in regulating M2 macrophage polarization. High levels of αKG are needed for JMJD3's enzymatic activity to remove tri-methylated groups from the lysine 27 residue on histone H3 (H3K27me3) (128). H3K27 tri-methylation is a repressive epigenetic mark that usually blocks the expression of M2-associated gene products (215). Therefore, the metabolic reprogramming towards mitochondrial metabolism during M2 polarization is needed to generate sufficient αKG to activate JMJD3-dependent demethylation of H3K27me3 marks to allow for transcriptional expression.

Interestingly, MIF depletion or inhibition functionally repolarizes macrophages from a pro-tumor/immunosuppressive M2 phenotype to an anti-tumor/immunostimulatory M1 phenotype (156). Given that both of these phenotypes are regulated by relative αKG/succinate levels, MIF-dependent control of macrophage phenotypes may be due to mitochondrial metabolism-mediated

balancing of the αKG/succinate ratio. In this model, MIF supports the mitochondrial metabolism needed to prevent succinate accumulation that would otherwise block the αKG-dependent, JMJD3-mediated demethylation of repressive H3K27me3 marks that must be removed for maximal M2 macrophage polarization. Conversely, MIF inhibition would lead to mitochondrial dysfunction, with a resultant accumulation of succinate, thus lowering the αKG/succinate ratio to enable LPS-induced NF-κβ signaling needed for M1 macrophage polarization.

The MIF/CSN5/NRF2 pathway in mitochondrial metabolism

Although MIF regulates mitochondrial metabolism in cancer cell lines (208), the underlying mechanistic effectors are undefined. Previously, the Mitchell Laboratory determined that MIF-dependent M2 macrophage polarization occurs independently of its cognate receptor CD74 (*unpublished*). This indicates that MIF regulates M2 polarization in a receptor-independent manner, potentially by binding to CSN5. Interestingly, nuclear factor E2-related factor 2 (NRF2) – a master regulator of mitochondrial biogenesis and integrity (216) – is regulated by CSN5 activity in macrophages (217), which suggests that NRF2 may be a mechanistic link between MIF and M2 macrophage-associated mitochondrial metabolism (218). Mechanistically, kelch-like ECH-associated protein 1 (KEAP1) negatively regulates NRF2 by forming a complex with cullin-RING ligase 3 (CUL3) to mediate the ubiquitination and subsequent proteasomal degradation of NRF2 (219). Previous investigations have identified that CSN5 mediates NRF2 stabilization by controlling the KEAP1:CUL3 complex (217). Therefore, MIF may functionally bind

to CSN5 to promote NRF2 stability to sustain subsequent mitochondrial biogenesis/metabolism needed for M2 macrophage polarization (Figure 7).

The following Aims will examine these hypotheses:

- **Aim 1: Delineate the mechanistic effectors of mitochondrial lactate metabolism in M2-macrophage polarization:** This aim will utilize metabolic flux assays, isotope tracing metabolomic analyses, and chromatin immunoprecipitation (ChIP) in *ex vivo* M2 macrophage polarization models to test the hypothesis that mitochondrial lactate metabolism supports M2 polarization through TCA cycle-derived citrate production and subsequent ACLY-dependent histone acetylation. The findings of this aim will be validated *in vivo* using a subcutaneous tumor model of lung cancer.

- **Aim 2: Determine the mechanistic contributions of MIF in lactate/pyruvate-mediated M2 TAM polarization:** This aim will utilize metabolic flux assays, gene expression assays, and ChIP to identify the contribution of MIF-dependent mitochondrial lactate/pyruvate metabolism and M2 polarization to determine if MIF supports these processes by functionally controlling CSN5-dependent NRF2 stabilization and ensuing mitochondrial metabolism.
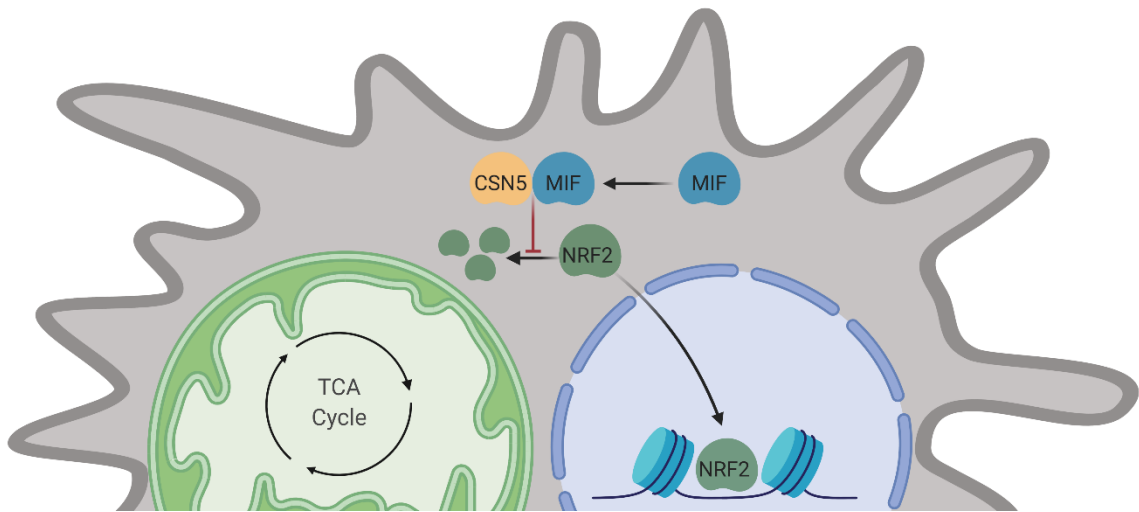
Figure 7: Schematic of the hypothesized mechanism of MIF-dependent mitochondrial metabolism during M2 macrophage polarization. Intracellular MIF binds to CSN5 to promote the stabilization of NRF2 to allow for NRF2 nuclear translocation and transcriptional expression of NRF2-dependent genes required for metabolic reprogramming toward mitochondrial metabolism during M2 macrophage polarization.

CHAPTER 2: MITOCHONDRIAL LACTATE METABOLISM SUPPORTS M2 MACROPHAGE POLARIZATION THROUGH ACLY-DEPENDENT HISTONE ACETYLATION

Introduction

Highly glycolytic "Warburg-like" cancer cells take up glucose and produce lactate, which fundamentally changes the metabolic landscape of tumor microenvironments (TME) (146,147). Although lactate was long considered a metabolic waste product of glycolytic tumors solely, it is increasingly becoming recognized as a vital TME signal that regulates the effector functions of various tumor-infiltrating immune cells (129,151,152). A paradigm-shifting study revealed that circulating lactate – derived from glucose metabolism following glycolysis and lactate secretion – is actively metabolized in the mitochondrial tricarboxylic acid (TCA) cycle (153). Perhaps relatedly, tumor-derived lactate drives M2 macrophage polarization in a HIF-1α-dependent manner (17), although the metabolic mechanism(s) are not fully elucidated. As M2 polarized tumor-associated macrophages (TAMs) occupy a low glucose/high lactate TME (18) and rely on mitochondrial metabolism (107,109), an understanding of how lactate is metabolized and whether/how it regulates gene expression patterns will help to elucidate the mechanisms by which the TME influences tumor-infiltrating macrophage functions

Macrophages carry out both physiologic and pathophysiologic functions leading to health and disease (41). For example, M2- TAMs promote wound

healing and resolution of immune responses (220), but in late-stage cancers, the tumors co-opt this phenotype to evade anti-tumor immunity (103). Conversely, while M1-TAMs eradicate tumors by enhancing anti-tumor immune responses, they also drive tumor development by contributing to chronic inflammation-associated cellular damage (95). Accumulating evidence demonstrates that macrophage phenotypes are sensitive to local metabolites within the TME that, in turn, influence their immunophenotypes and effector functions (104,126,127).

ATP-citrate lyase (ACLY) forms an essential link between the TCA cycle and epigenetic histone acetylation (130). Specifically, glucose is converted to pyruvate through glycolysis and then incorporated into the TCA cycle to produce citrate (119). A subfraction of this glucose-derived citrate is extruded out of the mitochondria and cleaved by ACLY, resulting in nucleo-cytoplasmic pools of Ac-CoA for histone acetylation (130).

ACLY has pleiotropic roles in macrophage polarization as Ac-CoA can support histone acetylation and *de novo* lipogenesis (122). Initial studies found that ACLY inhibitors suppress M1 macrophage-mediated cytokine and PGE$_2$ production (132,221). In contrast, interleukin-4 (IL-4)-dependent M2 macrophage polarization triggers Akt-mTORC1-dependent ACLY activation (140). More recently, a conditional macrophage *Acly*-knockout transgenic model identified a novel ACLY contribution to macrophage-dependent atherosclerotic plaque stability (142). However, the requirements for ACLY, and the metabolic substrates involved, in direct M0→M2 TAM polarization and effector functions are not fully elucidated.

Using gene expression analyses, chromatin immunoprecipitation, and metabolomic approaches, we report that direct M0→M2 macrophage polarization interchangeably utilizes glucose or lactate as TCA cycle carbon sources to maximally drive ACLY-dependent histone acetylation at M2 gene-specific promoters, resulting in T cell suppressive functionality.

Materials and Methods

Mice: Wild-type C57BL/6 mice were obtained from Harlan Laboratories (Dublin, VA). B6/SJL mice were obtained from Jackson Laboratory (Bar Harbor, ME). *ACLY*^f/f mice have been previously reported (222), and bones from UBC-Cre ERT2; ACLY^f/f mice were kindly provided by Dr. Kathryn Wellen. Animals were maintained under specific pathogen-free conditions and handled in accordance with the Association for Assessment and Accreditation of Laboratory Animals Care international guidelines. The Institutional Animal Care and Use Committee (IACUC) at the University of Louisville approved experiments. 6-16-week-old mice were used in all experiments.

Cell culture and BMDM differentiation: Mice were euthanized by CO_2 asphyxiation, and death was confirmed by cervical dislocation. Bone marrow cells from the tibias and femurs were differentiated in RPMI-1640 supplemented with FBS (5%) and recombinant murine M-CSF (25 ng/mL: Peprotech) for seven days. For the inducible *Acly*-depletion experiments, *Acly*^fl/fl UBC Cre ERT2 BMDMs were treated with 4-hydroxytamoxifen (5 μM) or vehicle control on day four of differentiation. Following differentiation, the cells were counted and plated at 1.3×10^6 BMDMs/mL in RPMI-1640 supplemented with 10% FBS (without M-CSF) overnight. The following day the BMDMs were washed with PBS and starved of glucose by addition of glucose-free RPMI-1640 supplemented with 10% dialyzed FBS and

2mM L-glutamine for 4-6 hours before treatment with the indicated compounds and stimulated with recombinant murine IL-4 (20 ng/ml: Peprotech) for 4-48 hours.

RNA purification and RT-qPCR: Total RNA was extracted using RNeasy Mini Kit (QIAGEN) following the manufacturer's instructions. The resulting RNA was quantified using a Nanodrop 8000 UV-visible spectrophotometer (Thermo Scientific), and the cDNA was synthesized with a High-Capacity cDNA Reverse Transcription Kit (Applied Biosystems). Quantitative measurement of cDNA levels was performed using TaqMan Fast Advanced Master Mix (Applied Biosystems) with TaqMan Gene Expression Primers (Applied Biosystems) on a 7500 Fast Real-Time PCR System (Applied Biosystems). Relative expression profiles of mRNA levels were calculated using the comparative Ct method ($2^{-(\Delta\Delta Ct)}$) using 18s rRNA levels as an endogenous reference control.

Immunoblotting: Cells were lysed in RIPA buffer supplemented with protease and phosphatase inhibitors, homogenized, and samples were denatured in LB sample buffer at 98°C. 5-20 µg of protein was loaded into a 4-20% Mini-PROTEAN TGX Gel (Bio-Rad Laboratories) and separated by electrophoresis before being transferred onto Immobilon-P PVDF membrane (EMD Millipore). After blocking, membranes were probed overnight at 4°C with primary Abs and then for 1 hour at room temperature with secondary Abs. The blots were developed using Pierce ECL Plus Western Blotting Substrate (Thermo Scientific).

In vitro BMDM-T cell coculture assay: BMDMs were treated with UK-5099 (25 µM) or DMSO in the presence of the indicated metabolites ± IL-4 for 24 hours before being collected, washed, counted via trypan blue exclusion, and live cells were plated in 96-well plates. BMDMs were then co-cultured with CFSE-labeled splenocytes from syngeneic mice in the presence of anti-CD3/anti-CD28 agonistic antibodies for three days. The cells were stimulated with PMA/Ionomycin plus GolgiPlug for 6 hours and then stained with anti-CD8 or anti-CD4 mAbs and fixed/permeabilized for intracellular IFN-γ staining. The data was acquired using a FACSCanto cytometer (BD Biosciences) and analyzed using FlowJo V10 software (Tree Star, Ashland, OR).

Extracellular Flux Analysis: For extracellular flux assays, BMDMs were plated in Seahorse XF96 cell culture microplates (Seahorse Biosciences, Agilent) and incubated in 5% CO_2 at 37°. The next day, wells were pre-treated with UK-5099 (25µM) or DMSO for 30 mins, followed by polarization with IL-4 for 16 hours. One hour prior to extracellular flux analysis, the growth medium was replaced with XF Assay Medium (Seahorse Bioscience, Billerica, MA, USA) and incubated in a non-CO_2 incubator. The oxygen consumption rate (OCR) and extracellular acidification rate (ECAR) were measured using an XF96 Extracellular Flux Analyzer (Seahorse Bioscience, Billerica, MA, USA) according to the manufacturer's instructions. During the assay, wells were injected with oligomycin (5 µM), FCCP (2 µM), and rotenone (1 µM)/antimycin A (5 µM). Each condition was performed in 4-6 replicates and analyzed using Seahorse Wave 2.6 Desktop Software (Agilent).

<u>^{13}C-Lactate Labeling:</u> 1×10^7 BMDMs were plated for 24 hours in complete RPMI-1640. The next day the cells were switched to glucose-free RPMI-1640 for six hours. The BMDMs were then pre-treated with UK-5099 or DMSO for 30 minutes before IL-4 polarization in ^{13}C-Lactate. After six hours of labeling, cells were washed twice with ice-cold 0.1x PBS and extracted with 1 mL 50% methanol containing 20 µM L-norvaline (internal control). Polar (aqueous layer) and insoluble fractions (protein) were separated by centrifugation at 4°C and 15,000 rpm for 10 minutes. The polar fraction was dried by SpeedVac (Thermo) followed by derivatization. The protein pellet was subsequently washed four times with 50% methanol and once with 100% methanol to remove polar contaminants and dried by SpeedVac.

<u>Pellet Hydrolysis:</u> Hydrolysis of the protein pellet was performed by first resuspending the dried pellet in deionized H_2O followed by the addition of equal part 6N HCl. The samples were vortexed thoroughly and incubated at 95 °C for 2 hours. All reactions were quenched with 100% methanol with 200 µM L-norvaline and then incubated on ice for 30 minutes. The supernatant was collected after centrifugation at 15,000 rpm at 4 °C for 10 minutes and was subsequently dried by SpeedVac followed by derivatization.

<u>Sample Derivatization:</u> Dried polar and hydrolyzed pellet samples were derivatized by the addition of 50 µL of 20 mg/ml methoxyamine hydrochloride in pyridine. Samples were incubated at 30°C for 90 minutes, followed by centrifugation at

15,000 rpm for 10 minutes. The supernatant was transferred to a V-shaped amber glass chromatography vial, followed by the addition of 80 µL of N-methyl-trimethylsilyl-trifluoroacetamide (MSTFA) and incubation for 30 minutes at 37°C. The derivatized samples were then analyzed by GC-MS.

GC-MS Quantitation: An Agilent 7800B gas-chromatography (GC) coupled to a 7010A triple quadrupole mass spectrometry detector equipped with a high-efficiency source was used for this study. GC-MS protocols were similar to those described previously(223), except a modified temperature gradient was used for GC: Initial temperature was 130°C, held for 4 minutes, rising at 6°C/min to 243°C, rising at 60°C/min to 280°C, and held for 2 minutes. The electron ionization (EI) energy was set to 70 eV. ^{13}C isotopologues were identified by selected ion monitoring (SIM) of the following ions at known retention times: alpha-ketoglutarate; 304-209, alanine; 218-221, citrate; 465-471, lactate; 219-222, pyruvate; 174-177. Scan (m/z:50-800) and full scan mode were used for target metabolite analysis. Metabolites were identified using the FiehnLib metabolomics library (available through Agilent) by retention time and fragmentation pattern, and quantitation was performed using Agilent MassHunter Workstation Software. Natural abundance correction was performed using IsoCorrectoR software, and relative abundance was corrected for recovery using the L-norvaline standard and adjusted to protein input (224).

Histone acetylation ELISA: Histones were extracted using the EpiQuick Total Histone Extraction Kit (EpiGentek) and analyzed using the EpiQuick Total Histone H3 Acetylation Detection Fast Kit (EpiGentek) according to the manufacturer's protocols. Briefly, $1x10^7$ BMDMs were polarized for 4-6 hours in the indicated conditions before collection using Cell Striper (Corning), incubation with pre-lysis, and then lysis buffer. The histone-containing supernatant fraction was collected and treated with the balance buffer before 150 ng of the histone extract was added to the ELISA assay wells for two hours at room temperature. The wells were then washed and incubated with the secondary antibody-containing solution for one hour on an orbital shaker. The wells were then developed with the enzyme reaction solution for 5 minutes before being quenched and measured for absorbance at 450 nm.

Chromatin immunoprecipitation (ChIP): ChIP was performed using the SimpleChip Enzymatic Chromatin IP Kit (Cell Signaling Technology; CST) according to the manufacturer's instructions. Briefly, $1.2x10^7$ BMDMs were fixed with 1% formaldehyde, lysed, and then the nuclei were isolated. The chromatin was digested with Micrococcal Nuclease and then sonicated to lyse the nuclear membrane. The cross-linked chromatin was immunoprecipitated with anti-H3K9ac antibody (CST – C5B11) overnight at 4° C. The chromatin was recovered with Protein G Agarose Beads, eluted, and the cross-links were reversed with Elution Buffer and Proteinase K overnight at 65° C. Input and immunoprecipitated DNA

was analyzed by Real-Time qPCR, and the data are presented as percent of the total input chromatin.

In vivo tumor admixture model: The tumor admixture model was performed as previously described (225). Briefly, $Acly^{+/+}$ and $Acly^{-/-}$ BMDMs (CD45.2$^+$) were polarized with IL-4 for 24 hours before being mixed with LLC cells (CD45.2$^+$) at a 1:2.5 ratio, respectively, in Matrigel (Corning) and injected s.c. into the flanks of congenic B6.SJL mice (CD45.1$^+$). On day seven post-injection, palpable tumors were measured three times a week, and the tumor volume was calculated by the following formula: (length x width^2)/2. At the experimental endpoint on day 16 post-injection, the mice were euthanized, and the tumors were resected, weighed, and digested in RPMI-1640 containing collagenase IV, hyaluronidase, and DNase I for 30 minutes at 37°. Aliquots of the single-cell suspensions were either stimulated with PMA/I plus GolgiPlug for 6 hours before staining or directly stained with the indicated mAbs.

Statistical Analysis: All representative data are presented as the mean ± SEM and are presented and analyzed for statistical significance using GraphPad Prism 8.3 (GraphPad Software. La Jolla, California, USA). Analysis with one-way or two-way ANOVA was utilized when the data presented had one or more independent variables, respectively. Tukey's post-test was utilized for multiple comparisons.

Results

Lactate supports direct M0→M2 macrophage polarization through mitochondrial pyruvate metabolism

To investigate how changing TME metabolite concentrations differentially impact M2 macrophage polarization, we treated primary murine bone marrow-derived macrophages (BMDMs) with the Th2 cytokine IL-4 in the presence/absence of various concentrations of glucose and lactate. Removal of extracellular glucose reduced the expression of canonical M2-associated gene products Arginase 1 (*Arg1*) and C-C motif chemokine 22 (*Ccl22*) – an effect that was rescued in a dose-dependent manner with molar equivalent additions of exogenous lactate as determined by qPCR and immunoblotting (Figure 8). Notably, the concentrations of lactate added are comparable to levels found in the TME, which are as high as 10-30 mM (149). In addition to *Arg1* and *Ccl22*, lactate also rescued the reduced expression of M2 macrophage-associated gene products *Retnla* and *Il-10* in glucose-free culture conditions (Figure 9).

Since M2 macrophages rely on mitochondrial metabolism (107,109), and lactate is converted to pyruvate that enters the TCA cycle by mitochondrial import via mitochondrial pyruvate carrier 1 (MPC1) (119,120), we asked whether MPC1 inhibition by UK-5099 (226) blocks lactate and glucose-dependent M2 polarization. As shown in Figure 10, UK-5099 inhibited IL-4-induced expression of M2-associated gene products in primary BMDMs cultured in glucose, lactate, and, as shown in (Figure 11), pyruvate.

A

Arg1

IL-4:	-	+	+	+	+	+	+	+
Glucose:	5	5	2.5	0.5	-	-	-	-
Lactate:	-	-	-	-	-	1	5	10

Ccl22

IL-4:	-	+	+	+	+	+	+	+
Glucose:	5	5	2.5	0.5	-	-	-	-
Lactate:	-	-	-	-	-	1	5	10

B

Glu(mM):	5	5	2.5	.5	-	-	-	-
Lac(mM):	-	-	-	-	-	1	5	10
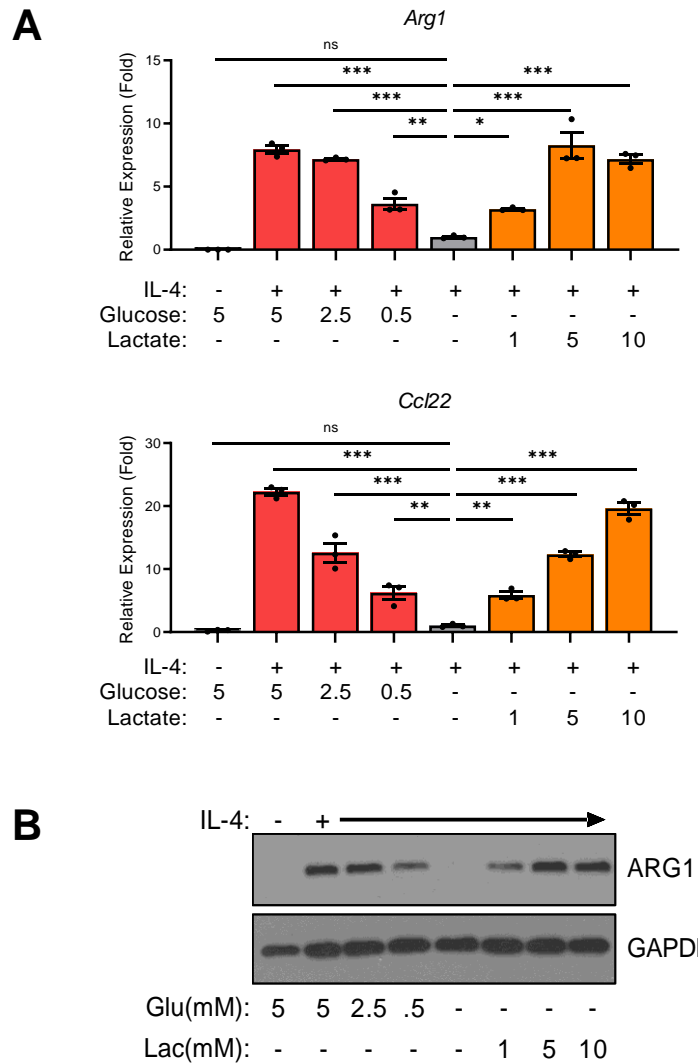
Figure 8: Lactate dose-dependently rescues loss of M2 polarization following glucose deficiency. (A) qPCR analysis of *Arg1* and *Ccl22* expression in BMDMs treated with IL-4 (48hr) in glucose-free media supplemented with glucose or lactate at the indicated concentrations. **(B)** Immunoblot of *Arg1* expression in BMDMs treated with IL-4 (48hr) in glucose-free media supplemented with glucose (Glu) or lactate (Lac) at the indicated concentrations. Data are the mean ± SEM of three replicates. *p≤0.05, **p≤0.01, ***p≤0.001 by two-way ANOVA with Tukey's post-test. Immunoblot is representative of three replicates.
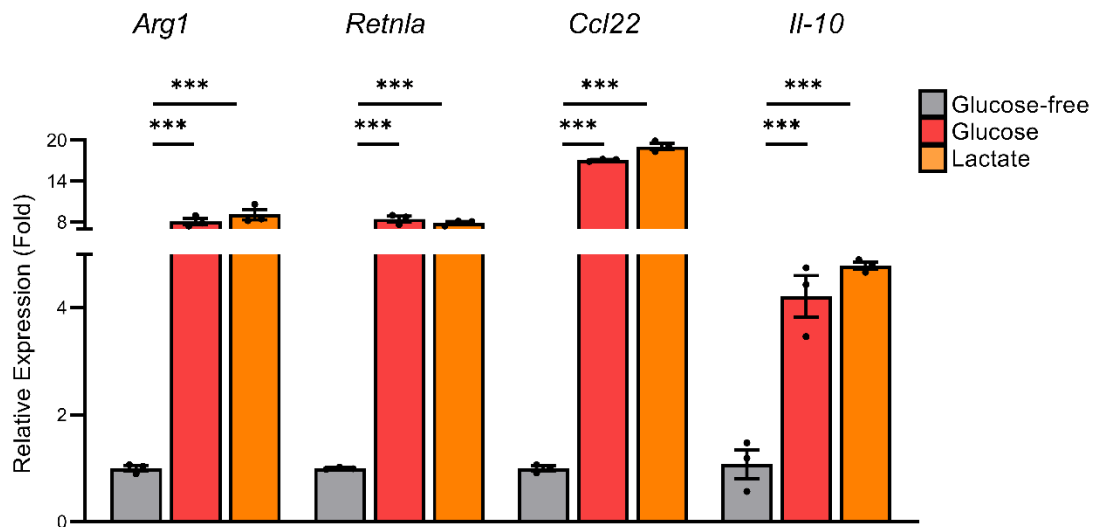
Figure 9: M2 macrophage polarization is maintained in tumor microenvironment-like conditions of low glucose/high lactate. qPCR analysis of M2 macrophage-associated gene product expression in BMDMs treated with IL-4 (48hr) in glucose-free media supplemented with glucose (5mM) or lactate (10mM). Data are the mean ± SEM of three replicates. *p≤0.05, **p≤0.01, ***p≤0.001 by one-way ANOVA with Tukey's post-test.
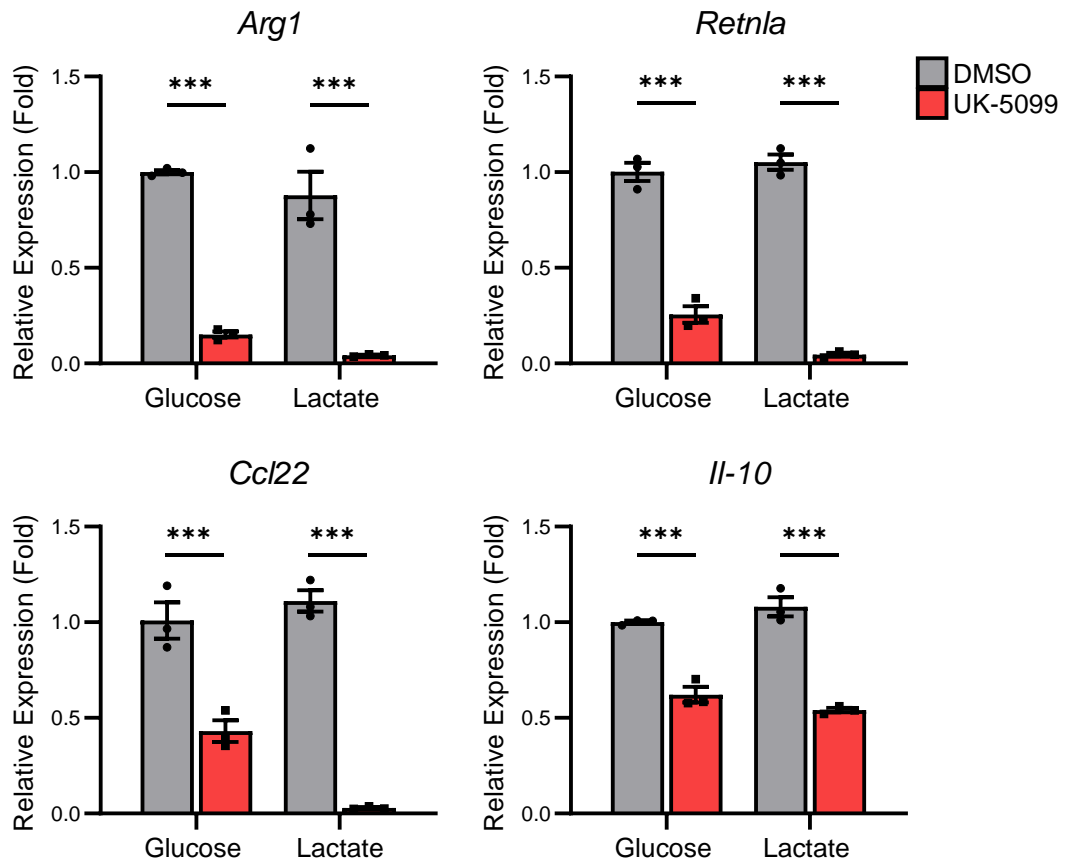
Figure 10: Mitochondrial pyruvate/lactate metabolism is a critical requirement of M2 macrophage polarization. qPCR analysis of M2 macrophage-associated gene product expression in BMDMs treated with IL-4 (48hr) ± UK-5099 (25µM) in glucose-free media supplemented with glucose (5mM) or lactate (10mM). Data are the mean ± SEM of three replicates. *p≤0.05, **p≤0.01, ***p≤0.001 by two-way ANOVA with Tukey's post-test.
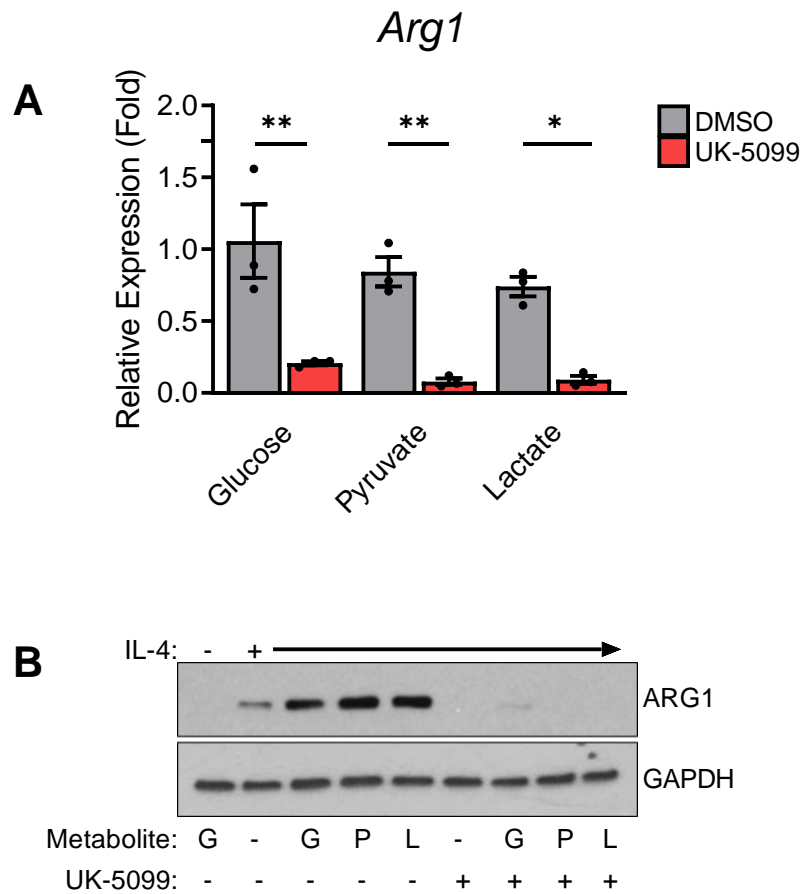
Figure 11: Glucose and lactate support M2 polarization through the production of pyruvate. (A) qPCR analysis of M2 macrophage-associated gene product expression in BMDMs treated with IL-4 (48hr) ± UK-5099 (25μM) in glucose-free media supplemented with glucose (5mM), pyruvate (10mM), or lactate (10mM). **(B)** Immunoblot of *Arg1* expression in BMDMs treated with IL-4 (48hr) ± UK-5099 (25μM) in glucose-free media supplemented with glucose (G, 5mM), pyruvate (P, 10mM), or lactate (L, 10mM). Data are the mean ± SEM of three replicates. *p≤0.05, **p≤0.01, ***p≤0.001 by two-way ANOVA with Tukey's post-test. Immunoblot is representative of three replicates.

To ensure that the inhibitory effects with UK-5099 were due to specific MPC1 inhibition, we tested Mitoglitazone, a molecularly distinct MPC inhibitor (227). Pre-treatment with Mitoglitazone both inhibited Arg1 expression in a dose-dependent manner and phenocopied the inhibition of UK-5099-sensitive M2-associated gene products (Figure 12).

Arguably, the most critical effector function of M2-TAMs is their immune-suppressive activity that inhibits the activation and anti-tumor cytolytic function of tumor-infiltrating CD8^{+} T cells (103). As such, we tested if lactate supports M2 macrophage immunosuppression and whether it also requires mitochondrial pyruvate uptake. As shown in Figure 12, M2 macrophage polarization in the presence of glucose or lactate significantly suppresses the proliferation and IFN-γ production of anti-CD3/anti-CD28-activated CD8^{+} splenocytes. Consistent with the requirement for mitochondrial pyruvate uptake in glucose/lactate-dependent M2 gene expression, UK-5099 abrogated glucose/lactate-dependent M2 macrophage-mediated immune-suppressive activity allowing for improved CD8^{+} T cell proliferation and IFN-γ production (Figure 13). Altogether, these data suggest that glucose- or lactate-derived mitochondrial pyruvate metabolism is necessary for maximal M0→M2 macrophage polarization and immunosuppressive function.

M2 macrophages actively metabolize lactate within the TCA cycle

M2 polarization induces a metabolic shift towards mitochondrial metabolism, TCA cycle activity, and OXPHOS (107,109), but the relative contribution of mitochondrial pyruvate metabolism to this metabolic reprogramming during M2 macrophage polarization is largely unresolved.
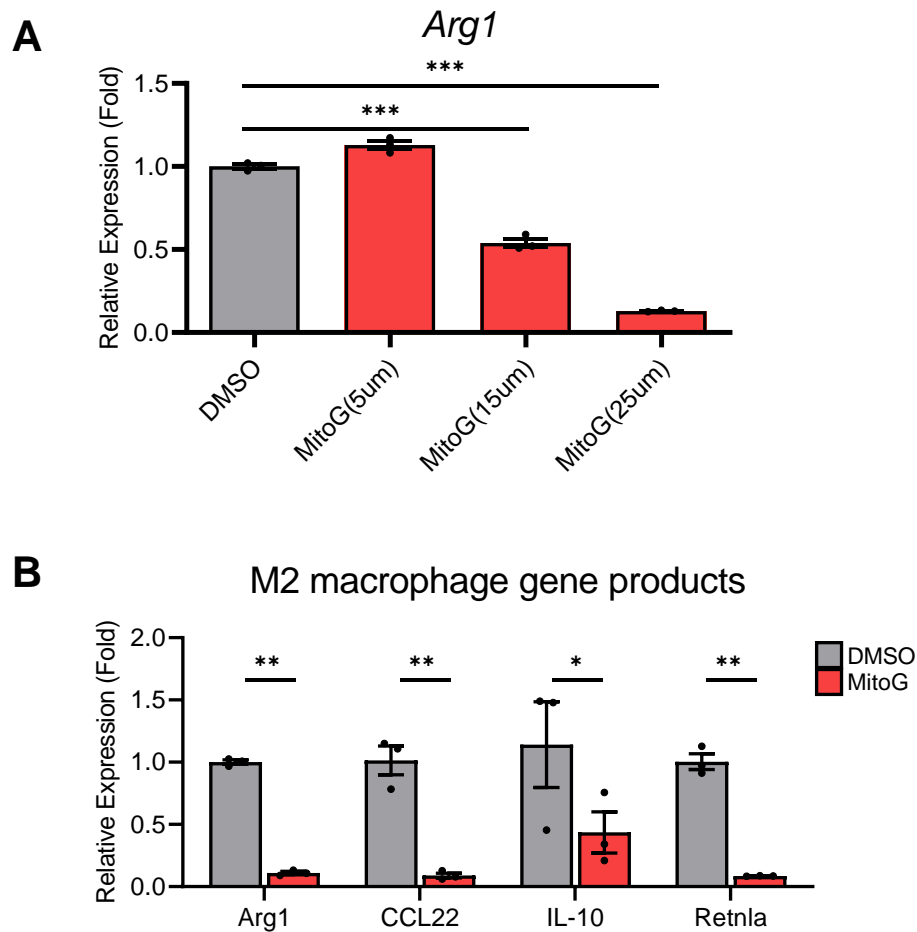
Figure 12: Inhibition of mitochondrial pyruvate uptake with Mitoglitazone phenocopies the loss of M2 macrophage polarization following UK-5099 pre-treatment. (A) qPCR analysis of *Arg1* expression in BMDMs treated with IL-4 (48hr) ± Mitoglitazone (MitoG) at the indicated concentrations. **(B)** qPCR analysis of M2 macrophage-associated gene product expression in BMDMs treated with IL-4 (48hr) ± MitoG (25µM). Data are the mean ± SEM of three replicates. *p≤0.05, **p≤0.01, ***p≤0.001 by one-way ANOVA **(A)** or two-way ANOVA **(B)** with Tukey's post-test.

A T Cell Proliferation
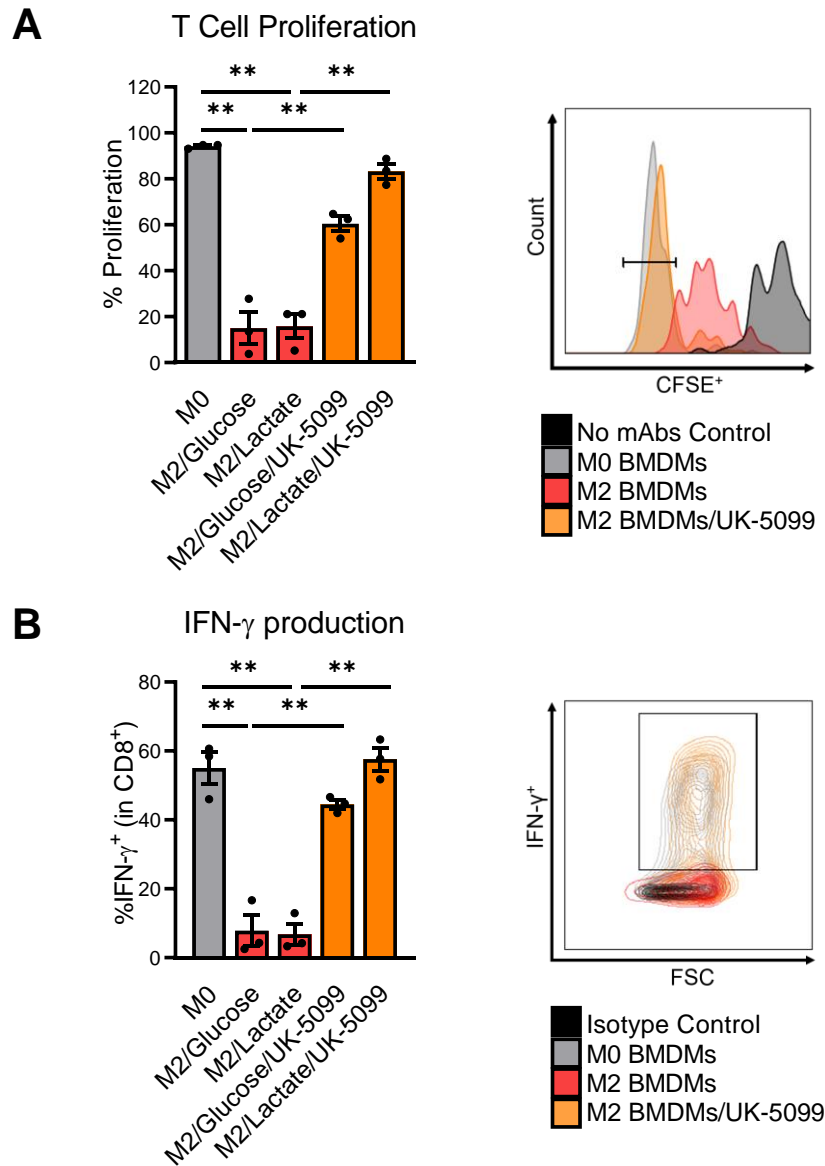
B IFN-γ production

Figure 13: Mitochondrial lactate/pyruvate metabolism is required for macrophage-mediated suppression of T cell activation. (A) Proliferation and **(B)** IFN-γ production, with representative images, of CD8+ T cells co-cultured with the indicated macrophages. Data are the mean ± SEM of three replicates. *p≤0.05, **p≤0.01, ***p≤0.001 by one-way ANOVA with Tukey's post-test.

Utilizing extracellular flux analysis of BMDMs, we confirmed that, as previously reported (107,109), IL-4 increases basal and maximal oxygen consumption rates (OCR) and spare respiratory capacity (SRC) (Figure 14). In contrast, pre-treatment with UK-5099 reduces both steady-state and IL-4-induced OCR and SRC (Figure 14). These findings indicate that mitochondrial lactate/pyruvate uptake is required for M2 macrophage metabolic reprogramming

Tumor-derived lactate supports M2 polarization (17), and lactate can be catabolized in the TCA cycle (153) – but whether M2 macrophage-specific lactate metabolism occurs is largely unknown. To address this, we conducted isotope tracing using uniformly labeled lactate ([U-^{13}C]-lactate) in M2 polarized BMDMs treated with and without UK-5099. As shown in Figure 15, ^{13}C-lactate accumulates intracellularly as fully labeled lactate (M+3 isotopologue) in M2 polarized macrophages and is not affected by UK-5099 treatment. In untreated M2 polarized BMDMs, ^{13}C-lactate is converted to fully labeled pyruvate (M+3) and incorporated into the initial round of the TCA cycle as (M+2) citrate and (M+3 – M+6) citrate following subsequent TCA cycling (Figure 15). In contrast, UK-5099 treatment reduces the fractional enrichment of initial and cycling citrate isotopologues, with a corresponding increase in fully labeled pyruvate. Comparison of un-labeled versus labeled lactate, pyruvate, and citrate shows the shift in the distribution of isotopologue labeling following UK-5099 treatment (Figure 16), which results in significant decreases in the metabolic influx of ^{13}C-lactate-derived carbons into the TCA cycle (Figure 16).
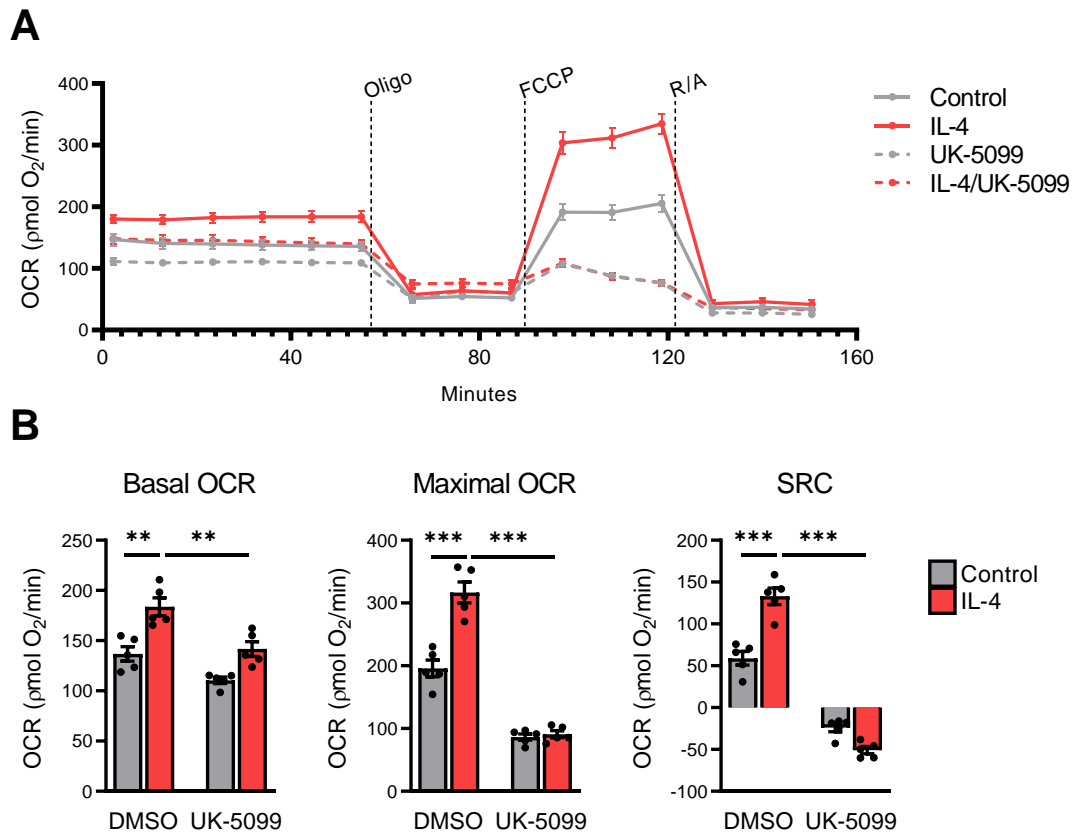
Figure 14: Mitochondrial lactate/pyruvate metabolism supports metabolic reprogramming during M2 macrophage polarization. (A) Extracellular flux analysis of the trace, **(B, left)** basal oxygen consumption rate (OCR), **(B, middle)** maximal OCR, **(B, right)** and spare respiratory capacity (SRC) in BMDMs treated with IL-4 (24hr) ± UK-5099 (25µM) before extracellular flux analysis with oligomycin (oligo), FCCP, and rotenone plus antimycin A (Rot/Ant). Data are the mean ± SEM of four replicates. *p≤0.05, **p≤0.01, ***p≤0.001 by two-way ANOVA with Tukey's post-test.
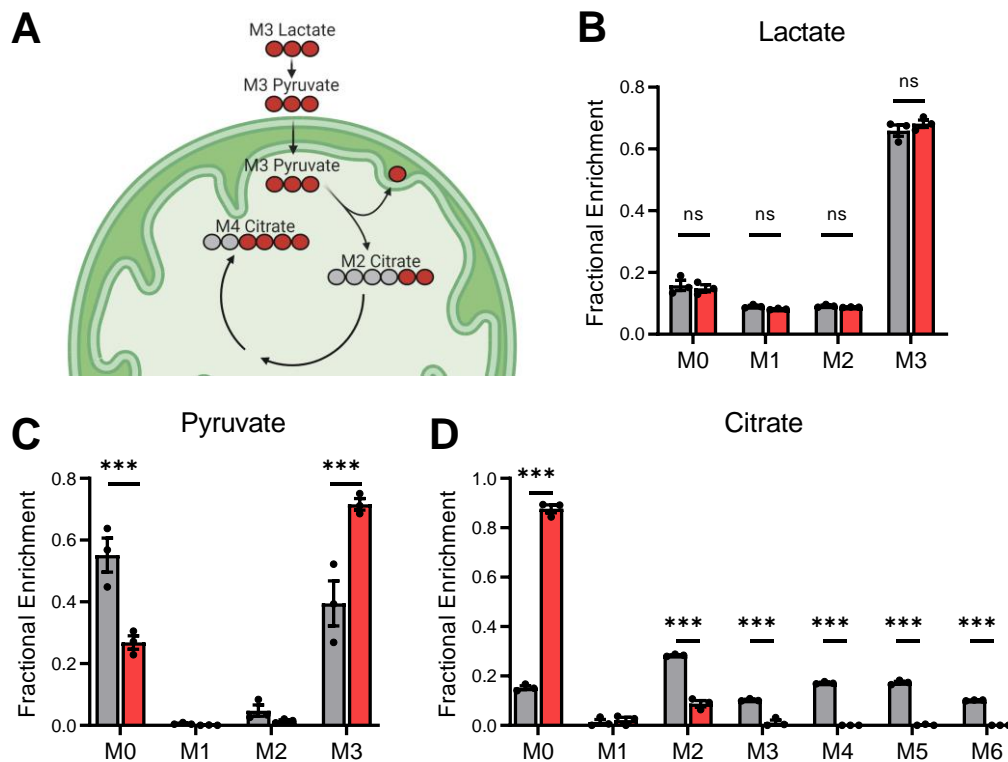
Figure 15: M2 macrophages actively metabolize lactate within the mitochondrial TCA cycle. (A) Schematic of metabolomic isotope tracing of ^{13}C-lactate-derived carbons (labeled in red) being incorporated into the TCA cycle (above, left). Fractional enrichment of **(B)** lactate, **(C)** pyruvate, **(D)** and citrate in BMDMs treated with IL-4 (6hr) ± UK-5099 (25µM) in glucose-free media supplemented with ^{13}C-lactate (10mM). Data are the mean ± SEM of three replicates. *p≤0.05, **p≤0.01, ***p≤0.001 by two-way ANOVA with Tukey's post-test.
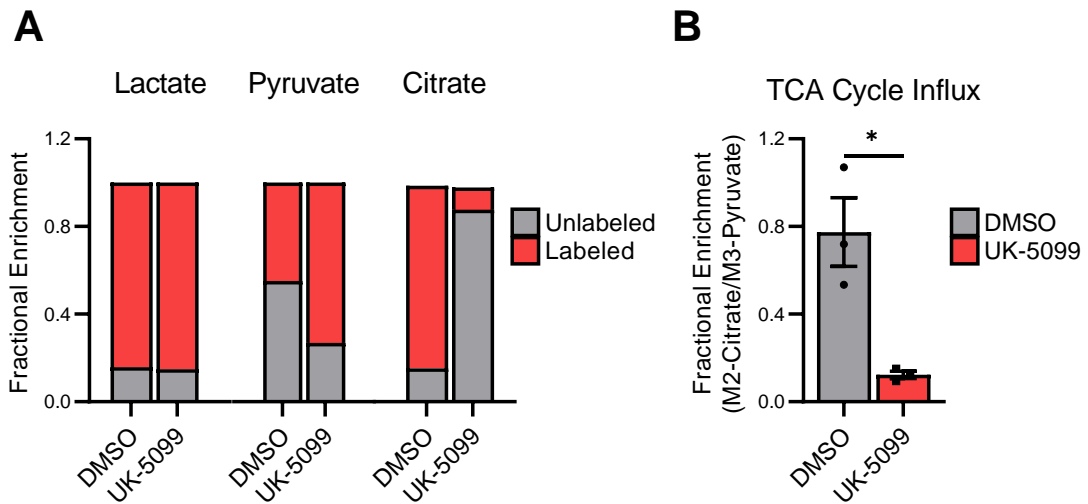
Figure 16: Lactate-derived carbons are incorporated into the TCA cycle during M2 polarization (A) Cumulative comparison of unlabeled (M0) *vs.* labeled lactate (M1 – M2), pyruvate (M1 – M2), and citrate (M1 – M6) (left) in BMDMs treated with IL-4 (6hr) ± UK-5099 (25µM) in glucose-free media supplemented with ^{13}C-lactate (10mM). **(B)** Metabolic influx of lactate-derived carbons into the TCA cycle in BMDMs treated with IL-4 (6hr) ± UK-5099 (25µM) in glucose-free media supplemented with ^{13}C-lactate (10mM). Data are the mean ± SEM of three replicates. *p≤0.05, **p≤0.01, ***p≤0.001 by student's t-test.

Altogether, these findings suggest that lactate-derived mitochondrial pyruvate is sufficient for IL-4-induced metabolic reprogramming and that lactate is efficiently taken up in M2 macrophages and catabolized within the TCA cycle.

M2 macrophages link lactate metabolism and M2 gene transcription through mitochondrial pyruvate-dependent histone acetylation

Initial studies designed to identify a mechanistic link between lactate-derived mitochondrial pyruvate metabolism and expression of M2 macrophage-associated gene products ruled out STAT6 phosphorylation and HIF-1α stabilization (126). Neither glucose-deprivation nor UK-5099 pre-treatment affected the phosphorylation of STAT6 in BMDMs when examined at both shorter (15 min) or longer (120 min) time points following IL-4 induced M2 polarization (Figure 17). Using HIF-ODD-luciferase BMDMs to quantify HIF-1α stability demonstrated that, while IL-4 induced a modest increase in luciferase activity (i.e., HIF-1α stability), no effect was observed with either UK-5099 or a succinate dehydrogenase inhibitor (228), Atpenin A5 (Figure 17).

A recent study described a functional role for endogenous, macrophage-derived lactate being metabolized into an acyl-CoA (*i.e.,* lactyl-CoA) and resulting in histone lactylation, thus promoting M1→M2 macrophage repolarization (129). However, it is not known whether protein lactylation plays a role in direct M0→M2 in our studies investigating M0→M2 direct polarization. Analysis of isotope tracing data, we found very low relative abundance and no fractional enrichment of the M3 isotopologue of lactylated-substrates (Figure 18). This finding suggests that M2 polarization occurs independently of histone lactylation.
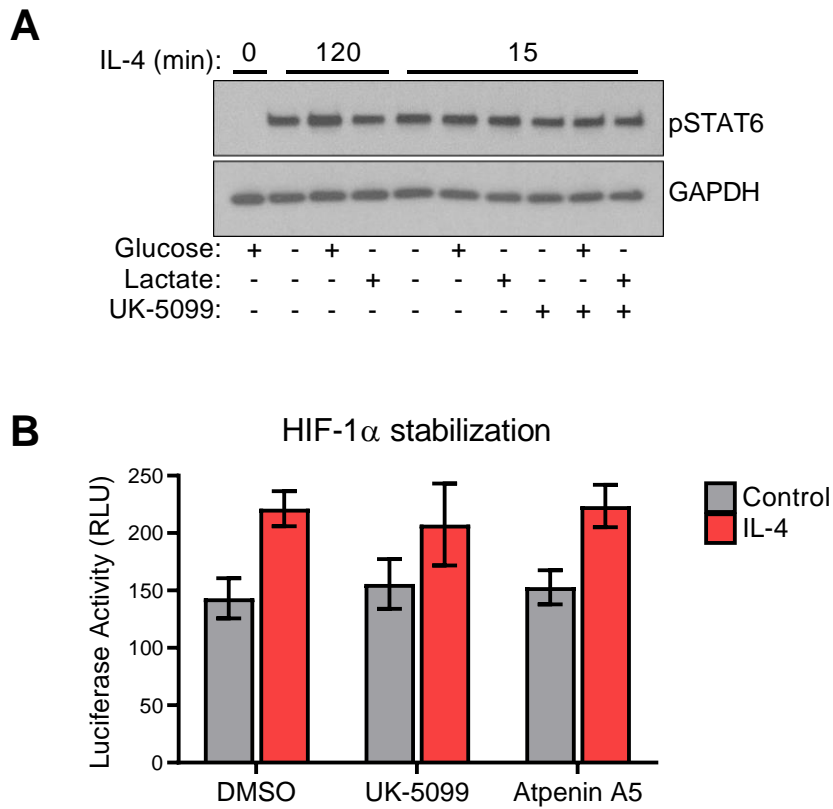
Figure 17: Mitochondrial lactate metabolism supports M2 macrophage polarization independent of STAT6 signaling and HIF-1α stabilization. (A) Immunoblotting analysis of phosphorylated STAT6 (pSTAT6) in BMDMs treated with IL-4 (as indicated) ± UK-5099 (25µM) in glucose-free media supplemented with glucose (10mM) or lactate (10mM). **(B)** Luciferase activity in ODD-Luc BMDMs treated with IL-4 (24hr) ± UK-5099 (25µM) or Atpenin A5 (25µM). Data are the mean ± SEM of two replicates. Immunoblot is representative of three replicates.

A

Protein Lactylation

B

Protein Lactylation
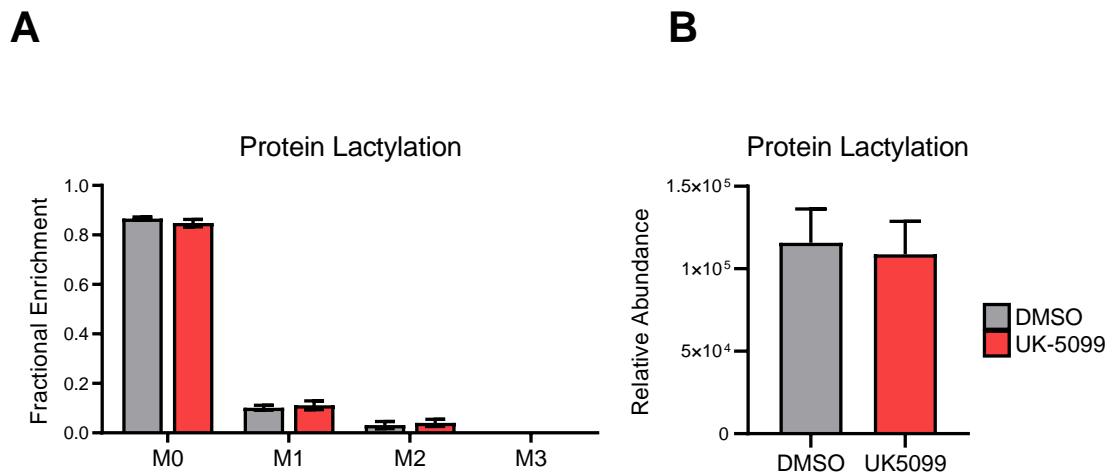
Figure 18: Mitochondrial lactate metabolism does not affect protein lactylation during M2 macrophage polarization: (A) Fractional enrichment and **(B)** relative abundance of protein lactylation in BMDMs treated with IL-4 (6hr) ± UK-5099 (25µM) in glucose-free media supplemented with ^{13}C-lactate (10mM). Data are the mean ± SEM of three replicates.

Finally, α-ketoglutarate serves as a substrate for histone demethylation-dependent M0→M2 macrophage polarization (128), and pyruvate catabolism can sustain the production of α-ketoglutarate through two distinct metabolic pathways – indirectly through the TCA cycle itself and directly through alanine transaminase, which converts glutamate and pyruvate into α-ketoglutarate and alanine. Analysis of the ^{13}C-lactate tracer studies revealed no noticeable changes in the relative abundance or fractional enrichment of α-ketoglutarate or alanine (Figure 19). These findings suggest that lactate-mediated M0→M2 macrophage polarization occurs independently of these previously identified pathways/mechanisms.

ATP-citrate lyase supports M0→M2 macrophage polarization and histone acetylation

Citrate can undergo mitochondrial export and subsequent cleavage by ATP-citrate lyase (ACLY) to form Ac-CoA substrates for histone acetylation (122,130). Analysis of our isotope tracing studies indicated that 20.32% and 20.52% of lactate-derived citrate isotopologues from the first TCA cycle round (M+2 citrate) and subsequent TCA cycling (M+3 – M+6 citrate), respectively, are not incorporated into α-ketoglutarate (Figure 20A), suggesting TCA cycle efflux. Consistent with a role for mitochondrial pyruvate-dependent histone acetylation, glucose and lactate independently increase total H3 (Figure 20B), lysine-residue specific H3 (Figure 20C), and M2 gene promoter-specific (Figure 20D) histone acetylation. These findings suggest that mitochondrial lactate metabolism can sustain the Ac-CoA levels that are needed for histone acetylation during M2 macrophage polarization.
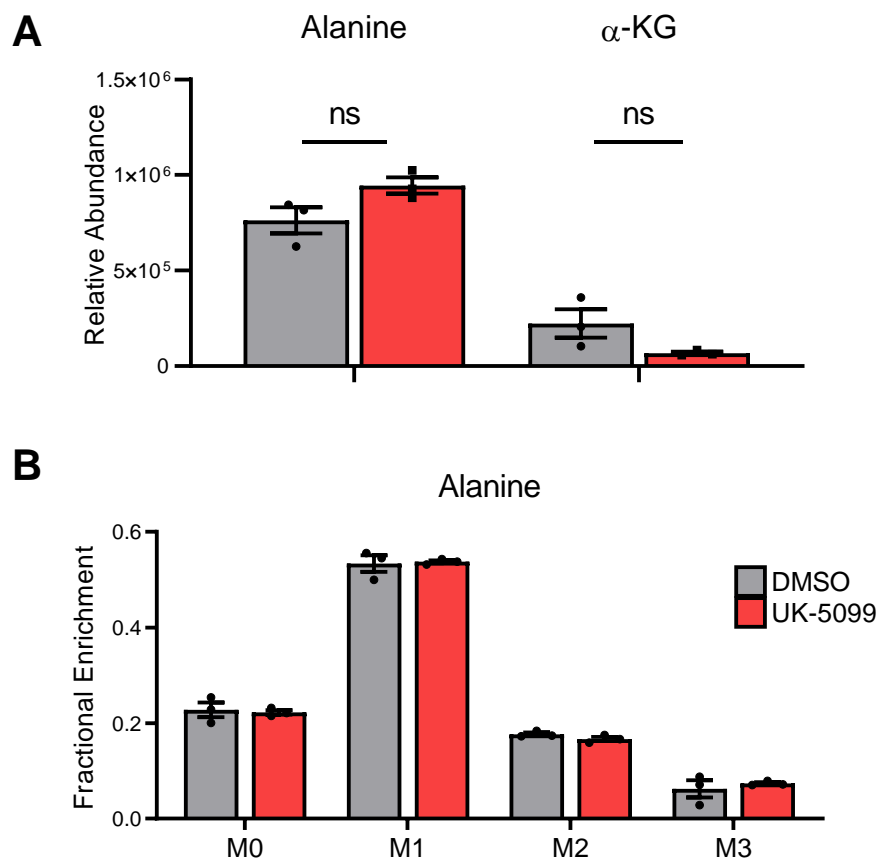
Figure 19: Mitochondrial lactate metabolism supports M2 macrophage polarization independent of α-ketoglutarate and alanine levels. (A) Relative abundance and **(B)** fractional enrichment of alpha-ketoglutarate (αKG) and alanine in BMDMs treated with IL-4 (6hr) ± UK-5099 (25μM) in glucose-free media supplemented with ^{13}C-lactate (10mM). Data are the mean ± SEM of three replicates.
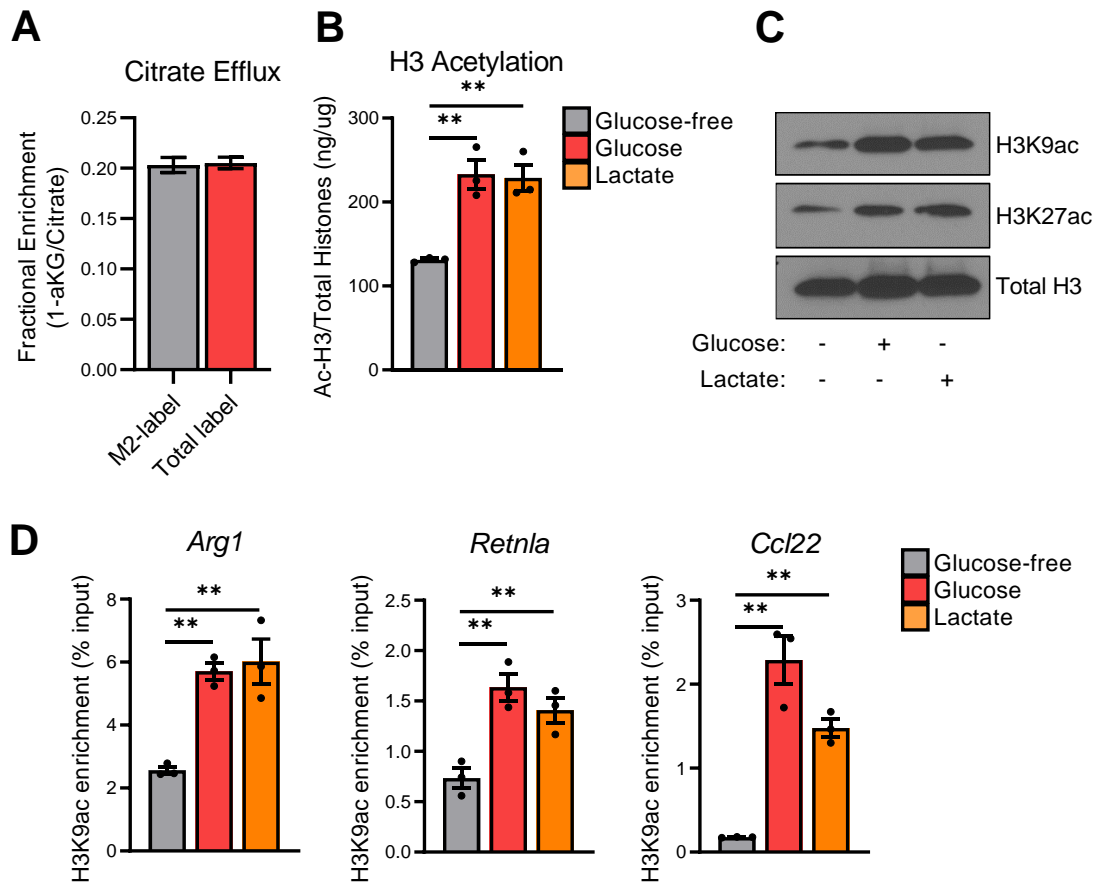
Figure 20: Histone acetylation during M2 polarization is maintained in low glucose/high lactate tumor microenvironment-like conditions. (A) Metabolic efflux of lactate-derived carbons, via citrate, out of the TCA cycle in BMDMs treated with IL-4 (6hr) ± UK-5099 (25μM) in glucose-free media supplemented with ^{13}C-lactate (10mM). **(B)** Total acetylated histone H3 ELISA, **(C)** lysine residue-specific acetylation immunoblot, and **(D)** H3K9ac chromatin-immunoprecipitation (ChIP) in BMDMs treated with IL-4 (6hr) in glucose-free media supplemented with glucose (5mM) or lactate (10mM). Data are the mean ± SEM of three replicates. *p≤0.05, **p≤0.01, ***p≤0.001 by one-way ANOVA with Tukey's post-test.

Nucleo-cytoplasmic Ac-CoA is produced by the ACLY-dependent cleavage of mitochondrial-derived citrate or by an alternative, mitochondrial-independent pathway via Ac-CoA synthetase short-chain family member 2 (ACSS2)-dependent activation of acetate. Interestingly, exogenous acetate rescues the loss of M2 macrophage-associated gene product expression (Figure 21), global lysine-residue-specific histone acetylation (Figure 22), and M2 gene promoter-specific histone acetylation (Figure 22) when mitochondrial lactate metabolism is inhibited by UK-5099. Conversely, small-molecule inhibition of ACSS2 reduces the expression of M2-specific gene products in BMDMs polarized with exogenous acetate but not lactate (Figure 23). These findings indicate a requirement for Ac-CoA in M2 macrophage histone acetylation/gene expression and suggest a role for ACLY in lactate-dependent M2 polarization.

ATP-citrate lyase is necessary for M2-associated gene expression, immune-suppressive activity, and M2 TAM-dependent tumor progression

To validate a requirement for ACLY in M0→M2 macrophage polarization, we used a small molecule inhibitor of ACLY, BMS-303141, and asked whether it can inhibit lactate-dependent M2 macrophage Arg1 expression. Unexpectedly, while BMS-303141 attenuated IL-4/lactate-induced Arg1 expression, exogenous acetate was not able to reverse this inhibition is in contrast to the effect with UK-5099 (Figure 24). However, prior investigations have identified that ACLY inhibitors may have off-target effects (143), and this was further validated through discussions with Dr. Kathryn Wellen, who discovered ACLY-dependent histone acetylation (130).
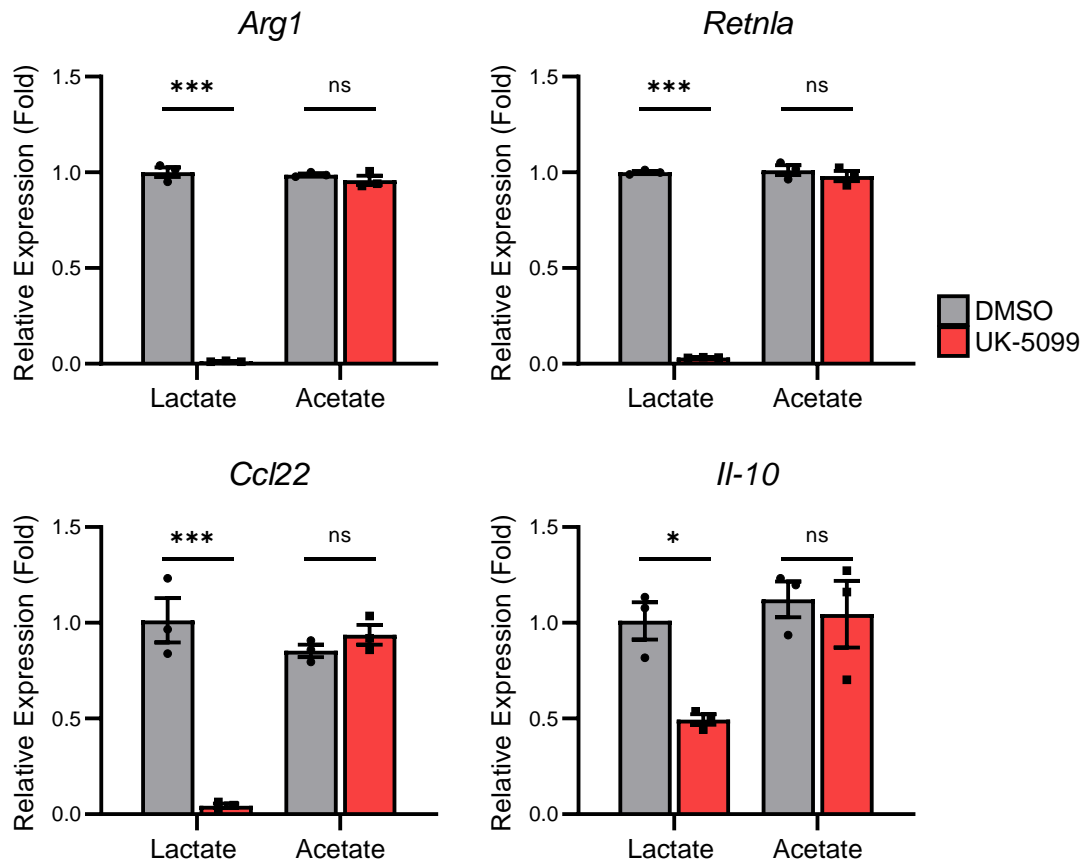
Figure 21: Exogenous acetate rescues the loss of lactate-enhanced M2 macrophage polarization following MPC1 inhibition. qPCR analysis of M2 macrophage-associated gene product expression in BMDMs treated with IL-4 (48hr) ± UK-5099 (25µM) in glucose-free media supplemented with lactate (10mM) or acetate (10mM). Data are the mean ± SEM of three replicates. *p≤0.05, **p≤0.01, ***p≤0.001 by two-way ANOVA with Tukey's post-test.
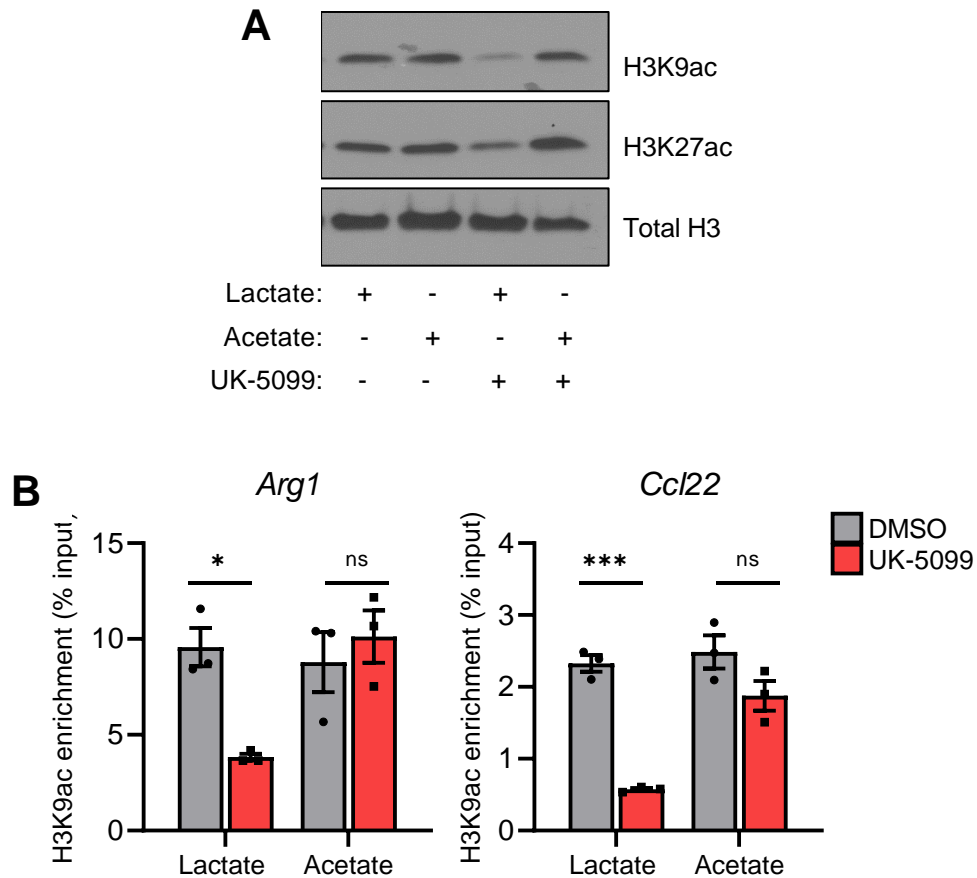
Figure 22: Exogenous acetate maintains histone acetylation during M2 macrophage polarization following MPC1 inhibition. (A) Immunoblot of lysine residue-specific acetylation and **(B)** H3K9ac ChIP in BMDMs treated with IL-4 (6hr) ± UK-5099 (25µM) in glucose-free media supplemented with lactate (10mM) or acetate (10mM). Data are the mean ± SEM of three replicates. *p≤0.05, **p≤0.01, ***p≤0.001 by two-way ANOVA with Tukey's post-test. Immunoblot is representative of three replicates.
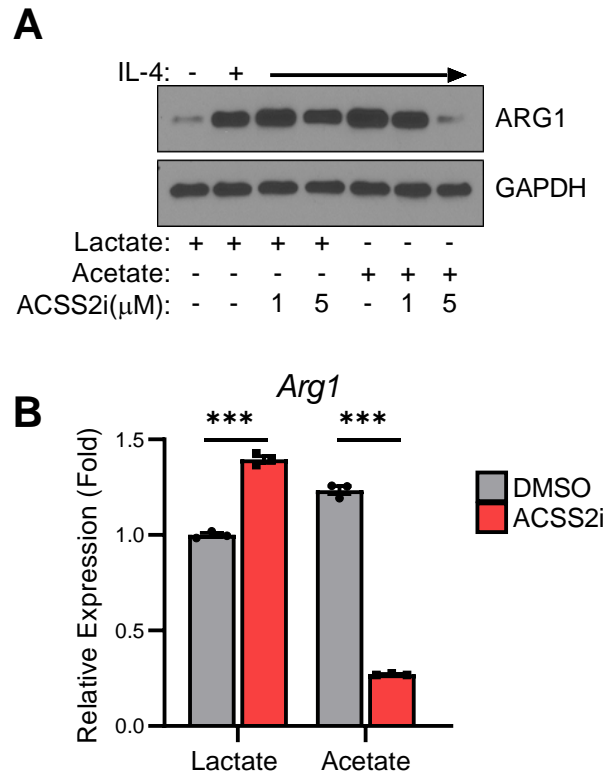
Figure 23: ACSS2 is required for acetate- but not lactate-enhanced M2 macrophage polarization. (A) Immunoblot and **(B)** qPCR analysis of *Arg1* expression in BMDMs treated with IL-4 (48hr) ± ACSS2i (as indicated) in glucose-free media supplemented with lactate (10mM) or acetate (10mM). Data are the mean ± SEM of three replicates. *p≤0.05, **p≤0.01, ***p≤0.001 by two-way ANOVA with Tukey's post-test. Immunoblot is representative of three replicates.

IL-4: - + ⟶

ARG1

GAPDH

Glucose: + - + - - - - - -
Lactate: - - - + + + - - -
Acetate: - - - - - - + + +
UK-5099: - - - - + - - + -
BMS-303141: - - - - - + - - +

Figure 24: Acetate does not rescue the loss of M2 polarization following pharmacological ACLY inhibition. Immunoblot of *Arg1* expression in BMDMs treated with IL-4 (48hhr) ± UK-5099 (25µM) or BMS-303141 (20µM) in glucose-free media supplemented with glucose (5mM), lactate (10mM), or acetate (10mM). Immunoblot is representative of three replicates.

Given that potential off-target effects may explain why acetate could not rescue the loss of M2 macrophage polarization following pharmacological ACLY inhibitions, we next utilized an inducible *Acly*-knockout transgenic mouse model (UBC-Cre-ERT2 *Acly*$^{f/f}$ mice). As shown in Figure 25, ACLY-deficiency phenocopies UK-5099-mediated inhibition of mitochondrial pyruvate uptake on reducing M2-associated gene expression in macrophages polarized in lactate but did not affect acetate-dependent polarization. Additionally, ACLY-deficiency reduces lysine-residue-specific histone acetylation, which can be rescued with the addition of exogenous acetate (Figure 26). Notably, ACLY-deficient BMDMs maintained high viability and expression of the macrophage terminal differentiation marker F4/80 (Figure 27), suggesting that loss of M2 polarization following ACLY depletion is not due to these factors.

Given that the defining effector function hallmark of M2 macrophages is their ability to suppress anti-tumor immunity leading to enhanced tumor growth, we utilized an *in vivo* tumor admixture murine model to investigate a requirement for ACLY in M2 macrophage-mediated tumor progression (225). Lewis Lung Carcinoma (LLC) cells were co-injected with *Acly*$^{+/+}$ or *Acly*$^{-/-}$ M2 polarized BMDMs (CD45.2^{+}) into congenic B6.SJL mice (CD45.1^{+}) (Figure 28). While tumors bearing *Acly*$^{+/+}$ M2 polarized BMDMs had increased tumor growth, end-point tumor weight, and gross tumor burden *vs.* LLC cells alone, tumors bearing *Acly*$^{-/-}$ M2 polarized BMDMs exhibited marked reductions in tumor outgrowth and end-point tumor burden compared to tumors bearing *Acly*$^{+/+}$ M2 BMDMs (Figure 29).
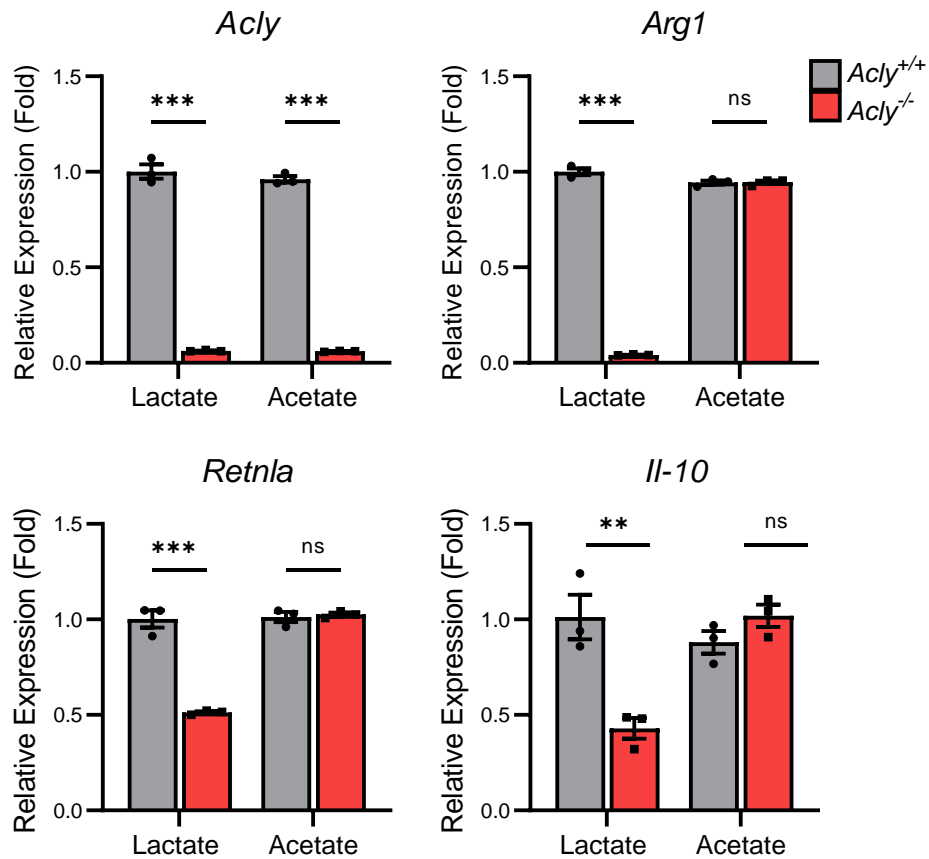
Figure 25: Exogenous acetate rescues the loss of lactate-enhanced M2 macrophage polarization from ACLY-deficiency. qPCR analysis of M2 macrophage-associated gene product expression in *Acly*^{+/+} and *Acly*^{-/-} BMDMs treated with IL-4 (48hr) in glucose-free media supplemented with lactate (10mM) or acetate (10mM). Data are the mean ± SEM of three replicates. *p≤0.05, **p≤0.01, ***p≤0.001 by two-way ANOVA with Tukey's post-test.
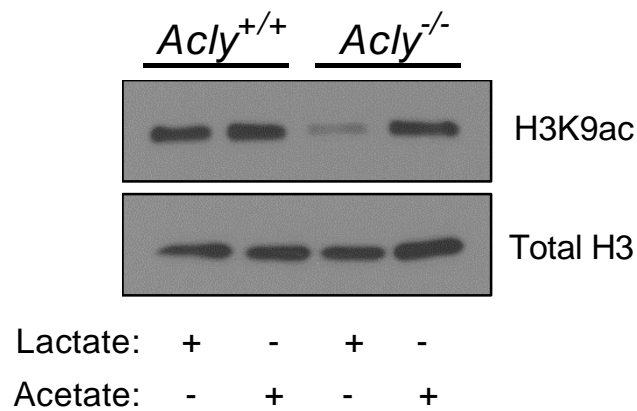
Figure 26: Exogenous acetate maintains histone acetylation ACLY-deficient macrophages during M2 polarization. Immunoblot of lysine residue-specific acetylation in *Acly*$^{+/+}$ and *Acly*$^{-/-}$ BMDMs treated with IL-4 (6hr) in glucose-free media supplemented with lactate (10mM) or acetate (10mM). Immunoblot is representative of three replicates.
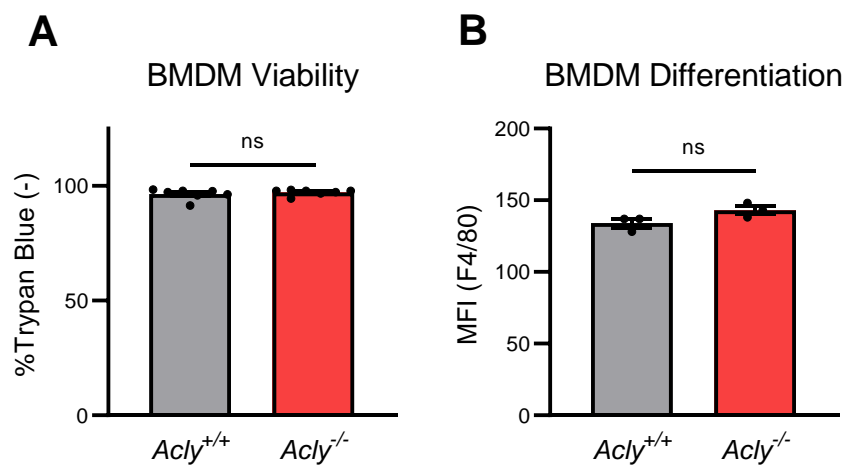
Figure 27: BMDM differentiation is intact in ACLY-deficient macrophages. (A) Viability and **(B)** differentiation in *Acly*^{+/+} and *Acly*^{-/-} BMDMs treated with M-CSF (7d) in complete RPMI medium. Data are the mean ± SEM of **(A)** seven and **(B)** three replicates. *p≤0.05, **p≤0.01, ***p≤0.001 by students t-test.
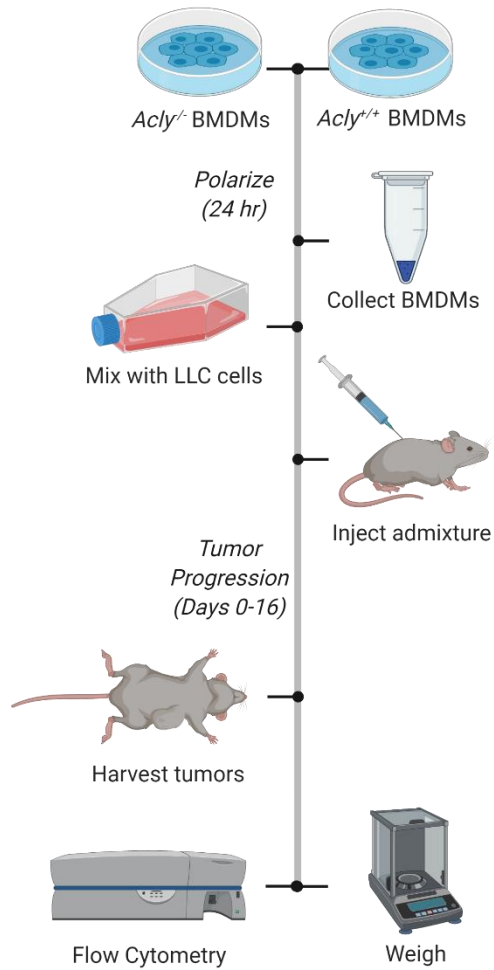
Figure 28: Schematic of experimental workflow for the *in vivo* ACLY tumor-admixture model. *Acly⁺/⁺* and *Acly⁻/⁻* BMDMs are polarized with IL-4 for 24 hours before being mixed with LLC cells (ratio 1:2.5) and injected s.c. into congenic B6.SJL mice. Tumor volume is measure over 16 days with digital calipers, and mice are euthanized at the experimental endpoint. The resultant tumors are surgically resected, weighed, and digested into single-cell suspensions for flow cytometric analyses.
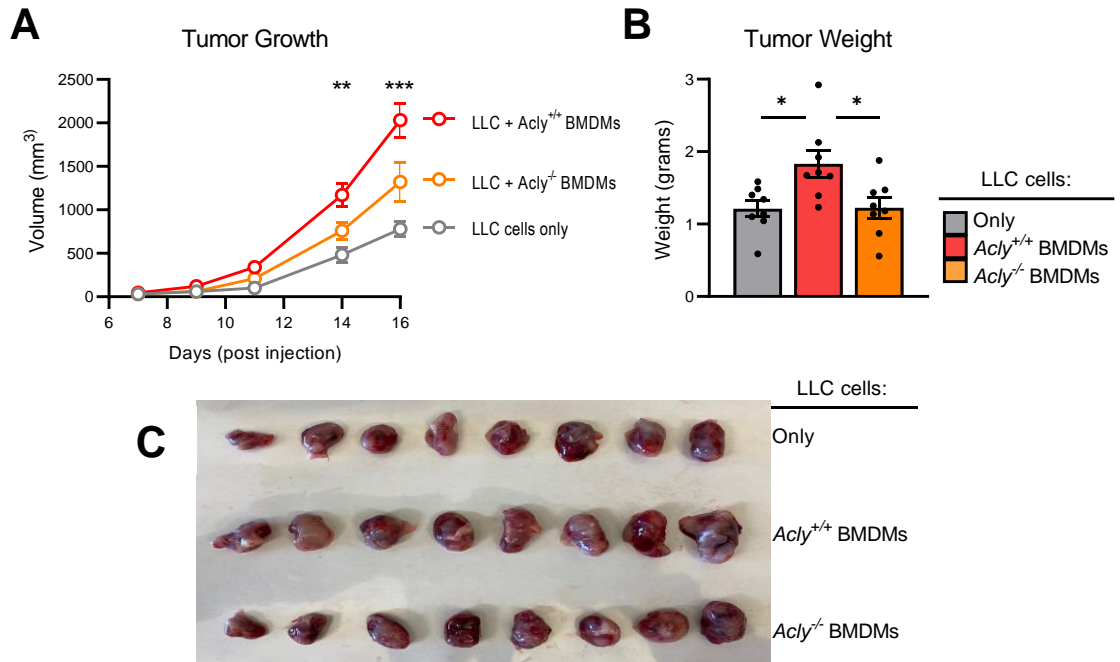
Figure 29: ACLY is required for maximal macrophage-mediated tumor progression. (A) Growth **(B)** weight, **(C)** gross dissections of tumors consisting of LLC cells only, LLC cells + M2 polarized $Acly^{+/+}$ BMDMs, or LLC cells + M2 polarized $Acly^{-/-}$ BMDMs. Data are the mean ± SEM of eight replicates. *$p \leq 0.05$, **$p \leq 0.01$, ***$p \leq 0.001$ by two-way ANOVA with Tukey's post-test.
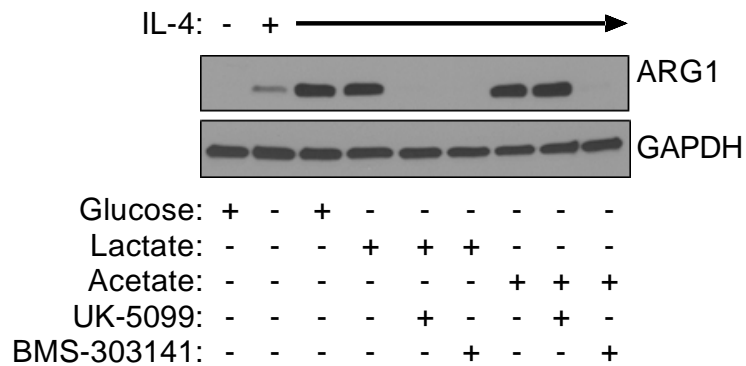
Flow cytometric analyses of intratumoral immune cells revealed a lack of residual $Acly^{+/+}$ or $Acly^{-/-}$ CD45.2$^+$ TAMs (Figure 30), suggesting nearly complete loss of initiator TAMs at the time of our end-point analysis. No discernable differences were found between percentages of infiltrating CD4$^+$ T cells, CD8$^+$ T cells, or CD4$^+$/CD8$^+$ T cell ratio (Figure 31), suggesting that macrophage-derived ACLY did not affect total intratumoral T cell infiltration *per se* in this model. However, tumors from LLC/$Acly^{-/-}$ macrophage co-injection had significantly fewer IFN-γ-expressing CD8$^+$ T cells and CD4$^+$ helper T cells compared to LLC/$Acly^{+/+}$ macrophage co-injection tumors (Figure 32). These findings suggest that intratumoral, M2 macrophage-derived ACLY is necessary for maximal TAM immunosuppressive activity and that loss of ACLY allows for a more robust anti-tumor immune response resulting, ultimately, in reduced tumor growth and progression.
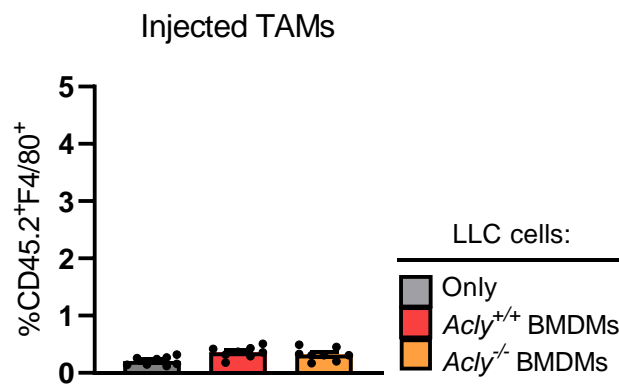
Figure 30: Injected TAMs are absent at tumor end-point. Percentage of CD45.2$^+$F4/80$^+$ cells at day 16 from tumors consisting of LLC cells only, LLC cells + M2 polarized *Acly+/+* BMDMs, or LLC cells + M2 polarized *Acly-/-* BMDMs. Data are the mean ± SEM of eight replicates. *p≤0.05, **p≤0.01, ***p≤0.001 by two-way ANOVA with Tukey's post-test.
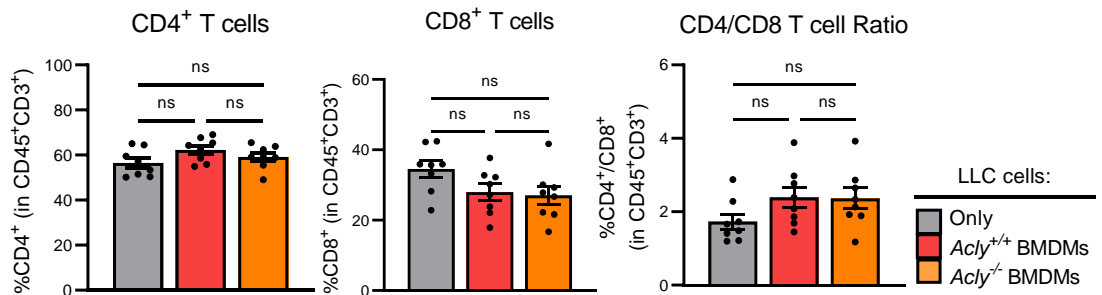
Figure 31: ACLY-deficient TAMs did not alter T cell accumulation in an *in vivo* tumor admixture model. Percentage of **(A)** CD4+ T cells, **(B)** CD8+ T cells, and **(C)** CD4+/CD8+ T cell ratio from tumors consisting of LLC cells only, LLC cells + M2 polarized *Acly+/+* BMDMs, or LLC cells + M2 polarized *Acly-/-* BMDMs. Data are the mean ± SEM of eight replicates. *p≤0.05, **p≤0.01, ***p≤0.001 by two-way ANOVA with Tukey's post-test.
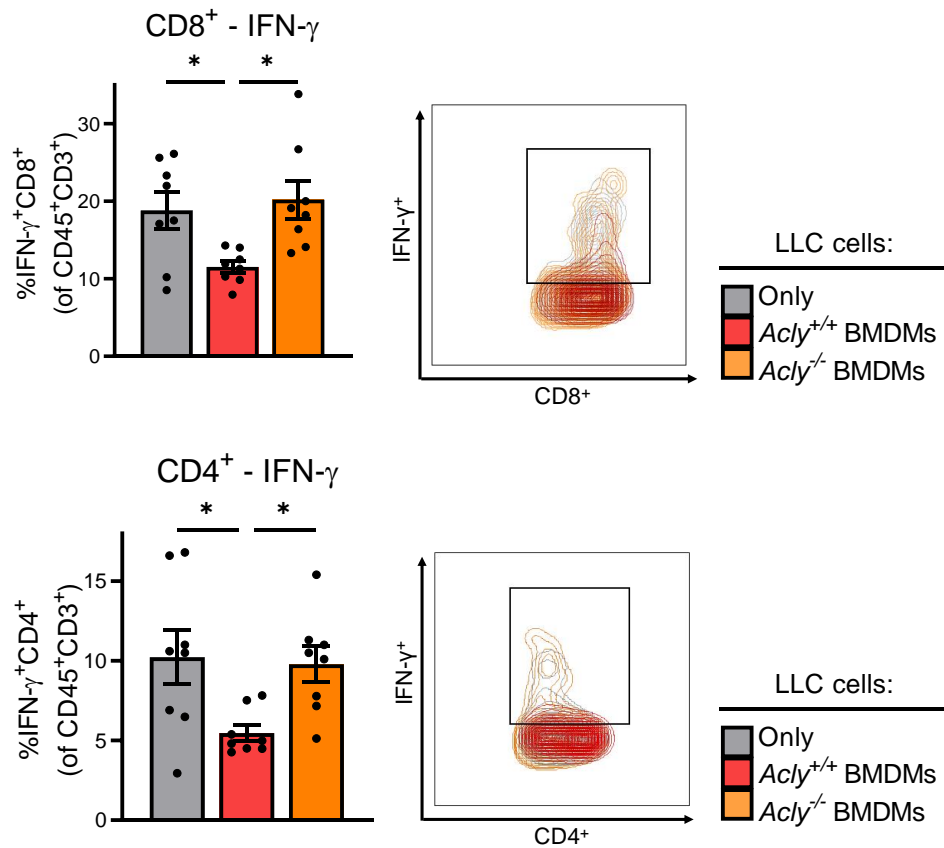
Figure 32: TAM-derived ACLY mediates the suppression of anti-tumor immune responses Percentage of **(A)** IFN-γ+CD8+ T cells and **(B)** IFN-γ+CD4+ T cells, with respective representative flow plots, from tumors consisting of LLC cells only, LLC cells + M2 polarized *Acly+/+* BMDMs, or LLC cells + M2 polarized *Acly-/-* BMDMs. Data are the mean ± SEM of eight replicates. *p≤0.05, **p≤0.01, ***p≤0.001 by two-way ANOVA with Tukey's post-test

Discussion

Solid TMEs represent a unique, physiologic paradigm of a high lactate/low glucose metabolic compartment in human pathology (147,151). Prior studies have shown that higher lactate concentrations in the TME drive both innate and adaptive immune responses (17,152), but whether, and if so how, lactate controls gene expression patterns and functional immune phenotypes is largely unknown.

Our studies reveal that M2 polarized macrophages utilize extracellular lactate to fuel mitochondrial TCA cycling and oxidative metabolism. Lactate fully compensates for low or absent glucose in driving M2 macrophage-associated gene expression patterns and immune suppressive activity. ^{13}C-lactate tracing metabolomics demonstrates that extracellular lactate is efficiently converted to pyruvate, imported into mitochondria, and further metabolized by the TCA cycle to citrate, of which ~20% is calculated to be effluxed out of the mitochondria. Our data further suggest that this lactate metabolism drives histone acetylation in a manner that requires Ac-CoA generation by ACLY, which is necessary for maximal M2 gene expression, immune-suppressive activity, and tumor progression.

Recently, a metabolic-epigenetic link was identified where M1 macrophages utilize glycolysis for *lactate anabolism* to generate lactyl-CoA for histone lactylation-dependent M1→M2 macrophage transition (129). Our findings, however, indicate that M0→M2 macrophage metabolic reprogramming preferentially allows for *lactate catabolism* – via mitochondrial pyruvate (155) – to generate Ac-CoA for use in histone acetylation-dependent gene expression. It's not unreasonable to speculate that, in early developing tumors where glucose

supplies are high and lactate is low, M1 macrophages with high glycolytic/low TCA activity (i.e., low citrate levels) can afford to utilize glycolysis-derived lactate as a source of epigenetic lactylation and initiation of M1→M2 transition. As these same tumors grow and expand (with concomitant reductions in glucose and increases in extracellular lactate), M2 macrophage metabolic reprogramming occurs, resulting in high TCA activity and, since glucose is scarce, these M2 macrophages begin to utilize lactate as a source of *both* oxidative fuel and, via citrate efflux, histone acetylation.

Although our studies did not find a direct link between lactate or glucose-dependent M2 polarization and HIF-1α stabilization, they do support the previously described requirement for HIF-1α in driving lactate-induced M2 polarization (17). In this scenario, we envision that lactate-dependent histone acetylation allows for maximally efficient HIF-1α-dependent transcription at a subset of HIF-1α-sensitive M2-associated acetylated gene promoters (17).

ACLY serves as a metabolic nexus to supply nucleo-cytosolic pools of Ac-CoA from mitochondrial citrate for lipid synthesis, prostaglandin production, and histone acetylation (122,131). We show that ACLY is necessary to support histone acetylation and subsequent maximal expression of M2 macrophage-associated gene products. In a recent study, Van den Bossche and colleagues utilized an independent, macrophage-specific, conditional *Acly* transgenic model to show that chronic loss of ACLY *in vivo* stabilized atherosclerotic plaques and suggested that ACLY contributes to fatty acid metabolism, efferocytosis, and M2 polarization phenotypes (142). In our current study, we utilized bone marrow-derived

macrophages from an inducible *Acly* knock-out transgenic model to assess acute ACLY deletion on direct M0→M2 polarization and to validate defective histone acetylation using exogenous acetate. Importantly, using *in vitro* M2 polarized *Acly*$^{+/+}$ and *Acly*$^{-/-}$ primary macrophages, we identified that in a more chronic model of macrophage ACLY deficiency, M2 macrophage-dependent tumor growth and progression were significantly impaired coincident with increased numbers of infiltrating IFN-γ$^+$CD8$^+$ and CD4$^+$ T lymphocytes.

Numerous ACLY inhibitory compounds are being developed as anti-cancer agents (229). Although the initial rationale for ACLY antagonists as anti-tumor agents was based on disrupting tumor cell fatty acid biosynthesis secondary to glucose addiction, it will be important in future translational studies to assess collateral effects on tumor-infiltrating immune effector cells and the relative disruption of transcriptional reprogramming, polarization/ differentiation phenotypes, and immune suppressive functions. Since infiltrating TAMs are a dominant source of anti-tumor T cell suppressive activity in late-stage malignant tumors, which can functionally skew immune checkpoint blockade (ICB) clinical efficacy (103), ACLY targeting may represent a unique immunotherapeutic approach to alleviate ICB resistance in the future.

CHAPTER 3: MIF-DEPENDENT REGULATION OF M2 MACROPHAGE POLARIZATION THROUGH MITOCHONDRIAL METABOLISM

Introduction

Macrophage migration inhibitory factor (MIF) is an atypical cytokine that is highly secreted in several tumor types (158-160), and elevated levels of MIF drive enhanced tumor progression that ultimately results in poorer patient outcomes (161-163). Although initially described as having pro-inflammatory roles in acute pathologies (179), MIF is increasingly being recognized as a critical regulator of immunosuppressive phenotypes in a variety of tumor-infiltrating immune cells in a malignant setting (230). MIF has pleiotropic roles in the suppression of anti-tumor immunity – in particular, several reports have identified that MIF promotes TAM/MDSC-mediated tumor progression (231,232).

Previously, Yaddanapudi and colleagues discovered that host-derived MIF mediates maximal *in vivo* polarization of TAMs to an immunosuppressive/anti-inflammatory M2 phenotype (156), although the underlying mechanistic mechanism(s) have not been fully elucidated. Additionally, small-molecule inhibition of MIF with 4-IPP functionally repolarizes TAMs from an immunosuppressive M2 phenotype to a pro-inflammatory, anti-tumor M1-TAM phenotype with a resultant enhancement of tumor immunity and subsequent delay in tumor outgrowth. Therefore, therapies that include MIF targeting, in combination with current immune-checkpoint inhibitors, represent an attractive clinical strategy to enhance the anti-tumor immune response in patients with cancer.

MIF's pleiotropic nature in regulating infiltrating immune cell effector functions is likely due to its multiple downstream molecular mechanisms (183). Extracellular MIF can exert autocrine or paracrine signaling by binding to a variety of different receptor complexes that include its cognate receptor, CD74 (188), along with non-cognate receptors such as CD44, CXCR2, CXCR4, and CXCR7, to activate several intracellular signaling cascades including the PI3K/AKT and MEK/ERK pathways (189,190,233). In contrast, intracellular MIF – either endogenously derived or accumulated following extracellular uptake – binds to COPS signalosome subunit 5 (CSN5) to regulate the deneddylation of cullin RING ligases (CRLs) (196). CRLs mediate the ubiquitination of several proteinaceous substrates (194), which is necessary for the targeting of these proteins for proteasomal-dependent degradation. Interestingly, while several of the MIF-dependent receptor- and CSN5-mediated downstream effects have been identified to regulate specific immune cell phenotypes (203,204,234), the relative contribution(s) of extracellular or intracellular MIF in regulating M2-TAM polarization remain unelucidated.

A critical determinant of M2 macrophage polarization is the ability to undergo metabolic reprogramming towards enhanced tricarboxylic acid (TCA) cycle activity and mitochondrial oxidative phosphorylation (107,109,114,235). Previous investigations have identified that this metabolic reprogramming not only to fulfills necessary bioenergetic requirements but also that specific TCA cycle metabolites functionally regulate transcriptional mechanisms needed for the expression of M2-associated gene products (127). In particular, enhanced TCA

cycling supports the generation of alpha-ketoglutarate (αKG) to maintain a high αKG/succinate level that is needed for αKG-dependent demethylation of trimethylated lysine 27 residues on histone H3 (H3K27me3) via jumonji C demethylase (JMJD3) (128,215). In contrast, mitochondrial dysfunction causes defective activity of electron transport chain (ETC) complexes (212), such as succinate dehydrogenase (SDH), that results in the accumulation of succinate – a pro-inflammatory TCA cycle metabolite (28). Interestingly, recent studies in non-immune cells have found that MIF regulates mitochondrial dynamics to maintain functional ETC activity (208), which suggests that macrophage-derived MIF may support maximal M2 macrophage polarization by sustaining the mitochondrial metabolism needed to maintain the correct relative balance of TCA cycle metabolites.

MIF's intracellular binding partner CSN5 has been implicated in controlling mitochondrial metabolism in macrophages by regulating the stabilization of nuclear factor erythroid 2-related factor (NRF2) (217,236). NRF2 is a critical regulator of mitochondrial metabolism by affecting mitochondrial membrane potential, ETC activity, and mitochondrial biogenesis (216). Under basal conditions, NRF2 is actively targeted for proteasomal degradation via the Cullin 3-containing CRL complex (219). Although whether MIF can regulate NRF2 stabilization through CSN5 in macrophages has not been determined, these findings suggest that a MIF/CSN5/NRF2 pathway may serve as an intermediary mechanistic link between macrophage-derived MIF and M2-TAM polarization through mitochondrial metabolism.

Using a combination gene expression assay, steady-state metabolomics, and chromatin immunoprecipitation, we report that MIF is a critical regulator for metabolic reprogramming during M0→M2 macrophage polarization by supporting mitochondrial metabolism for αKG-dependent H3K27me3 demethylation via the MIF/CSN5/NRF2 pathway. This study identifies a critical metabolic-epigenetic link by which MIF contributes to M2-TAM polarization and immunosuppressive capacity and provides a further rationale that pharmacological MIF targeting may be a clinically effective therapeutic strategy to enhance anti-tumor immunity.

Materials and Methods

Mice: Wild-type C57BL/6 mice were obtained from Harlan Laboratories (Dublin, VA). MIF$^{-/-}$ C57BL/6 mice were maintained by the Mitchell Laboratory. Animals were maintained under specific pathogen-free conditions and handled in accordance with the Association for Assessment and Accreditation of Laboratory Animals Care international guidelines. The Institutional Animal Care and Use Committee (IACUC) at the University of Louisville approved experiments. 6-16-week-old mice were used in all experiments.

Cell culture and BMDM differentiation: Mice were euthanized by CO_2 asphyxiation, and death was confirmed by cervical dislocation. Bone marrow cells from the tibias and femurs were differentiated in RPMI-1640 supplemented with FBS (5%) and recombinant murine M-CSF (25 ng/mL: Peprotech) for seven days. Following differentiation, the cells were counted and plated with RPMI-1640 supplemented with 10% FBS (without M-CSF) overnight. The following day the BMDMs were washed with PBS and starved of glucose by addition of glucose-free RPMI-1640 supplemented with 10% dialyzed FBS and 2mM L-glutamine for 4-6 hours before treatment with the indicated compounds and stimulated with recombinant murine IL-4 (20 ng/ml: Peprotech) for 4-48 hours.

RNA purification and RT-qPCR: Total RNA was extracted using RNeasy Mini Kit (QIAGEN) following the manufacturer's instructions. The resulting RNA was quantified using a Nanodrop 8000 UV-visible spectrophotometer (Thermo Scientific), and the cDNA was synthesized with a High-Capacity cDNA Reverse

Transcription Kit (Applied Biosystems). Quantitative measurement of cDNA levels was performed using TaqMan Fast Advanced Master Mix (Applied Biosystems) with TaqMan Gene Expression Primers (Applied Biosystems) on a 7500 Fast Real-Time PCR System (Applied Biosystems). Relative expression profiles of mRNA levels were calculated using the comparative Ct method ($2^{-(\Delta\Delta Ct)}$) using 18s rRNA levels as an endogenous reference control.

Immunoblotting: Cells were lysed in RIPA buffer supplemented with protease and phosphatase inhibitors, homogenized, and samples were denatured in LB sample buffer at 98°C. 5-20 µg of protein was loaded into a 4-20% Mini-PROTEAN TGX Gel (Bio-Rad Laboratories) and separated by electrophoresis before being transferred onto Immobilon-P PVDF membrane (EMD Millipore). After blocking, membranes were probed overnight at 4°C with primary Abs and then for 1 hour at room temperature with secondary Abs. The blots were developed using Pierce ECL Plus Western Blotting Substrate (Thermo Scientific).

Extracellular Flux Analysis: For extracellular flux assays of MIF-deficiency, $MIF^{+/+}$ and $MIF^{-/-}$ BMDMs were plated in Seahorse XF96 cell culture microplates (Seahorse Biosciences, Agilent) overnight followed by polarization with IL-4 for 16 hours. For extracellular flux assays of pharmacological MIF inhibition, $MIF^{+/+}$ BMDMs were plated in Seahorse XF96 cell culture microplates (Seahorse Biosciences, Agilent) overnight followed by treatment with or without 4-IPP (25µM) for thirty minutes and then polarization with IL-4 for 16 hours The oxygen consumption rate (OCR) and extracellular acidification rate (ECAR) was measured using an XF96 Extracellular Flux Analyzer (Seahorse Bioscience, Billerica, MA,

USA) according to manufacturer's instructions. During the assay, wells were injected with oligomycin (5 µM), FCCP (2 µM), and rotenone (1 µM)/antimycin A (5 µM). Each condition was performed in 4-6 replicates, and data was analyzed using Seahorse Wave 2.6 Desktop Software (Agilent).

Chromatin immunoprecipitation (ChIP): ChIP was performed using the SimpleChip Enzymatic Chromatin IP Kit (Cell Signaling Technology; CST) according to the manufacturer's instructions. Briefly, 1.2×10^7 BMDMs were fixed with 1% formaldehyde, lysed, and then the nuclei were isolated. The chromatin was digested with Micrococcal Nuclease and then sonicated to lyse the nuclear membrane. The cross-linked chromatin was immunoprecipitated with anti-H3K9ac antibody (CST – C5B11) overnight at 4° C. The chromatin was recovered with Protein G Agarose Beads, eluted, and the cross-links were reversed with Elution Buffer and Proteinase K overnight at 65° C. Input and Immunoprecipitated DNA was analyzed by Real-Time qPCR and the data are presented as percent of the total input chromatin.

Statistical Analysis: All results representative data presented as the mean ± SEM and analyzed for statistical significance using GraphPad Prism 8.3 (GraphPad Software. La Jolla, California, USA). Analysis with one-way or two-way ANOVA was utilized when the data presented had one or more independent variables, respectively. Tukey's post-test was utilized for multiple comparisons.

Results

MIF supports metabolic reprogramming during M0→M2 macrophage polarization

MIF can regulate glucose metabolism (208,237) to support pyruvate production, and we previously found that mitochondrial pyruvate metabolism is a critical determinant of M2 macrophage polarization (Chapter 2). To investigate whether MIF is necessary for mitochondrial pyruvate-mediated M2 polarization, we treated primary MIF$^{+/+}$ and MIF$^{-/-}$ bone marrow-derived macrophages (BMDMs) with the Th2 cytokine IL-4 in glucose-free RPMI supplemented with either glucose, pyruvate, or lactate. As shown in Figure 33, molar equivalent addition of exogenous glucose, pyruvate, or lactate is sufficient to restore expression of the canonical M2 macrophage associated gene product Arginase 1 (ARG1) in MIF$^{+/+}$ BMDMs polarized in glucose-free media. In contrast, these metabolites did not restore the loss of IL-4-induced ARG1 expression in MIF-deficient BMDMs (Figure 33), which suggests that the defect in M2 polarization following MIF deficiency is not due to decreased pyruvate production (i.e., glycolysis) and is instead downstream of pyruvate metabolism.

Following production, MPC1-mediated mitochondrial pyruvate import fuels TCA cycling and mitochondrial metabolism (119,120) for enhanced mitochondrial oxygen consumption rates (OCR) needed to support maximal M2 polarization (107,109). Therefore, we next utilized extracellular flux analysis and asked whether loss or inhibition of MIF affects mitochondrial OCR in BMDMs.

84
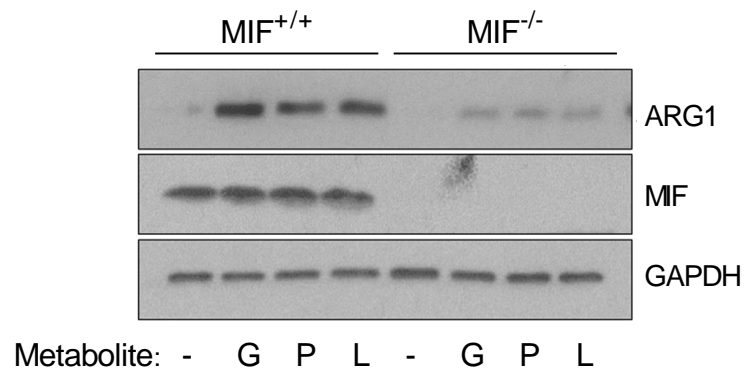
Figure 33: MIF-deficiency impairs M2 polarization downstream of cytosolic pyruvate production. Immunoblot of ARG1 expression in MIF$^{+/+}$ and MIF$^{-/-}$ BMDMs treated with IL-4 (24hr) in glucose-free media supplemented with or without glucose (G, 5mM), pyruvate (P, 10mM), or Lactate (L, 10mM). Immunoblot is representative of three replicates.

Remarkably, while IL-4 increases basal and maximal OCR, as previously reported (109), in MIF$^{+/+}$ BMDMs, MIF-deficiency decreases *both* steady-state and IL-4-induced mitochondrial OCR in BMDMs (Figure 34A). Importantly, small molecule pharmacological inhibition of MIF with 4-IPP entirely recapitulates the defect in mitochondrial OCR following MIF deficiency (Figure 34B). Given the defect in OCR in MIF-deficient BMDMS, *even at steady-state*, these findings indicate the MIF is an underlying requirement for metabolic reprogramming during naïve M0→M2 macrophage polarization and that acute MIF inhibition is capable of impairing mitochondrial metabolism in MIF-sufficient BMDMs.

Given our previous findings that mitochondrial pyruvate metabolism is mechanistically linked to histone acetylation-mediated M2 polarization (Chapter 2), we next hypothesized that MIF-dependent mitochondrial metabolism supports M2 polarization through TCA cycle-derived Ac-CoA production. Unexpectedly, in contrast with UK-5099-dependent inhibition of mitochondrial pyruvate uptake, loss of M2 polarization following acute MIF inhibition with 4-IPP was not able to be rescued with the addition of exogenous acetate (Figure 35). This indicates that MIF-dependent mitochondrial metabolism supports M2 polarization independent of histone acetylation and instead through a different mechanism.

To further determine if loss of M2 macrophage polarization following MIF deficiency or inhibition was attributed to impaired mitochondrial metabolism, we next examined the effect of specific mitochondrial ETC Complex II (i.e., SDH) inhibition on the expression of M2 macrophage-associated gene products with comparison to MIF-deficiency (228).
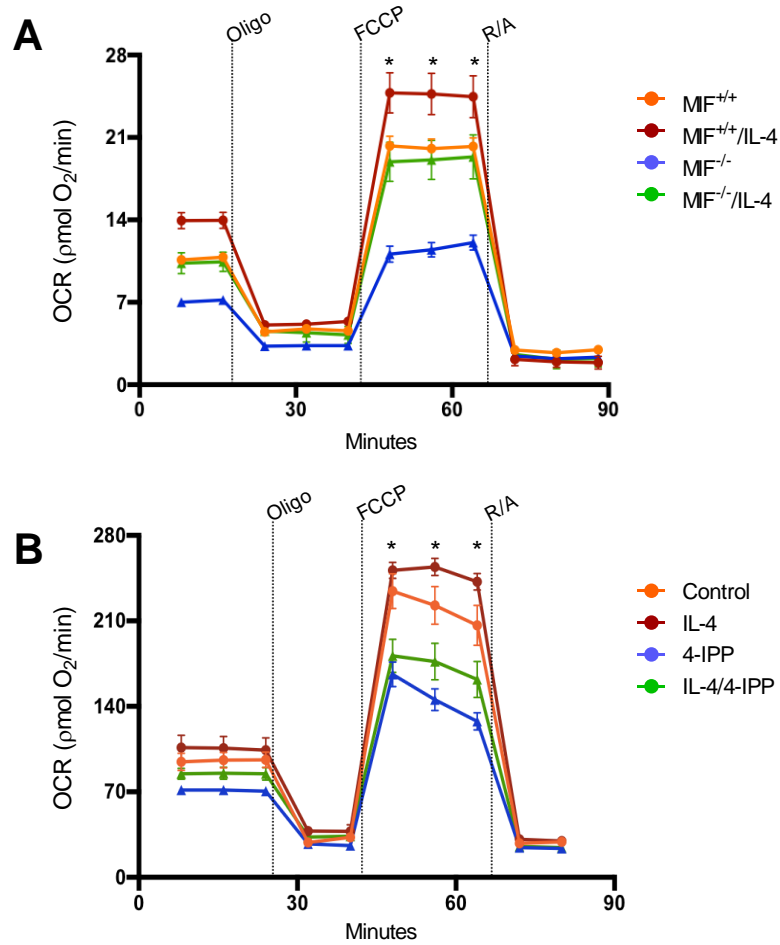
Figure 34: Deficiency and pharmacological inhibition of MIF impair metabolic reprogramming during M2 polarization. (A) Oxygen consumption rates (OCR) trace in MIF$^{+/+}$ and MIF$^{-/-}$ BMDMs treated with or without IL-4 (24hr) and **(B)** MIF$^{+/+}$ BMDMs treated with or without IL-4 (24hr) ± 4-IPP (25μM) before extracellular flux analysis with oligomycin (oligo), FCCP, and rotenone plus antimycin A (R/A). Data are the mean ± SEM of three replicates. *p≤0.05 by two-way ANOVA with Tukey's post-test.

	DMSO			UK-5099			4-IPP		
Glucose:	+	-	-	+	-	-	+	-	-
Lactate:	-	+	-	-	+	-	-	+	-
Acetate:	-	-	+	-	-	+	-	-	+
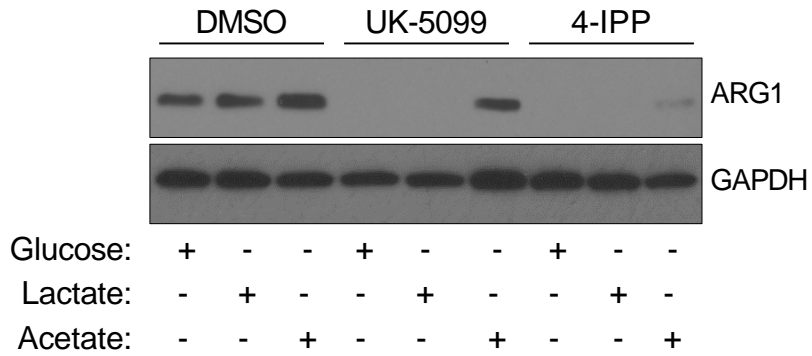
Figure 35: MIF-deficiency impairs M2 polarization independent of mitochondrial pyruvate metabolism-dependent histone acetylation. Immunoblot of ARG1 expression in BMDMs treated with IL-4 (24hr) ± UK-5099 (25µM) or 4-IPP (25µM) in glucose-free media supplemented with glucose (5mM), lactate (10mM), or acetate (10mM). Immunoblot is representative of three replicates.

As seen in Figure 36, inhibition of SDH with Atpenin A5 pre-treatment in MIF$^{+/+}$ BMDMs decreases *Arg1* expression in a dose-dependent manner to levels that are comparable to those found with MIF-deficiency. Although Atpenin A5 treatment also reduces *Arg1* expression in MIF$^{-/-}$ BMDMs – likely due to residual mitochondrial metabolism in MIF-deficient M2 macrophages as seen in Figure 34A – the decrease in *Arg1* expression in Atpenin A5-treated, M2-polarized MIF$^{+/+}$ BMDMs is comparable to the levels found in untreated M2-polarized MIF$^{-/-}$ BMDMs (Figure 36). These findings indicate that ETC Complex II (SDH) inhibition phenocopies MIF-deficiency and further suggests that MIF supports M2 macrophage polarization by sustaining mitochondrial metabolism.

SDH oxidizes succinate, thus decreasing intracellular succinate levels (228) that would otherwise inhibit αKG-dependent enzymes through competitive feedback inhibition (213). A previous study identified that enhanced αKG levels are required to support an elevated αKG/succinate ratio for the maximal enzymatic activity of JMJD3-mediated H3K27me3 demethylation (128). Therefore, we next utilized steady-state metabolomics to determine whether MIF-deficiency alters the relative αKG/succinate ratio during M2 macrophage polarization. Interestingly, while our findings identified that MIF-deficiency did not change αKG levels *per se,* there was a dramatic increase in succinate levels with a resulting decrease in the relative αKG/succinate levels (Figure 37), which is consistent with impaired histone demethylation-dependent M2 macrophage polarization (128). These findings suggest that MIF sustains mitochondrial metabolism to prevent the accumulation of succinate that would otherwise impair M2 macrophage polarization.
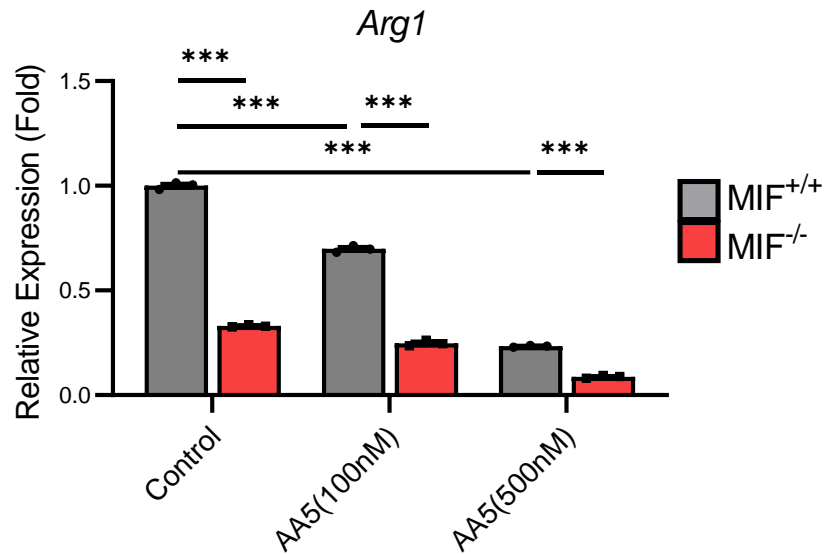
Figure 36: Inhibition of Succinate Dehydrogenase phenocopies MIF-deficiency during M2 macrophage polarization. qPCR analysis of *Arg1* expression in MIF$^{+/+}$ and MIF$^{-/-}$ BMDMs treated with IL-4 (24hr) ± Atpenin A5 (AA5) at the indicated concentrations. Data are the mean ± SEM of three replicates. *p≤0.05, **p≤0.01, ***p≤0.001 by two-way ANOVA with Tukey's post-test.
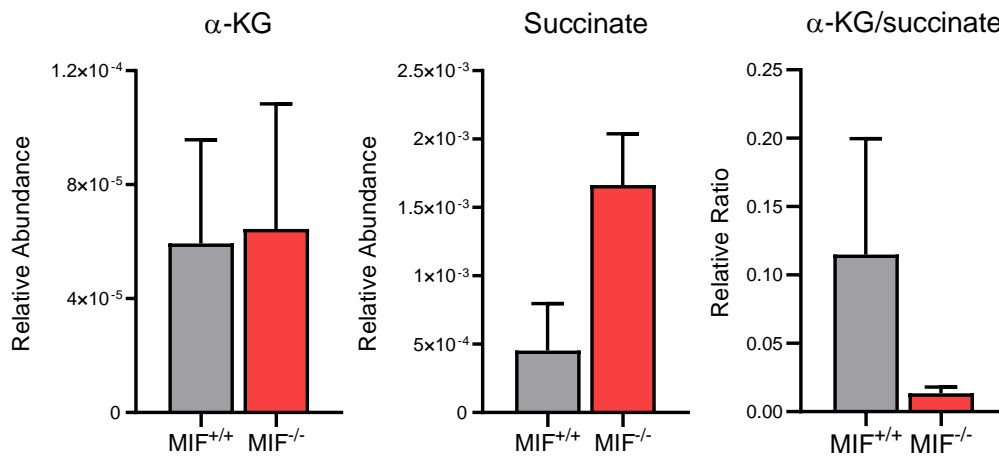
Figure 37: MIF deficiency impairs the α-ketoglutarate/succinate ratio. Relative abundance of α-ketoglutarate (αKG, left), succinate (middle), αKG/succinate ratio (right) in MIF^{+/+} and MIF^{-/-} BMDMs treated with IL-4 (6 hr). Data are the mean ± SEM of two replicates.

To determine whether the altered αKG/succinate ratio following MIF-deficiency functionally regulates M2 macrophage polarization, we next utilized a cell-permeable analog of αKG, dimethyl-αKG (DM-αKG) (128), and examined the expression of M2 macrophage-associated gene products. As shown in Figure 38A, DM-αKG can rescue the loss of ARG1 expression in M2-polarized MIF^{-/-} BMDMs in a dose-dependent manner. Furthermore, the addition of 5mM DM-αKG to 4-IPP-treated MIF^{+/+} BMDMs functionally rescues the loss of M2 macrophage polarization (Figure 38B). Interestingly, the functional rescue with 5mM DM-αKG was attenuated when higher concentrations of 4-IPP were administered, which suggests that complete inhibition of MIF further exacerbates a decrease in the αKG/succinate ratio that then requires higher concentrations of DM-αKG for a functional rescue.

A high αKG/succinate ratio is needed for JMJD3-dependent H3K27me3 demethylation during M2 macrophage polarization (128,215). Therefore, we utilized ChIP to investigate the hypothesis that MIF-dependent mitochondrial metabolism maintains a high αKG/succinate ratio to promote H3K27me3 demethylation. Remarkably, inhibition of MIF with 4-IPP significantly increased the levels of both enhancer- and promoter-specific H3K27me3 in M2 polarized BMDMs, and the addition of exogenous DM-αKG was sufficient to decrease H3K27me3 levels to those comparable to control BMDMs (Figure 39). This finding suggests that MIF functionally supports αKG-dependent histone demethylation of M2 macrophage gene enhancers and promoters through mitochondrial metabolism.
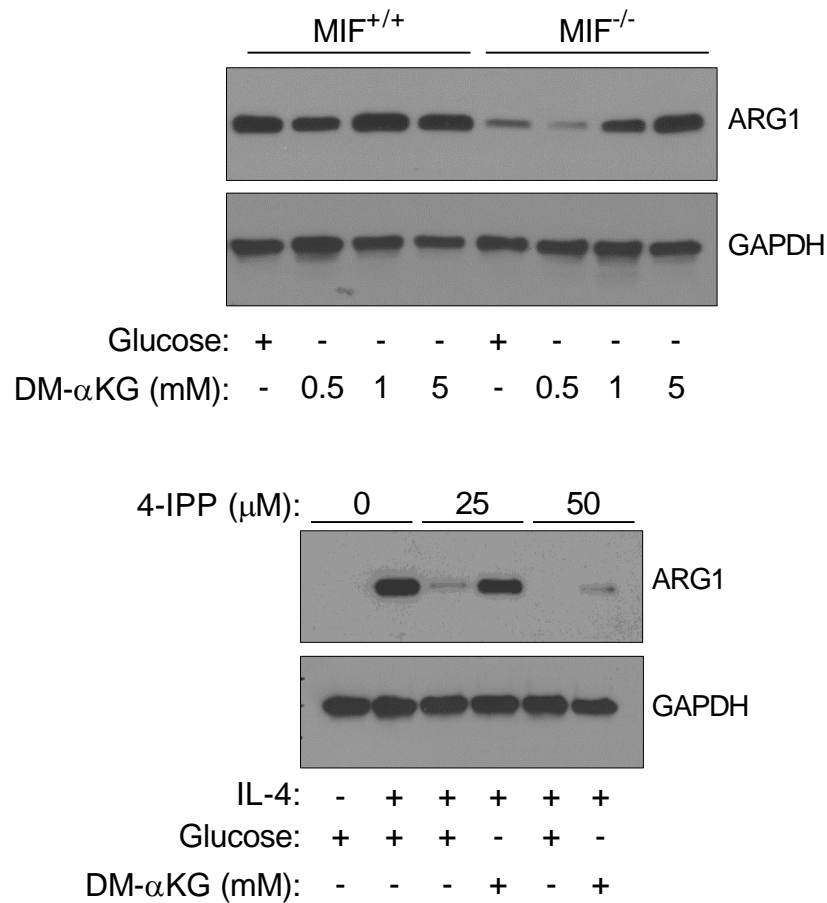
Figure 38: Exogenous α-ketoglutarate functionally rescues M2 polarization in MIF-deficient or -inhibited macrophages. (A) Immunoblot of ARG1 expression in MIF^{+/+} and MIF^{-/-} BMDMs treated with IL-4 (48hrs) in glucose-free media supplemented with glucose (5mM) or dimethyl-α-ketoglutarate (DM-αKG) at the indicated concentrations. **(B)** Immunoblot of ARG1 expression in MIF^{+/+} BMDMs treated with IL-4 (48hrs) ± 4-IPP (at indicated concentrations) in glucose-free media supplemented with glucose (5mM) or DM-αKG (5mM). Immunoblots are representative of three replicates.
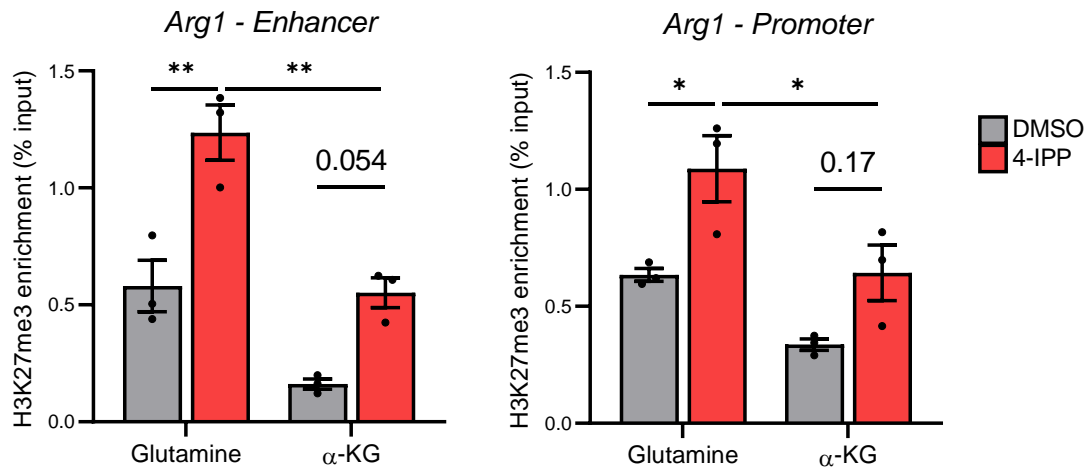
Figure 39: MIF-inhibition impairs αKG-dependent histone demethylation during M2 macrophage polarization. H3K27me3 chromatin-immunoprecipitation (ChIP) of *Arg1* enhancer (left) and promoter (right) in BMDMs treated with IL-4 (6hr) in glucose-free media supplemented with glutamine (2mM) or dimethyl-αKG (DM-αKG, 2mM). Data are the mean ± SEM of three replicates. *p≤0.05, **p≤0.01, ***p≤0.001 by two-way ANOVA with Tukey's post-test.

To identify the intermediary mechanistic effectors between MIF and mitochondrial metabolism-dependent M2 macrophage polarization, we first determined the requirement of MIF's cognate cell-surface receptor CD74 during M2 polarization (188). Surprisingly, IL-4-induced *Arg1* expression is fully intact in CD74$^{-/-}$ BMDMs (*data are not shown*), suggesting that MIF promotes M2 polarization independent of CD74 signaling. An alternative but equally important receptor-independent function for MIF involves COP9 signalosome subunit 5 (CSN5) (196), which regulates CRL-dependent protein degradation. Therefore, we next treated MIF$^{+/+}$ and MIF$^{-/-}$ BMDMs with MLN4924 – a NEDD8 activating enzyme inhibitor that mimics CSN5's deneddylase activity (236). While MLN4924 dose-dependently increased ARG1 expression in M2-polarized MIF$^{+/+}$ BMDMs, this effect was dramatically more pronounced in M2-polarized MIF$^{-/-}$ BMDMs to the extent that there were no significant differences in ARG1 expression between MIF$^{+/+}$ and MIF$^{-/-}$ BMDMs (Figure 40), which suggests that MIF promotes M2 macrophage polarization, in part, by regulating CSN5 activity.

In macrophages, CSN5 regulates the stability of nuclear respiratory factor 2 (NRF2) (217), which is a master regulator of mitochondrial metabolism, biogenesis, and M2 polarization (216). To determine if MIF influences NRF2 stabilization, we next examined nuclear NRF2 levels (i.e., NRF2 stabilization results in nuclear translocation (219)) at steady-state and during M2 polarization in MIF$^{+/+}$ and MIF$^{-/-}$ BMDMs and identified noticeable reductions in NRF2 levels in MIF-deficient BMDMs (Figure 41), suggesting that MIF may bind to CSN5 to support NRF2 stabilization during M2 macrophage polarization.
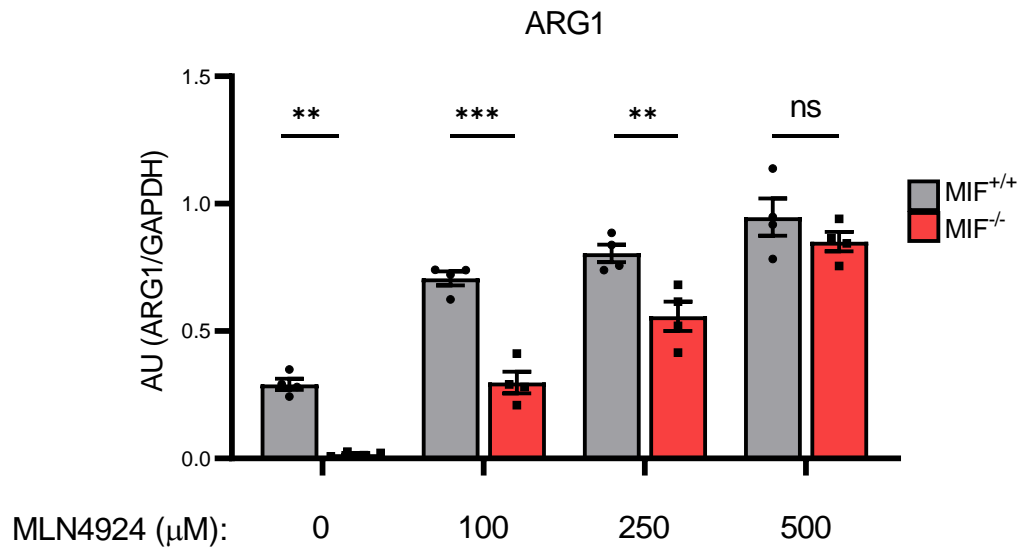
Figure 40: CSN5-like inhibition of CRL neddylation restores M2 polarization in MIF-deficient macrophages. Densitometric analysis of ARG1 expression in MIF$^{+/+}$ and MIF$^{-/-}$ BMDMs treated with IL-4 (6hr) ± MLN4924 at the indicated concentrations. Data are the mean ± SEM of four replicates. *p≤0.05, **p≤0.01, ***p≤0.001 by one-way ANOVA with Tukey's post-test.
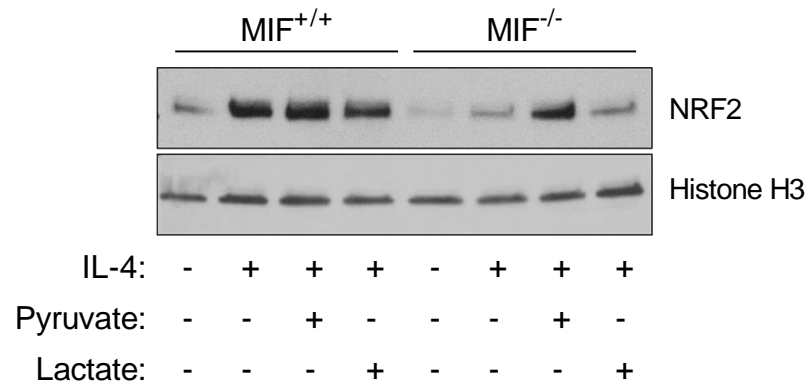
Figure 41: Nuclear NRF2 stabilization is lost in M2-polarized MIF-deficient macrophages. Immunoblot of NRF2 expression in MIF$^{+/+}$ and MIF$^{-/-}$ BMDMs treated with IL-4 (24hrs) in glucose-free media supplemented with pyruvate (10mM) or lactate (10mM). Immunoblot is representative of three replicates.

DISCUSSION

The findings of this study suggest that macrophage-derived MIF contributes to IL-4-induced M2 polarization by supporting a metabolic-epigenetic link through mitochondrial metabolism and αKG-dependent histone demethylation. During this study, it was reported that MIF deficiency in cancer cells leads to a loss of mitochondrial integrity (208). Our extracellular flux analyses validate and extend these findings as we found that loss of MIF in macrophages leads to a defect in mitochondrial OCR. Notably, MIF-deficiency impaired both steady-state and IL-4 enhanced mitochondrial metabolism, which suggests that MIF is an underlying requirement for metabolic reprogramming during M2 polarization. Additionally, pharmacological inhibition of MIF with 4-IPP phenocopies the loss of mitochondrial metabolism with MIF-deficiency. Previous studies have found that 4-IPP treatment impairs M2 macrophage polarization while also functionally promoting an M2→M1 macrophage re-polarization that in turn allows for an efficient anti-tumor immune response and subsequently delayed tumor outgrowth (156,232). As M2 polarization relies on metabolic reprogramming towards mitochondrial metabolism (107,109), it is interesting to speculate that the immunotherapeutic benefit of 4-IPP treatment for malignancies is attributed, in part, to the impairment of metabolic reprogramming in M2-polarized TAMs.

Mitochondrial metabolism in M2 macrophages allows for the dynamic regulation and accumulation of specific TCA cycle metabolites (127). In our earlier investigations, we identified that mitochondrial lactate metabolism supports TCA

cycle production of citrate for ACLY-dependent Ac-CoA synthesis for subsequent histone acetylation. Unexpectedly, exogenous acetate was not able to rescue the loss of M2 macrophage polarization in MIF-deficient BMDMs, which suggests that MIF supports M2 polarization through a different mitochondrial-dependent mechanism. Fortuitously, during our study, Liu and colleagues identified that another TCA cycle metabolite, αKG, is critical during M2 macrophage polarization for αKG-dependent histone demethylation (128). These findings were particularly intriguing because the enzymatic activity of these histone demethylases is dynamically regulated agonistically by αKG and antagonistically by succinate (213,214), coupled with the fact that SDH is ETC Complex II that forms a critical link between the TCA cycle and OXPHOS (211). Therefore, loss of mitochondrial integrity and disruption of the mitochondrial ETC, in particular Complex II (i.e., SDH), leads to succinate accumulation that in turn antagonizes histone demethylases (213,215). Consistent with our findings of decreased OCR in MIF-deficient BMDMs, our steady-state metabolomics analysis identified that MIF-deficiency in macrophages leads to a significant increase in succinate levels, which suggests that MIF regulates intracellular αKG/succinate levels through mitochondrial metabolism.

Using the cell-permeable analog of αKG, DM-αKG, to modulate intracellular αKG/succinate levels, we found that DM-αKG fully rescues loss of M2 polarization in MIF-deficient and MIF-inhibited macrophages. This finding further supports the suggestion that MIF regulates mitochondrial reprogramming during M2 polarization to support αKG-dependent histone demethylases. This is also

consistent with the results that DM-αKG supplementation decreases H3K27 trimethylation in 4-IPP treated BMDMs. Therefore, 4-IPP treatment to increase succinate levels in combination with glutaminase inhibitors, which lower αKG levels (238), represents an attractive therapeutic strategy to synergistically reduce intracellular αKG/succinate levels to inhibit histone demethylase-dependent M2 macrophage polarization.

Lastly, identifying the intermediary molecular mechanism(s) between MIF and mitochondrial metabolism is critical to understanding 4-IPP's mechanism of action and its further development as a viable immunotherapeutic treatment. The findings that MLN-4924 increases M2 polarization in MIF-deficient BMDMs suggest that MIF regulates M2 macrophages, in part, by binding to and regulating CSN5 activity. Previous studies have identified that CSN5 regulates NRF2 stabilization in macrophages (217). As NRF2 is a notable rheostat of mitochondrial metabolism (216) and that MIF-deficient macrophages have decreased nuclear NRF2 levels, this suggests that a MIF/CSN5/NRF2 axis regulates metabolic reprogramming towards mitochondrial metabolism during M2 macrophage polarization. Given that MIF regulates several downstream signaling pathways (183), it will be essential to identify the relative contributions of the MIF/CSN5/NRF2 axis in combination with other downstream MIF-dependent effectors in M2 macrophage polarization.

CHAPTER 4: SUMMARY AND FUTURE DIRECTIONS

Altogether this body of work identifies and describes critical metabolic-epigenetic links that regulate M2 macrophage polarization. Specifically, mitochondrial lactate/pyruvate metabolism supports the transcriptional expression of M2 macrophage-associated gene products through ACLY-dependent histone acetylation (Chapter 2). This metabolic-epigenetic link is then, in turn, reliant on MIF-dependent metabolic reprogramming and mitochondrial metabolism for αKG-mediated histone demethylation (Chapter 3). These two aims identify the interdependence between these two metabolic-epigenetics links to obtain efficient and maximal M2 macrophage polarization.

The principal novel findings presented in the first aim are: 1) Macrophages undergoing direct M0→M2 polarization utilize lactate catabolism within the mitochondria, 2) Macrophage-derived ACLY mechanistically links mitochondrial metabolism with histone acetylation and tumor-associated macrophage (TAM)-dependent tumor progression, and 3) Lactate-derived carbons are utilized in a direct metabolic-epigenetic link between mitochondrial TCA cycle metabolism and histone acetylation.

We identified for the first time, to our knowledge, that lactate is a *bona fide* catabolic mitochondrial substrate in M2-polarized macrophages. Our ^{13}C-lactate isotope tracing metabolomics identified that M2 polarized macrophages efficiently take up exogenous lactate, with subsequent conversion to pyruvate, mitochondrial entry via MPC1, and incorporation into the TCA cycle as citrate. The use of isotope

tracing versus steady-state metabolomics was advantageous as this allowed us to definitively track the metabolic path of lactate-derived carbons into TCA cycle metabolites (116). Notably, this study utilized pharmacological inhibition of mitochondrial pyruvate uptake via the canonical MPC1 inhibitor UK-5099 (119,120), which was then further validated by a molecularly distinct MPC1 inhibitor (227). Since full-body homozygous transgenic knockout of MPC1 is embryonic lethal (239,240), it will be intriguing in future studies to determine the feasibility of developing an inducible or conditional macrophage MPC1 transgenic model to validate macrophage-specific mitochondrial lactate metabolism during M2 polarization

In this study, we developed an *inducible* macrophage ACLY transgenic model to study the contribution of TAM-specific ACLY in tumor progression. We identified that ACLY-dependent histone acetylation is required for M0→M2 polarization and that TAM-derived ACLY supports *in vivo* suppression of infiltrating anti-tumor T cell responses and subsequent TAM-mediated tumor outgrowth. During this study, Baardman and colleagues developed a *conditional* ACLY knockout mouse model to study the contribution of macrophage-derived ACLY in atherosclerotic plaque progression (142). Since our study is the first report to describe a role for macrophage-specific ACLY in driving suppression of anti-tumor immunity, future utilization of the recently described macrophage conditional ACLY transgenic model will be informative to extend further our understanding of ACLY's regulation of macrophage-mediated tumor immunosuppression.

Our studies also suggest that lactate provides a direct carbon source for Ac-CoA production via citrate conversion and functionally determines the relative accumulation of acetyl groups onto M2 gene promoter-specific histone lysine residues. To our knowledge, this is the first description of specific lactate-derived carbons being used for acetyl-histone modifications that ultimately drive macrophage gene expression and T cell immune suppressive activity. During our study, we attempted to indirectly trace lactate-derived carbons into acetyl-histone groups by quantifying histone bound acetate based on an alkylation and GC-MS/MS (241), but this method was not sensitive enough to detect ^{13}C-lactate-derived acetate in primary M2-polarized BMDMs. The development of a more robust protocol that combines isotope tracing, peptide immunoprecipitation, and HPLC-MS/MS will be helpful to quantify lactate-derived acetyl-histone modifications directly (129).

The principal novel findings presented in the second aim are 1) MIF is a critical underlying requirement of metabolic reprogramming during M2 macrophage polarization, 2) MIF-dependent mitochondrial metabolism maintains an α-ketoglutarate/succinate ratio conducive histone demethylation-mediated M2 polarization, and 3) MIF supports metabolic reprogramming during M2 macrophage polarization by regulating a CSN5/NRF2 axis.

We identified for the first time, to our knowledge, that MIF regulates metabolic reprogramming in macrophages to allow for IL-4-enhanced mitochondrial metabolism. Our extracellular flux analyses identified defective mitochondrial OCR in both naïve M0 and M2-polarized MIF-deficient or 4-IPP-

inhibited macrophages, which suggests that MIF is an underlying requirement for the ability of macrophages to undergo metabolic reprogramming. Previous studies have indicated that MIF modulates mitochondrial dynamics in human cancer cell lines (208). Further investigations into whether macrophage-derived MIF regulates mitochondrial quality (i.e., integrity and activity) *vs.* quantity (i.e., biogenesis) will be particularly informative to extending this newly identified molecular contribution of MIF in macrophage polarization.

In this study, we identified that MIF serves as a metabolic-epigenetic link during macrophage polarization through mitochondrial metabolism and αKG-dependent, M2 macrophage-associated gene promoter and enhancer-specific H3K27me3 demethylation. Intriguingly, the relative αKG/succinate ratio – which is impaired with MIF deficiency – is a critical determinant on M2 polarization (128), and restoration of this ratio with exogenous αKG functionally rescues M2 polarization and histone demethylation in MIF-deficient macrophages. It will be interesting to determine whether combinatorial therapeutic targeting of MIF (i.e., increasing succinate) and glutaminolysis (i.e., decreasing αKG (238)) provides synergistic effects in reducing the αKG/succinate ratio to further potentiate a functional immunosuppressive, pro-tumor M2-TAM→immunostimulatory, anti-tumor M1-TAM repolarization with subsequent enhancement of tumor immunity.

Lastly, our studies also suggest that MIF supports metabolic reprogramming during M2 macrophage polarization, in part, by regulating a CSN5/NRF2 axis. Several studies have identified that MIF is a critical regulator of TAM- and MDSC-dependent immunosuppression and subsequent tumor

progression (156,232,242), but the underlying mechanistic effects have not been fully elucidated. The finding that intracellular MIF likely plays a dominant role in TAM/MDSC effector functions is particularly exciting as this suggests that therapeutic MIF targeting with small molecule inhibitors, such as 4-IPP (243), will be more clinically efficacious than the currently available antibody-based therapies that target MIF's extracellular, receptor-dependent mechanisms (242,244). Therefore, further head-to-head comparisons of these differential therapeutic strategies will be informative in validating and extending the potential clinical benefit of 4-IPP, and other small molecule MIF inhibitors, in targeting MIF-dependent immunosuppression and tumor progression.

Altogether, these findings highlight the functional significance of metabolic-epigenetic links in the regulation of M2 macrophage polarization. Understanding the metabolic-epigenetic coordinations needed to activate specific transcriptional networks that are required to elicit macrophage phenotypes and effector functions is critical in developing immunotherapeutic targeting strategies. The findings in this body of work identified multiple insights that can, and should, be leveraged for the future development of immunotherapies to enhance tumor immunity leading to robust and durable clinical responses in patients diagnosed with cancer.

REFERENCES

1.   Brahmer, J. R., Tykodi, S. S., Chow, L. Q., Hwu, W. J., Topalian, S. L., Hwu, P., Drake, C. G., Camacho, L. H., Kauh, J., Odunsi, K., Pitot, H. C., Hamid, O., Bhatia, S., Martins, R., Eaton, K., Chen, S., Salay, T. M., Alaparthy, S., Grosso, J. F., Korman, A. J., Parker, S. M., Agrawal, S., Goldberg, S. M., Pardoll, D. M., Gupta, A., and Wigginton, J. M. (2012) Safety and activity of anti-PD-L1 antibody in patients with advanced cancer. *N Engl J Med* **366**, 2455-2465

2.   Topalian, S. L., Hodi, F. S., Brahmer, J. R., Gettinger, S. N., Smith, D. C., McDermott, D. F., Powderly, J. D., Carvajal, R. D., Sosman, J. A., Atkins, M. B., Leming, P. D., Spigel, D. R., Antonia, S. J., Horn, L., Drake, C. G., Pardoll, D. M., Chen, L., Sharfman, W. H., Anders, R. A., Taube, J. M., McMiller, T. L., Xu, H., Korman, A. J., Jure-Kunkel, M., Agrawal, S., McDonald, D., Kollia, G. D., Gupta, A., Wigginton, J. M., and Sznol, M. (2012) Safety, activity, and immune correlates of anti-PD-1 antibody in cancer. *N Engl J Med* **366**, 2443-2454

3.   Gonzalez, H., Hagerling, C., and Werb, Z. (2018) Roles of the immune system in cancer: from tumor initiation to metastatic progression. *Genes Dev* **32**, 1267-1284

4.   Cortez-Retamozo, V., Etzrodt, M., Newton, A., Rauch, P. J., Chudnovskiy, A., Berger, C., Ryan, R. J., Iwamoto, Y., Marinelli, B., Gorbatov, R., Forghani, R., Novobrantseva, T. I., Koteliansky, V., Figueiredo, J. L., Chen, J. W., Anderson, D. G., Nahrendorf, M., Swirski, F. K., Weissleder, R., and Pittet, M. J. (2012) Origins of tumor-associated macrophages and neutrophils. *Proc Natl Acad Sci U S A* **109**, 2491-2496

5.   Franklin, R. A., Liao, W., Sarkar, A., Kim, M. V., Bivona, M. R., Liu, K., Pamer, E. G., and Li, M. O. (2014) The cellular and molecular origin of tumor-associated macrophages. *Science* **344**, 921-925

6.   Kumar, V., Cheng, P., Condamine, T., Mony, S., Languino, L. R., McCaffrey, J. C., Hockstein, N., Guarino, M., Masters, G., Penman, E., Denstman, F., Xu, X., Altieri, D. C., Du, H., Yan, C., and Gabrilovich, D. I. (2016) CD45 Phosphatase Inhibits STAT3 Transcription Factor Activity in Myeloid Cells and Promotes Tumor-Associated Macrophage Differentiation. *Immunity* **44**, 303-315

7.   Qian, B. Z., Li, J., Zhang, H., Kitamura, T., Zhang, J., Campion, L. R., Kaiser, E. A., Snyder, L. A., and Pollard, J. W. (2011) CCL2 recruits

inflammatory monocytes to facilitate breast-tumour metastasis. *Nature* **475**, 222-225

8. Laviron, M., and Boissonnas, A. (2019) Ontogeny of Tumor-Associated Macrophages. *Front Immunol* **10**, 1799

9. Lin, E. Y., Nguyen, A. V., Russell, R. G., and Pollard, J. W. (2001) Colony-stimulating factor 1 promotes progression of mammary tumors to malignancy. *J Exp Med* **193**, 727-740

10. Loyher, P. L., Hamon, P., Laviron, M., Meghraoui-Kheddar, A., Goncalves, E., Deng, Z., Torstensson, S., Bercovici, N., Baudesson de Chanville, C., Combadiere, B., Geissmann, F., Savina, A., Combadiere, C., and Boissonnas, A. (2018) Macrophages of distinct origins contribute to tumor development in the lung. *J Exp Med* **215**, 2536-2553

11. Zhu, Y., Herndon, J. M., Sojka, D. K., Kim, K. W., Knolhoff, B. L., Zuo, C., Cullinan, D. R., Luo, J., Bearden, A. R., Lavine, K. J., Yokoyama, W. M., Hawkins, W. G., Fields, R. C., Randolph, G. J., and DeNardo, D. G. (2017) Tissue-Resident Macrophages in Pancreatic Ductal Adenocarcinoma Originate from Embryonic Hematopoiesis and Promote Tumor Progression. *Immunity* **47**, 597

12. Gocheva, V., Wang, H. W., Gadea, B. B., Shree, T., Hunter, K. E., Garfall, A. L., Berman, T., and Joyce, J. A. (2010) IL-4 induces cathepsin protease activity in tumor-associated macrophages to promote cancer growth and invasion. *Genes Dev* **24**, 241-255

13. Gupta, S., Jain, A., Syed, S. N., Snodgrass, R. G., Pfluger-Muller, B., Leisegang, M. S., Weigert, A., Brandes, R. P., Ebersberger, I., Brune, B., and Namgaladze, D. (2018) IL-6 augments IL-4-induced polarization of primary human macrophages through synergy of STAT3, STAT6 and BATF transcription factors. *Oncoimmunology* **7**, e1494110

14. Pyonteck, S. M., Akkari, L., Schuhmacher, A. J., Bowman, R. L., Sevenich, L., Quail, D. F., Olson, O. C., Quick, M. L., Huse, J. T., Teijeiro, V., Setty, M., Leslie, C. S., Oei, Y., Pedraza, A., Zhang, J., Brennan, C. W., Sutton, J. C., Holland, E. C., Daniel, D., and Joyce, J. A. (2013) CSF-1R inhibition alters macrophage polarization and blocks glioma progression. *Nat Med* **19**, 1264-1272

15. Casazza, A., Laoui, D., Wenes, M., Rizzolio, S., Bassani, N., Mambretti, M., Deschoemaeker, S., Van Ginderachter, J. A., Tamagnone, L., and Mazzone, M. (2013) Impeding macrophage entry into hypoxic tumor areas by Sema3A/Nrp1 signaling blockade inhibits angiogenesis and restores antitumor immunity. *Cancer Cell* **24**, 695-709

16. Henze, A. T., and Mazzone, M. (2016) The impact of hypoxia on tumor-associated macrophages. *J Clin Invest* **126**, 3672-3679

17. Colegio, O. R., Chu, N. Q., Szabo, A. L., Chu, T., Rhebergen, A. M., Jairam, V., Cyrus, N., Brokowski, C. E., Eisenbarth, S. C., Phillips, G. M., Cline, G. W., Phillips, A. J., and Medzhitov, R. (2014) Functional polarization of tumour-associated macrophages by tumour-derived lactic acid. *Nature* **513**, 559-563

18. Carmona-Fontaine, C., Deforet, M., Akkari, L., Thompson, C. B., Joyce, J. A., and Xavier, J. B. (2017) Metabolic origins of spatial organization in the tumor microenvironment. *Proc Natl Acad Sci U S A* **114**, 2934-2939

19. Munder, M., Eichmann, K., and Modolell, M. (1998) Alternative metabolic states in murine macrophages reflected by the nitric oxide synthase/arginase balance: competitive regulation by CD4+ T cells correlates with Th1/Th2 phenotype. *J Immunol* **160**, 5347-5354

20. Barrios-Rodiles, M., and Chadee, K. (1998) Novel regulation of cyclooxygenase-2 expression and prostaglandin E2 production by IFN-gamma in human macrophages. *J Immunol* **161**, 2441-2448

21. Biswas, S. K., Gangi, L., Paul, S., Schioppa, T., Saccani, A., Sironi, M., Bottazzi, B., Doni, A., Vincenzo, B., Pasqualini, F., Vago, L., Nebuloni, M., Mantovani, A., and Sica, A. (2006) A distinct and unique transcriptional program expressed by tumor-associated macrophages (defective NF-kappaB and enhanced IRF-3/STAT1 activation). *Blood* **107**, 2112-2122

22. Weiskopf, K., Jahchan, N. S., Schnorr, P. J., Cristea, S., Ring, A. M., Maute, R. L., Volkmer, A. K., Volkmer, J. P., Liu, J., Lim, J. S., Yang, D., Seitz, G., Nguyen, T., Wu, D., Jude, K., Guerston, H., Barkal, A., Trapani, F., George, J., Poirier, J. T., Gardner, E. E., Miles, L. A., de Stanchina, E., Lofgren, S. M., Vogel, H., Winslow, M. M., Dive, C., Thomas, R. K., Rudin, C. M., van de Rijn, M., Majeti, R., Garcia, K. C., Weissman, I. L., and Sage, J. (2016) CD47-blocking immunotherapies stimulate macrophage-mediated destruction of small-cell lung cancer. *J Clin Invest* **126**, 2610-2620

23. Oldenborg, P. A., Gresham, H. D., and Lindberg, F. P. (2001) CD47-signal regulatory protein alpha (SIRPalpha) regulates Fcgamma and complement receptor-mediated phagocytosis. *J Exp Med* **193**, 855-862

24. Chao, M. P., Alizadeh, A. A., Tang, C., Myklebust, J. H., Varghese, B., Gill, S., Jan, M., Cha, A. C., Chan, C. K., Tan, B. T., Park, C. Y., Zhao, F., Kohrt, H. E., Malumbres, R., Briones, J., Gascoyne, R. D., Lossos, I. S., Levy, R., Weissman, I. L., and Majeti, R. (2010) Anti-CD47 antibody synergizes with rituximab to promote phagocytosis and eradicate non-Hodgkin lymphoma. *Cell* **142**, 699-713

25. Muraoka, D., Seo, N., Hayashi, T., Tahara, Y., Fujii, K., Tawara, I., Miyahara, Y., Okamori, K., Yagita, H., Imoto, S., Yamaguchi, R., Komura, M., Miyano, S., Goto, M., Sawada, S. I., Asai, A., Ikeda, H., Akiyoshi, K., Harada, N., and Shiku, H. (2019) Antigen delivery targeted to tumor-

associated macrophages overcomes tumor immune resistance. *J Clin Invest* **129**, 1278-1294

26. Kerkar, S. P., Goldszmid, R. S., Muranski, P., Chinnasamy, D., Yu, Z., Reger, R. N., Leonardi, A. J., Morgan, R. A., Wang, E., Marincola, F. M., Trinchieri, G., Rosenberg, S. A., and Restifo, N. P. (2011) IL-12 triggers a programmatic change in dysfunctional myeloid-derived cells within mouse tumors. *J Clin Invest* **121**, 4746-4757

27. Ghiringhelli, F., Apetoh, L., Tesniere, A., Aymeric, L., Ma, Y., Ortiz, C., Vermaelen, K., Panaretakis, T., Mignot, G., Ullrich, E., Perfettini, J. L., Schlemmer, F., Tasdemir, E., Uhl, M., Genin, P., Civas, A., Ryffel, B., Kanellopoulos, J., Tschopp, J., Andre, F., Lidereau, R., McLaughlin, N. M., Haynes, N. M., Smyth, M. J., Kroemer, G., and Zitvogel, L. (2009) Activation of the NLRP3 inflammasome in dendritic cells induces IL-1beta-dependent adaptive immunity against tumors. *Nat Med* **15**, 1170-1178

28. Tannahill, G. M., Curtis, A. M., Adamik, J., Palsson-McDermott, E. M., McGettrick, A. F., Goel, G., Frezza, C., Bernard, N. J., Kelly, B., Foley, N. H., Zheng, L., Gardet, A., Tong, Z., Jany, S. S., Corr, S. C., Haneklaus, M., Caffrey, B. E., Pierce, K., Walmsley, S., Beasley, F. C., Cummins, E., Nizet, V., Whyte, M., Taylor, C. T., Lin, H., Masters, S. L., Gottlieb, E., Kelly, V. P., Clish, C., Auron, P. E., Xavier, R. J., and O'Neill, L. A. (2013) Succinate is an inflammatory signal that induces IL-1beta through HIF-1alpha. *Nature* **496**, 238-242

29. Coussens, L. M., and Werb, Z. (2002) Inflammation and cancer. *Nature* **420**, 860-867

30. Kryczek, I., Wei, S., Zou, L., Zhu, G., Mottram, P., Xu, H., Chen, L., and Zou, W. (2006) Cutting edge: induction of B7-H4 on APCs through IL-10: novel suppressive mode for regulatory T cells. *J Immunol* **177**, 40-44

31. Lin, H., Wei, S., Hurt, E. M., Green, M. D., Zhao, L., Vatan, L., Szeliga, W., Herbst, R., Harms, P. W., Fecher, L. A., Vats, P., Chinnaiyan, A. M., Lao, C. D., Lawrence, T. S., Wicha, M., Hamanishi, J., Mandai, M., Kryczek, I., and Zou, W. (2018) Host expression of PD-L1 determines efficacy of PD-L1 pathway blockade-mediated tumor regression. *J Clin Invest* **128**, 805-815

32. Gordon, S. R., Maute, R. L., Dulken, B. W., Hutter, G., George, B. M., McCracken, M. N., Gupta, R., Tsai, J. M., Sinha, R., Corey, D., Ring, A. M., Connolly, A. J., and Weissman, I. L. (2017) PD-1 expression by tumour-associated macrophages inhibits phagocytosis and tumour immunity. *Nature* **545**, 495-499

33. Lau, J., Cheung, J., Navarro, A., Lianoglou, S., Haley, B., Totpal, K., Sanders, L., Koeppen, H., Caplazi, P., McBride, J., Chiu, H., Hong, R., Grogan, J., Javinal, V., Yauch, R., Irving, B., Belvin, M., Mellman, I., Kim, J. M., and Schmidt, M. (2017) Tumour and host cell PD-L1 is required to

mediate suppression of anti-tumour immunity in mice. *Nat Commun* **8**, 14572

34. Rodriguez, P. C., Quiceno, D. G., Zabaleta, J., Ortiz, B., Zea, A. H., Piazuelo, M. B., Delgado, A., Correa, P., Brayer, J., Sotomayor, E. M., Antonia, S., Ochoa, J. B., and Ochoa, A. C. (2004) Arginase I production in the tumor microenvironment by mature myeloid cells inhibits T-cell receptor expression and antigen-specific T-cell responses. *Cancer Res* **64**, 5839-5849

35. Rodriguez, P. C., Zea, A. H., DeSalvo, J., Culotta, K. S., Zabaleta, J., Quiceno, D. G., Ochoa, J. B., and Ochoa, A. C. (2003) L-arginine consumption by macrophages modulates the expression of CD3 zeta chain in T lymphocytes. *J Immunol* **171**, 1232-1239

36. Zea, A. H., Rodriguez, P. C., Atkins, M. B., Hernandez, C., Signoretti, S., Zabaleta, J., McDermott, D., Quiceno, D., Youmans, A., O'Neill, A., Mier, J., and Ochoa, A. C. (2005) Arginase-producing myeloid suppressor cells in renal cell carcinoma patients: a mechanism of tumor evasion. *Cancer Res* **65**, 3044-3048

37. Murdoch, C., Muthana, M., Coffelt, S. B., and Lewis, C. E. (2008) The role of myeloid cells in the promotion of tumour angiogenesis. *Nat Rev Cancer* **8**, 618-631

38. Dirkx, A. E., Oude Egbrink, M. G., Wagstaff, J., and Griffioen, A. W. (2006) Monocyte/macrophage infiltration in tumors: modulators of angiogenesis. *J Leukoc Biol* **80**, 1183-1196

39. Gordon, S. (2003) Alternative activation of macrophages. *Nat Rev Immunol* **3**, 23-35

40. Murray, P. J., Allen, J. E., Biswas, S. K., Fisher, E. A., Gilroy, D. W., Goerdt, S., Gordon, S., Hamilton, J. A., Ivashkiv, L. B., Lawrence, T., Locati, M., Mantovani, A., Martinez, F. O., Mege, J. L., Mosser, D. M., Natoli, G., Saeij, J. P., Schultze, J. L., Shirey, K. A., Sica, A., Suttles, J., Udalova, I., van Ginderachter, J. A., Vogel, S. N., and Wynn, T. A. (2014) Macrophage activation and polarization: nomenclature and experimental guidelines. *Immunity* **41**, 14-20

41. Sica, A., and Mantovani, A. (2012) Macrophage plasticity and polarization: in vivo veritas. *J Clin Invest* **122**, 787-795

42. McWhorter, F. Y., Wang, T., Nguyen, P., Chung, T., and Liu, W. F. (2013) Modulation of macrophage phenotype by cell shape. *Proc Natl Acad Sci U S A* **110**, 17253-17258

43. Gabrilovich, D. I., Ostrand-Rosenberg, S., and Bronte, V. (2012) Coordinated regulation of myeloid cells by tumours. *Nat Rev Immunol* **12**, 253-268

44. Gajewski, T. F., Schreiber, H., and Fu, Y. X. (2013) Innate and adaptive immune cells in the tumor microenvironment. *Nat Immunol* **14**, 1014-1022

45. Mitchem, J. B., Brennan, D. J., Knolhoff, B. L., Belt, B. A., Zhu, Y., Sanford, D. E., Belaygorod, L., Carpenter, D., Collins, L., Piwnica-Worms, D., Hewitt, S., Udupi, G. M., Gallagher, W. M., Wegner, C., West, B. L., Wang-Gillam, A., Goedegebuure, P., Linehan, D. C., and DeNardo, D. G. (2013) Targeting tumor-infiltrating macrophages decreases tumor-initiating cells, relieves immunosuppression, and improves chemotherapeutic responses. *Cancer Res* **73**, 1128-1141

46. Raes, G., De Baetselier, P., Noel, W., Beschin, A., Brombacher, F., and Hassanzadeh Gh, G. (2002) Differential expression of FIZZ1 and Ym1 in alternatively versus classically activated macrophages. *J Leukoc Biol* **71**, 597-602

47. Zhu, Z., Zheng, T., Homer, R. J., Kim, Y. K., Chen, N. Y., Cohn, L., Hamid, Q., and Elias, J. A. (2004) Acidic mammalian chitinase in asthmatic Th2 inflammation and IL-13 pathway activation. *Science* **304**, 1678-1682

48. Stein, M., Keshav, S., Harris, N., and Gordon, S. (1992) Interleukin 4 potently enhances murine macrophage mannose receptor activity: a marker of alternative immunologic macrophage activation. *J Exp Med* **176**, 287-292

49. Geiger, R., Rieckmann, J. C., Wolf, T., Basso, C., Feng, Y., Fuhrer, T., Kogadeeva, M., Picotti, P., Meissner, F., Mann, M., Zamboni, N., Sallusto, F., and Lanzavecchia, A. (2016) L-Arginine Modulates T Cell Metabolism and Enhances Survival and Anti-tumor Activity. *Cell* **167**, 829-842 e813

50. Riabov, V., Gudima, A., Wang, N., Mickley, A., Orekhov, A., and Kzhyshkowska, J. (2014) Role of tumor associated macrophages in tumor angiogenesis and lymphangiogenesis. *Front Physiol* **5**, 75

51. Bergers, G., Brekken, R., McMahon, G., Vu, T. H., Itoh, T., Tamaki, K., Tanzawa, K., Thorpe, P., Itohara, S., Werb, Z., and Hanahan, D. (2000) Matrix metalloproteinase-9 triggers the angiogenic switch during carcinogenesis. *Nat Cell Biol* **2**, 737-744

52. Giraudo, E., Inoue, M., and Hanahan, D. (2004) An amino-bisphosphonate targets MMP-9-expressing macrophages and angiogenesis to impair cervical carcinogenesis. *J Clin Invest* **114**, 623-633

53. Murray, P. J., and Wynn, T. A. (2011) Protective and pathogenic functions of macrophage subsets. *Nat Rev Immunol* **11**, 723-737

54. Flavell, R. A., Sanjabi, S., Wrzesinski, S. H., and Licona-Limon, P. (2010) The polarization of immune cells in the tumour environment by TGFbeta. *Nat Rev Immunol* **10**, 554-567

55. Klarquist, J., Tobin, K., Farhangi Oskuei, P., Henning, S. W., Fernandez, M. F., Dellacecca, E. R., Navarro, F. C., Eby, J. M., Chatterjee, S., Mehrotra,

S., Clark, J. I., and Le Poole, I. C. (2016) Ccl22 Diverts T Regulatory Cells and Controls the Growth of Melanoma. *Cancer Res* **76**, 6230-6240

56. Wang, D., Yang, L., Yue, D., Cao, L., Li, L., Wang, D., Ping, Y., Shen, Z., Zheng, Y., Wang, L., and Zhang, Y. (2019) Macrophage-derived CCL22 promotes an immunosuppressive tumor microenvironment via IL-8 in malignant pleural effusion. *Cancer Lett* **452**, 244-253

57. Mogensen, T. H. (2009) Pathogen recognition and inflammatory signaling in innate immune defenses. *Clin Microbiol Rev* **22**, 240-273, Table of Contents

58. Nathan, C. F., Murray, H. W., Wiebe, M. E., and Rubin, B. Y. (1983) Identification of interferon-gamma as the lymphokine that activates human macrophage oxidative metabolism and antimicrobial activity. *J Exp Med* **158**, 670-689

59. Muller, E., Christopoulos, P. F., Halder, S., Lunde, A., Beraki, K., Speth, M., Oynebraten, I., and Corthay, A. (2017) Toll-Like Receptor Ligands and Interferon-gamma Synergize for Induction of Antitumor M1 Macrophages. *Front Immunol* **8**, 1383

60. Schroder, K., Hertzog, P. J., Ravasi, T., and Hume, D. A. (2004) Interferon-gamma: an overview of signals, mechanisms and functions. *J Leukoc Biol* **75**, 163-189

61. Akira, S., and Takeda, K. (2004) Toll-like receptor signalling. *Nat Rev Immunol* **4**, 499-511

62. Poltorak, A., He, X., Smirnova, I., Liu, M. Y., Van Huffel, C., Du, X., Birdwell, D., Alejos, E., Silva, M., Galanos, C., Freudenberg, M., Ricciardi-Castagnoli, P., Layton, B., and Beutler, B. (1998) Defective LPS signaling in C3H/HeJ and C57BL/10ScCr mice: mutations in Tlr4 gene. *Science* **282**, 2085-2088

63. Orecchioni, M., Ghosheh, Y., Pramod, A. B., and Ley, K. (2019) Macrophage Polarization: Different Gene Signatures in M1(LPS+) vs. Classically and M2(LPS-) vs. Alternatively Activated Macrophages. *Front Immunol* **10**, 1084

64. Sharif, O., Bolshakov, V. N., Raines, S., Newham, P., and Perkins, N. D. (2007) Transcriptional profiling of the LPS induced NF-kappaB response in macrophages. *BMC Immunol* **8**, 1

65. Meraz, M. A., White, J. M., Sheehan, K. C., Bach, E. A., Rodig, S. J., Dighe, A. S., Kaplan, D. H., Riley, J. K., Greenlund, A. C., Campbell, D., Carver-Moore, K., DuBois, R. N., Clark, R., Aguet, M., and Schreiber, R. D. (1996) Targeted disruption of the Stat1 gene in mice reveals unexpected physiologic specificity in the JAK-STAT signaling pathway. *Cell* **84**, 431-442

66. Gordon, S., and Martinez, F. O. (2010) Alternative activation of macrophages: mechanism and functions. *Immunity* **32**, 593-604

67. Nelms, K., Keegan, A. D., Zamorano, J., Ryan, J. J., and Paul, W. E. (1999) The IL-4 receptor: signaling mechanisms and biologic functions. *Annu Rev Immunol* **17**, 701-738

68. Kondo, M., Takeshita, T., Ishii, N., Nakamura, M., Watanabe, S., Arai, K., and Sugamura, K. (1993) Sharing of the interleukin-2 (IL-2) receptor gamma chain between receptors for IL-2 and IL-4. *Science* **262**, 1874-1877

69. Obiri, N. I., Debinski, W., Leonard, W. J., and Puri, R. K. (1995) Receptor for interleukin 13. Interaction with interleukin 4 by a mechanism that does not involve the common gamma chain shared by receptors for interleukins 2, 4, 7, 9, and 15. *J Biol Chem* **270**, 8797-8804

70. Welham, M. J., Learmonth, L., Bone, H., and Schrader, J. W. (1995) Interleukin-13 signal transduction in lymphohemopoietic cells. Similarities and differences in signal transduction with interleukin-4 and insulin. *J Biol Chem* **270**, 12286-12296

71. Reichel, M., Nelson, B. H., Greenberg, P. D., and Rothman, P. B. (1997) The IL-4 receptor alpha-chain cytoplasmic domain is sufficient for activation of JAK-1 and STAT6 and the induction of IL-4-specific gene expression. *J Immunol* **158**, 5860-5867

72. Chen, X. H., Patel, B. K., Wang, L. M., Frankel, M., Ellmore, N., Flavell, R. A., LaRochelle, W. J., and Pierce, J. H. (1997) Jak1 expression is required for mediating interleukin-4-induced tyrosine phosphorylation of insulin receptor substrate and Stat6 signaling molecules. *J Biol Chem* **272**, 6556-6560

73. Takeda, K., Tanaka, T., Shi, W., Matsumoto, M., Minami, M., Kashiwamura, S., Nakanishi, K., Yoshida, N., Kishimoto, T., and Akira, S. (1996) Essential role of Stat6 in IL-4 signalling. *Nature* **380**, 627-630

74. Ihle, J. N. (1996) STATs: signal transducers and activators of transcription. *Cell* **84**, 331-334

75. Kaplan, M. H., Schindler, U., Smiley, S. T., and Grusby, M. J. (1996) Stat6 is required for mediating responses to IL-4 and for development of Th2 cells. *Immunity* **4**, 313-319

76. McLeod, J. J., Baker, B., and Ryan, J. J. (2015) Mast cell production and response to IL-4 and IL-13. *Cytokine* **75**, 57-61

77. Ferrick, D. A., Schrenzel, M. D., Mulvania, T., Hsieh, B., Ferlin, W. G., and Lepper, H. (1995) Differential production of interferon-gamma and interleukin-4 in response to Th1- and Th2-stimulating pathogens by gamma delta T cells in vivo. *Nature* **373**, 255-257

78. Yoshimoto, T., and Paul, W. E. (1994) CD4pos, NK1.1pos T cells promptly produce interleukin 4 in response to in vivo challenge with anti-CD3. *J Exp Med* **179**, 1285-1295

79. Chen, H., and Paul, W. E. (1997) Cultured NK1.1+ CD4+ T cells produce large amounts of IL-4 and IFN-gamma upon activation by anti-CD3 or CD1. *J Immunol* **159**, 2240-2249

80. Min, B., Prout, M., Hu-Li, J., Zhu, J., Jankovic, D., Morgan, E. S., Urban, J. F., Jr., Dvorak, A. M., Finkelman, F. D., LeGros, G., and Paul, W. E. (2004) Basophils produce IL-4 and accumulate in tissues after infection with a Th2-inducing parasite. *J Exp Med* **200**, 507-517

81. Hsieh, C. S., Heimberger, A. B., Gold, J. S., O'Garra, A., and Murphy, K. M. (1992) Differential regulation of T helper phenotype development by interleukins 4 and 10 in an alpha beta T-cell-receptor transgenic system. *Proc Natl Acad Sci U S A* **89**, 6065-6069

82. Gascan, H., Gauchat, J. F., Roncarolo, M. G., Yssel, H., Spits, H., and de Vries, J. E. (1991) Human B cell clones can be induced to proliferate and to switch to IgE and IgG4 synthesis by interleukin 4 and a signal provided by activated CD4+ T cell clones. *J Exp Med* **173**, 747-750

83. Menges, M., Baumeister, T., Rossner, S., Stoitzner, P., Romani, N., Gessner, A., and Lutz, M. B. (2005) IL-4 supports the generation of a dendritic cell subset from murine bone marrow with altered endocytosis capacity. *J Leukoc Biol* **77**, 535-543

84. Chen, L., Grabowski, K. A., Xin, J. P., Coleman, J., Huang, Z., Espiritu, B., Alkan, S., Xie, H. B., Zhu, Y., White, F. A., Clancy, J., Jr., and Huang, H. (2004) IL-4 induces differentiation and expansion of Th2 cytokine-producing eosinophils. *J Immunol* **172**, 2059-2066

85. Fallon, P. G., Jolin, H. E., Smith, P., Emson, C. L., Townsend, M. J., Fallon, R., Smith, P., and McKenzie, A. N. (2002) IL-4 induces characteristic Th2 responses even in the combined absence of IL-5, IL-9, and IL-13. *Immunity* **17**, 7-17

86. Urban, J. F., Jr., Katona, I. M., Paul, W. E., and Finkelman, F. D. (1991) Interleukin 4 is important in protective immunity to a gastrointestinal nematode infection in mice. *Proc Natl Acad Sci U S A* **88**, 5513-5517

87. Biedermann, T., Zimmermann, S., Himmelrich, H., Gumy, A., Egeter, O., Sakrauski, A. K., Seegmuller, I., Voigt, H., Launois, P., Levine, A. D., Wagner, H., Heeg, K., Louis, J. A., and Rocken, M. (2001) IL-4 instructs TH1 responses and resistance to Leishmania major in susceptible BALB/c mice. *Nat Immunol* **2**, 1054-1060

88. Carvalho, L. H., Sano, G., Hafalla, J. C., Morrot, A., Curotto de Lafaille, M. A., and Zavala, F. (2002) IL-4-secreting CD4+ T cells are crucial to the

development of CD8+ T-cell responses against malaria liver stages. *Nat Med* **8**, 166-170

89. Todaro, M., Lombardo, Y., Francipane, M. G., Alea, M. P., Cammareri, P., Iovino, F., Di Stefano, A. B., Di Bernardo, C., Agrusa, A., Condorelli, G., Walczak, H., and Stassi, G. (2008) Apoptosis resistance in epithelial tumors is mediated by tumor-cell-derived interleukin-4. *Cell Death Differ* **15**, 762-772

90. Prokopchuk, O., Liu, Y., Henne-Bruns, D., and Kornmann, M. (2005) Interleukin-4 enhances proliferation of human pancreatic cancer cells: evidence for autocrine and paracrine actions. *Br J Cancer* **92**, 921-928

91. DeNardo, D. G., Barreto, J. B., Andreu, P., Vasquez, L., Tawfik, D., Kolhatkar, N., and Coussens, L. M. (2009) CD4(+) T cells regulate pulmonary metastasis of mammary carcinomas by enhancing protumor properties of macrophages. *Cancer Cell* **16**, 91-102

92. Pollard, J. W. (2004) Tumour-educated macrophages promote tumour progression and metastasis. *Nat Rev Cancer* **4**, 71-78

93. Qian, B. Z., and Pollard, J. W. (2010) Macrophage diversity enhances tumor progression and metastasis. *Cell* **141**, 39-51

94. Mantovani, A., Sozzani, S., Locati, M., Allavena, P., and Sica, A. (2002) Macrophage polarization: tumor-associated macrophages as a paradigm for polarized M2 mononuclear phagocytes. *Trends Immunol* **23**, 549-555

95. Biswas, S. K., and Mantovani, A. (2010) Macrophage plasticity and interaction with lymphocyte subsets: cancer as a paradigm. *Nat Immunol* **11**, 889-896

96. Mantovani, A., Allavena, P., Sica, A., and Balkwill, F. (2008) Cancer-related inflammation. *Nature* **454**, 436-444

97. Movahedi, K., Laoui, D., Gysemans, C., Baeten, M., Stange, G., Van den Bossche, J., Mack, M., Pipeleers, D., In't Veld, P., De Baetselier, P., and Van Ginderachter, J. A. (2010) Different tumor microenvironments contain functionally distinct subsets of macrophages derived from Ly6C(high) monocytes. *Cancer Res* **70**, 5728-5739

98. Mantovani, A., and Sica, A. (2010) Macrophages, innate immunity and cancer: balance, tolerance, and diversity. *Curr Opin Immunol* **22**, 231-237

99. Thorsson, V., Gibbs, D. L., Brown, S. D., Wolf, D., Bortone, D. S., Ou Yang, T. H., Porta-Pardo, E., Gao, G. F., Plaisier, C. L., Eddy, J. A., Ziv, E., Culhane, A. C., Paull, E. O., Sivakumar, I. K. A., Gentles, A. J., Malhotra, R., Farshidfar, F., Colaprico, A., Parker, J. S., Mose, L. E., Vo, N. S., Liu, J., Liu, Y., Rader, J., Dhankani, V., Reynolds, S. M., Bowlby, R., Califano, A., Cherniack, A. D., Anastassiou, D., Bedognetti, D., Mokrab, Y., Newman, A. M., Rao, A., Chen, K., Krasnitz, A., Hu, H., Malta, T. M., Noushmehr, H.,

Pedamallu, C. S., Bullman, S., Ojesina, A. I., Lamb, A., Zhou, W., Shen, H., Choueiri, T. K., Weinstein, J. N., Guinney, J., Saltz, J., Holt, R. A., Rabkin, C. S., Cancer Genome Atlas Research, N., Lazar, A. J., Serody, J. S., Demicco, E. G., Disis, M. L., Vincent, B. G., and Shmulevich, I. (2018) The Immune Landscape of Cancer. *Immunity* **48**, 812-830 e814

100. Zhang, Q. W., Liu, L., Gong, C. Y., Shi, H. S., Zeng, Y. H., Wang, X. Z., Zhao, Y. W., and Wei, Y. Q. (2012) Prognostic significance of tumor-associated macrophages in solid tumor: a meta-analysis of the literature. *PLoS One* **7**, e50946

101. Lin, Y., Xu, J., and Lan, H. (2019) Tumor-associated macrophages in tumor metastasis: biological roles and clinical therapeutic applications. *J Hematol Oncol* **12**, 76

102. Krieg, C., Nowicka, M., Guglietta, S., Schindler, S., Hartmann, F. J., Weber, L. M., Dummer, R., Robinson, M. D., Levesque, M. P., and Becher, B. (2018) High-dimensional single-cell analysis predicts response to anti-PD-1 immunotherapy. *Nat Med* **24**, 144-153

103. Mantovani, A., Marchesi, F., Malesci, A., Laghi, L., and Allavena, P. (2017) Tumour-associated macrophages as treatment targets in oncology. *Nat Rev Clin Oncol* **14**, 399-416

104. Viola, A., Munari, F., Sanchez-Rodriguez, R., Scolaro, T., and Castegna, A. (2019) The Metabolic Signature of Macrophage Responses. *Front Immunol* **10**, 1462

105. West, A. P., Brodsky, I. E., Rahner, C., Woo, D. K., Erdjument-Bromage, H., Tempst, P., Walsh, M. C., Choi, Y., Shadel, G. S., and Ghosh, S. (2011) TLR signaling augments macrophage bactericidal activity through mitochondrial ROS. *Nature* **472**, 476-480

106. Pavlou, S., Wang, L., Xu, H., and Chen, M. (2017) Higher phagocytic activity of thioglycollate-elicited peritoneal macrophages is related to metabolic status of the cells. *J Inflamm (Lond)* **14**, 4

107. Van den Bossche, J., Baardman, J., Otto, N. A., van der Velden, S., Neele, A. E., van den Berg, S. M., Luque-Martin, R., Chen, H. J., Boshuizen, M. C., Ahmed, M., Hoeksema, M. A., de Vos, A. F., and de Winther, M. P. (2016) Mitochondrial Dysfunction Prevents Repolarization of Inflammatory Macrophages. *Cell Rep* **17**, 684-696

108. Jin, Z., Wei, W., Yang, M., Du, Y., and Wan, Y. (2014) Mitochondrial complex I activity suppresses inflammation and enhances bone resorption by shifting macrophage-osteoclast polarization. *Cell Metab* **20**, 483-498

109. Van den Bossche, J., Baardman, J., and de Winther, M. P. (2015) Metabolic Characterization of Polarized M1 and M2 Bone Marrow-derived Macrophages Using Real-time Extracellular Flux Analysis. *J Vis Exp*

110. Freemerman, A. J., Johnson, A. R., Sacks, G. N., Milner, J. J., Kirk, E. L., Troester, M. A., Macintyre, A. N., Goraksha-Hicks, P., Rathmell, J. C., and Makowski, L. (2014) Metabolic reprogramming of macrophages: glucose transporter 1 (GLUT1)-mediated glucose metabolism drives a proinflammatory phenotype. *J Biol Chem* **289**, 7884-7896

111. Fukuzumi, M., Shinomiya, H., Shimizu, Y., Ohishi, K., and Utsumi, S. (1996) Endotoxin-induced enhancement of glucose influx into murine peritoneal macrophages via GLUT1. *Infect Immun* **64**, 108-112

112. Huang, S. C., Smith, A. M., Everts, B., Colonna, M., Pearce, E. L., Schilling, J. D., and Pearce, E. J. (2016) Metabolic Reprogramming Mediated by the mTORC2-IRF4 Signaling Axis Is Essential for Macrophage Alternative Activation. *Immunity* **45**, 817-830

113. Tan, Z., Xie, N., Cui, H., Moellering, D. R., Abraham, E., Thannickal, V. J., and Liu, G. (2015) Pyruvate dehydrogenase kinase 1 participates in macrophage polarization via regulating glucose metabolism. *J Immunol* **194**, 6082-6089

114. Vats, D., Mukundan, L., Odegaard, J. I., Zhang, L., Smith, K. L., Morel, C. R., Wagner, R. A., Greaves, D. R., Murray, P. J., and Chawla, A. (2006) Oxidative metabolism and PGC-1beta attenuate macrophage-mediated inflammation. *Cell Metab* **4**, 13-24

115. Martinez-Reyes, I., and Chandel, N. S. (2020) Mitochondrial TCA cycle metabolites control physiology and disease. *Nat Commun* **11**, 102

116. Jang, C., Chen, L., and Rabinowitz, J. D. (2018) Metabolomics and Isotope Tracing. *Cell* **173**, 822-837

117. Prochownik, E. V., and Wang, H. (2021) The Metabolic Fates of Pyruvate in Normal and Neoplastic Cells. *Cells* **10**

118. Kuhlbrandt, W. (2015) Structure and function of mitochondrial membrane protein complexes. *BMC Biol* **13**, 89

119. Bricker, D. K., Taylor, E. B., Schell, J. C., Orsak, T., Boutron, A., Chen, Y. C., Cox, J. E., Cardon, C. M., Van Vranken, J. G., Dephoure, N., Redin, C., Boudina, S., Gygi, S. P., Brivet, M., Thummel, C. S., and Rutter, J. (2012) A mitochondrial pyruvate carrier required for pyruvate uptake in yeast, Drosophila, and humans. *Science* **337**, 96-100

120. Herzig, S., Raemy, E., Montessuit, S., Veuthey, J. L., Zamboni, N., Westermann, B., Kunji, E. R., and Martinou, J. C. (2012) Identification and functional expression of the mitochondrial pyruvate carrier. *Science* **337**, 93-96

121. Patel, M. S., Nemeria, N. S., Furey, W., and Jordan, F. (2014) The pyruvate dehydrogenase complexes: structure-based function and regulation. *J Biol Chem* **289**, 16615-16623

122. Pietrocola, F., Galluzzi, L., Bravo-San Pedro, J. M., Madeo, F., and Kroemer, G. (2015) Acetyl coenzyme A: a central metabolite and second messenger. *Cell Metab* **21**, 805-821

123. Kurz, L. C., Drysdale, G. R., Riley, M. C., Evans, C. T., and Srere, P. A. (1992) Catalytic strategy of citrate synthase: effects of amino acid changes in the acetyl-CoA binding site on transition-state analog inhibitor complexes. *Biochemistry* **31**, 7908-7914

124. Link, H., Fuhrer, T., Gerosa, L., Zamboni, N., and Sauer, U. (2015) Real-time metabolome profiling of the metabolic switch between starvation and growth. *Nat Methods* **12**, 1091-1097

125. Zhao, R. Z., Jiang, S., Zhang, L., and Yu, Z. B. (2019) Mitochondrial electron transport chain, ROS generation and uncoupling (Review). *Int J Mol Med* **44**, 3-15

126. Noe, J. T., and Mitchell, R. A. (2019) Tricarboxylic acid cycle metabolites in the control of macrophage activation and effector phenotypes. *J Leukoc Biol* **106**, 359-367

127. Jha, A. K., Huang, S. C., Sergushichev, A., Lampropoulou, V., Ivanova, Y., Loginicheva, E., Chmielewski, K., Stewart, K. M., Ashall, J., Everts, B., Pearce, E. J., Driggers, E. M., and Artyomov, M. N. (2015) Network integration of parallel metabolic and transcriptional data reveals metabolic modules that regulate macrophage polarization. *Immunity* **42**, 419-430

128. Liu, P. S., Wang, H., Li, X., Chao, T., Teav, T., Christen, S., Di Conza, G., Cheng, W. C., Chou, C. H., Vavakova, M., Muret, C., Debackere, K., Mazzone, M., Huang, H. D., Fendt, S. M., Ivanisevic, J., and Ho, P. C. (2017) alpha-ketoglutarate orchestrates macrophage activation through metabolic and epigenetic reprogramming. *Nat Immunol* **18**, 985-994

129. Zhang, D., Tang, Z., Huang, H., Zhou, G., Cui, C., Weng, Y., Liu, W., Kim, S., Lee, S., Perez-Neut, M., Ding, J., Czyz, D., Hu, R., Ye, Z., He, M., Zheng, Y. G., Shuman, H. A., Dai, L., Ren, B., Roeder, R. G., Becker, L., and Zhao, Y. (2019) Metabolic regulation of gene expression by histone lactylation. *Nature* **574**, 575-580

130. Wellen, K. E., Hatzivassiliou, G., Sachdeva, U. M., Bui, T. V., Cross, J. R., and Thompson, C. B. (2009) ATP-citrate lyase links cellular metabolism to histone acetylation. *Science* **324**, 1076-1080

131. Icard, P., Wu, Z., Fournel, L., Coquerel, A., Lincet, H., and Alifano, M. (2020) ATP citrate lyase: A central metabolic enzyme in cancer. *Cancer Lett* **471**, 125-134

132. Infantino, V., Iacobazzi, V., Palmieri, F., and Menga, A. (2013) ATP-citrate lyase is essential for macrophage inflammatory response. *Biochem Biophys Res Commun* **440**, 105-111

133. Sivanand, S., Viney, I., and Wellen, K. E. (2018) Spatiotemporal Control of Acetyl-CoA Metabolism in Chromatin Regulation. *Trends Biochem Sci* **43**, 61-74

134. Infantino, V., Convertini, P., Cucci, L., Panaro, M. A., Di Noia, M. A., Calvello, R., Palmieri, F., and Iacobazzi, V. (2011) The mitochondrial citrate carrier: a new player in inflammation. *Biochem J* **438**, 433-436

135. Infantino, V., Iacobazzi, V., Menga, A., Avantaggiati, M. L., and Palmieri, F. (2014) A key role of the mitochondrial citrate carrier (SLC25A1) in TNFalpha- and IFNgamma-triggered inflammation. *Biochim Biophys Acta* **1839**, 1217-1225

136. Aktan, F. (2004) iNOS-mediated nitric oxide production and its regulation. *Life Sci* **75**, 639-653

137. Palmieri, E. M., Spera, I., Menga, A., Infantino, V., Porcelli, V., Iacobazzi, V., Pierri, C. L., Hooper, D. C., Palmieri, F., and Castegna, A. (2015) Acetylation of human mitochondrial citrate carrier modulates mitochondrial citrate/malate exchange activity to sustain NADPH production during macrophage activation. *Biochim Biophys Acta* **1847**, 729-738

138. Torres, A., Makowski, L., and Wellen, K. E. (2016) Immunometabolism: Metabolism fine-tunes macrophage activation. *Elife* **5**

139. Tessarz, P., and Kouzarides, T. (2014) Histone core modifications regulating nucleosome structure and dynamics. *Nat Rev Mol Cell Biol* **15**, 703-708

140. Covarrubias, A. J., Aksoylar, H. I., Yu, J., Snyder, N. W., Worth, A. J., Iyer, S. S., Wang, J., Ben-Sahra, I., Byles, V., Polynne-Stapornkul, T., Espinosa, E. C., Lamming, D., Manning, B. D., Zhang, Y., Blair, I. A., and Horng, T. (2016) Akt-mTORC1 signaling regulates Acly to integrate metabolic input to control of macrophage activation. *Elife* **5**

141. Mullican, S. E., Gaddis, C. A., Alenghat, T., Nair, M. G., Giacomin, P. R., Everett, L. J., Feng, D., Steger, D. J., Schug, J., Artis, D., and Lazar, M. A. (2011) Histone deacetylase 3 is an epigenomic brake in macrophage alternative activation. *Genes Dev* **25**, 2480-2488

142. Baardman, J., Verberk, S. G. S., van der Velden, S., Gijbels, M. J. J., van Roomen, C., Sluimer, J. C., Broos, J. Y., Griffith, G. R., Prange, K. H. M., van Weeghel, M., Lakbir, S., Molenaar, D., Meinster, E., Neele, A. E., Kooij, G., de Vries, H. E., Lutgens, E., Wellen, K. E., de Winther, M. P. J., and Van den Bossche, J. (2020) Macrophage ATP citrate lyase deficiency stabilizes atherosclerotic plaques. *Nat Commun* **11**, 6296

143. Namgaladze, D., Zukunft, S., Schnutgen, F., Kurrle, N., Fleming, I., Fuhrmann, D., and Brune, B. (2018) Polarization of Human Macrophages by Interleukin-4 Does Not Require ATP-Citrate Lyase. *Front Immunol* **9**, 2858

144. Hanahan, D., and Weinberg, R. A. (2011) Hallmarks of cancer: the next generation. *Cell* **144**, 646-674

145. Pavlova, N. N., and Thompson, C. B. (2016) The Emerging Hallmarks of Cancer Metabolism. *Cell Metab* **23**, 27-47

146. Warburg, O. (1956) On respiratory impairment in cancer cells. *Science* **124**, 269-270

147. Warburg, O. (1956) On the origin of cancer cells. *Science* **123**, 309-314

148. DeBerardinis, R. J., and Chandel, N. S. (2020) We need to talk about the Warburg effect. *Nat Metab* **2**, 127-129

149. de la Cruz-Lopez, K. G., Castro-Munoz, L. J., Reyes-Hernandez, D. O., Garcia-Carranca, A., and Manzo-Merino, J. (2019) Lactate in the Regulation of Tumor Microenvironment and Therapeutic Approaches. *Front Oncol* **9**, 1143

150. Vander Heiden, M. G., Cantley, L. C., and Thompson, C. B. (2009) Understanding the Warburg effect: the metabolic requirements of cell proliferation. *Science* **324**, 1029-1033

151. Certo, M., Tsai, C. H., Pucino, V., Ho, P. C., and Mauro, C. (2020) Lactate modulation of immune responses in inflammatory versus tumour microenvironments. *Nat Rev Immunol*

152. Angelin, A., Gil-de-Gomez, L., Dahiya, S., Jiao, J., Guo, L., Levine, M. H., Wang, Z., Quinn, W. J., 3rd, Kopinski, P. K., Wang, L., Akimova, T., Liu, Y., Bhatti, T. R., Han, R., Laskin, B. L., Baur, J. A., Blair, I. A., Wallace, D. C., Hancock, W. W., and Beier, U. H. (2017) Foxp3 Reprograms T Cell Metabolism to Function in Low-Glucose, High-Lactate Environments. *Cell Metab* **25**, 1282-1293 e1287

153. Hui, S., Ghergurovich, J. M., Morscher, R. J., Jang, C., Teng, X., Lu, W., Esparza, L. A., Reya, T., Le, Z., Yanxiang Guo, J., White, E., and Rabinowitz, J. D. (2017) Glucose feeds the TCA cycle via circulating lactate. *Nature* **551**, 115-118

154. Faubert, B., Li, K. Y., Cai, L., Hensley, C. T., Kim, J., Zacharias, L. G., Yang, C., Do, Q. N., Doucette, S., Burguete, D., Li, H., Huet, G., Yuan, Q., Wigal, T., Butt, Y., Ni, M., Torrealba, J., Oliver, D., Lenkinski, R. E., Malloy, C. R., Wachsmann, J. W., Young, J. D., Kernstine, K., and DeBerardinis, R. J. (2017) Lactate Metabolism in Human Lung Tumors. *Cell* **171**, 358-371 e359

155. Wang, F., Zhang, S., Vuckovic, I., Jeon, R., Lerman, A., Folmes, C. D., Dzeja, P. P., and Herrmann, J. (2018) Glycolytic Stimulation Is Not a Requirement for M2 Macrophage Differentiation. *Cell Metab* **28**, 463-475 e464

156. Yaddanapudi, K., Putty, K., Rendon, B. E., Lamont, G. J., Faughn, J. D., Satoskar, A., Lasnik, A., Eaton, J. W., and Mitchell, R. A. (2013) Control of

tumor-associated macrophage alternative activation by macrophage migration inhibitory factor. *J Immunol* **190**, 2984-2993

157. Barbosa de Souza Rizzo, M., Brasilino de Carvalho, M., Kim, E. J., Rendon, B. E., Noe, J. T., Darlene Wise, A., and Mitchell, R. A. (2018) Oral squamous carcinoma cells promote macrophage polarization in an MIF-dependent manner. *QJM* **111**, 769-778

158. Xiao, W., Dong, X., Zhao, H., Han, S., Nie, R., Zhang, X., and An, R. (2016) Expression of MIF and c-erbB-2 in endometrial cancer. *Mol Med Rep* **13**, 3828-3834

159. Tomiyasu, M., Yoshino, I., Suemitsu, R., Okamoto, T., and Sugimachi, K. (2002) Quantification of macrophage migration inhibitory factor mRNA expression in non-small cell lung cancer tissues and its clinical significance. *Clin Cancer Res* **8**, 3755-3760

160. Zhao, Y. M., Wang, L., Dai, Z., Wang, D. D., Hei, Z. Y., Zhang, N., Fu, X. T., Wang, X. L., Zhang, S. C., Qin, L. X., Tang, Z. Y., Zhou, J., and Fan, J. (2011) Validity of plasma macrophage migration inhibitory factor for diagnosis and prognosis of hepatocellular carcinoma. *Int J Cancer* **129**, 2463-2472

161. Olsson, L., Lindmark, G., Hammarstrom, M. L., Hammarstrom, S., and Sitohy, B. (2020) Evaluating macrophage migration inhibitory factor 1 expression as a prognostic biomarker in colon cancer. *Tumour Biol* **42**, 1010428320924524

162. Lippitz, B. E. (2013) Cytokine patterns in patients with cancer: a systematic review. *Lancet Oncol* **14**, e218-228

163. Koh, H. M., and Kim, D. C. (2020) Prognostic significance of macrophage migration inhibitory factor expression in cancer patients: A systematic review and meta-analysis. *Medicine (Baltimore)* **99**, e21575

164. Bloom, B. R., and Bennett, B. (1966) Mechanism of a reaction in vitro associated with delayed-type hypersensitivity. *Science* **153**, 80-82

165. David, J. R. (1966) Delayed hypersensitivity in vitro: its mediation by cell-free substances formed by lymphoid cell-antigen interaction. *Proc Natl Acad Sci U S A* **56**, 72-77

166. Bacher, M., Metz, C. N., Calandra, T., Mayer, K., Chesney, J., Lohoff, M., Gemsa, D., Donnelly, T., and Bucala, R. (1996) An essential regulatory role for macrophage migration inhibitory factor in T-cell activation. *Proc Natl Acad Sci U S A* **93**, 7849-7854

167. Calandra, T., Bernhagen, J., Mitchell, R. A., and Bucala, R. (1994) The macrophage is an important and previously unrecognized source of macrophage migration inhibitory factor. *J Exp Med* **179**, 1895-1902

168. Weiser, W. Y., Temple, P. A., Witek-Giannotti, J. S., Remold, H. G., Clark, S. C., and David, J. R. (1989) Molecular cloning of a cDNA encoding a human macrophage migration inhibitory factor. *Proc Natl Acad Sci U S A* **86**, 7522-7526

169. Calandra, T., and Roger, T. (2003) Macrophage migration inhibitory factor: a regulator of innate immunity. *Nat Rev Immunol* **3**, 791-800

170. Bernhagen, J., Calandra, T., Mitchell, R. A., Martin, S. B., Tracey, K. J., Voelter, W., Manogue, K. R., Cerami, A., and Bucala, R. (1993) MIF is a pituitary-derived cytokine that potentiates lethal endotoxaemia. *Nature* **365**, 756-759

171. Calandra, T., Bernhagen, J., Metz, C. N., Spiegel, L. A., Bacher, M., Donnelly, T., Cerami, A., and Bucala, R. (1995) MIF as a glucocorticoid-induced modulator of cytokine production. *Nature* **377**, 68-71

172. Calandra, T., and Bucala, R. (1995) Macrophage migration inhibitory factor: a counter-regulator of glucocorticoid action and critical mediator of septic shock. *J Inflamm* **47**, 39-51

173. Roger, T., Glauser, M. P., and Calandra, T. (2001) Macrophage migration inhibitory factor (MIF) modulates innate immune responses induced by endotoxin and Gram-negative bacteria. *J Endotoxin Res* **7**, 456-460

174. Morand, E. F., Leech, M., and Bernhagen, J. (2006) MIF: a new cytokine link between rheumatoid arthritis and atherosclerosis. *Nat Rev Drug Discov* **5**, 399-410

175. Mikulowska, A., Metz, C. N., Bucala, R., and Holmdahl, R. (1997) Macrophage migration inhibitory factor is involved in the pathogenesis of collagen type II-induced arthritis in mice. *J Immunol* **158**, 5514-5517

176. Donnelly, S. C., and Bucala, R. (1997) Macrophage migration inhibitory factor: a regulator of glucocorticoid activity with a critical role in inflammatory disease. *Mol Med Today* **3**, 502-507

177. Donnelly, S. C., Haslett, C., Reid, P. T., Grant, I. S., Wallace, W. A., Metz, C. N., Bruce, L. J., and Bucala, R. (1997) Regulatory role for macrophage migration inhibitory factor in acute respiratory distress syndrome. *Nat Med* **3**, 320-323

178. Asare, Y., Schmitt, M., and Bernhagen, J. (2013) The vascular biology of macrophage migration inhibitory factor (MIF). Expression and effects in inflammation, atherogenesis and angiogenesis. *Thromb Haemost* **109**, 391-398

179. Bach, J. P., Rinn, B., Meyer, B., Dodel, R., and Bacher, M. (2008) Role of MIF in inflammation and tumorigenesis. *Oncology* **75**, 127-133

180. Shah, Y. M., Ito, S., Morimura, K., Chen, C., Yim, S. H., Haase, V. H., and Gonzalez, F. J. (2008) Hypoxia-inducible factor augments experimental

colitis through an MIF-dependent inflammatory signaling cascade. *Gastroenterology* **134**, 2036-2048, 2048 e2031-2033

181. White, E. S., Strom, S. R., Wys, N. L., and Arenberg, D. A. (2001) Non-small cell lung cancer cells induce monocytes to increase expression of angiogenic activity. *J Immunol* **166**, 7549-7555

182. Wang, X., Chen, T., Leng, L., Fan, J., Cao, K., Duan, Z., Zhang, X., Shao, C., Wu, M., Tadmori, I., Li, T., Liang, L., Sun, D., Zheng, S., Meinhardt, A., Young, W., Bucala, R., and Ren, Y. (2012) MIF produced by bone marrow-derived macrophages contributes to teratoma progression after embryonic stem cell transplantation. *Cancer Res* **72**, 2867-2878

183. Jankauskas, S. S., Wong, D. W. L., Bucala, R., Djudjaj, S., and Boor, P. (2019) Evolving complexity of MIF signaling. *Cell Signal* **57**, 76-88

184. Stark, K., Eckart, A., Haidari, S., Tirniceriu, A., Lorenz, M., von Bruhl, M. L., Gartner, F., Khandoga, A. G., Legate, K. R., Pless, R., Hepper, I., Lauber, K., Walzog, B., and Massberg, S. (2013) Capillary and arteriolar pericytes attract innate leukocytes exiting through venules and 'instruct' them with pattern-recognition and motility programs. *Nat Immunol* **14**, 41-51

185. Bacher, M., Meinhardt, A., Lan, H. Y., Mu, W., Metz, C. N., Chesney, J. A., Calandra, T., Gemsa, D., Donnelly, T., Atkins, R. C., and Bucala, R. (1997) Migration inhibitory factor expression in experimentally induced endotoxemia. *Am J Pathol* **150**, 235-246

186. Fukuzawa, J., Nishihira, J., Hasebe, N., Haneda, T., Osaki, J., Saito, T., Nomura, T., Fujino, T., Wakamiya, N., and Kikuchi, K. (2002) Contribution of macrophage migration inhibitory factor to extracellular signal-regulated kinase activation by oxidative stress in cardiomyocytes. *J Biol Chem* **277**, 24889-24895

187. Mitchell, R. A., Metz, C. N., Peng, T., and Bucala, R. (1999) Sustained mitogen-activated protein kinase (MAPK) and cytoplasmic phospholipase A2 activation by macrophage migration inhibitory factor (MIF). Regulatory role in cell proliferation and glucocorticoid action. *J Biol Chem* **274**, 18100-18106

188. Leng, L., Metz, C. N., Fang, Y., Xu, J., Donnelly, S., Baugh, J., Delohery, T., Chen, Y., Mitchell, R. A., and Bucala, R. (2003) MIF signal transduction initiated by binding to CD74. *J Exp Med* **197**, 1467-1476

189. Shi, X., Leng, L., Wang, T., Wang, W., Du, X., Li, J., McDonald, C., Chen, Z., Murphy, J. W., Lolis, E., Noble, P., Knudson, W., and Bucala, R. (2006) CD44 is the signaling component of the macrophage migration inhibitory factor-CD74 receptor complex. *Immunity* **25**, 595-606

190. Bernhagen, J., Krohn, R., Lue, H., Gregory, J. L., Zernecke, A., Koenen, R. R., Dewor, M., Georgiev, I., Schober, A., Leng, L., Kooistra, T., Fingerle-Rowson, G., Ghezzi, P., Kleemann, R., McColl, S. R., Bucala, R., Hickey,

M. J., and Weber, C. (2007) MIF is a noncognate ligand of CXC chemokine receptors in inflammatory and atherogenic cell recruitment. *Nat Med* **13**, 587-596

191. Alampour-Rajabi, S., El Bounkari, O., Rot, A., Muller-Newen, G., Bachelerie, F., Gawaz, M., Weber, C., Schober, A., and Bernhagen, J. (2015) MIF interacts with CXCR7 to promote receptor internalization, ERK1/2 and ZAP-70 signaling, and lymphocyte chemotaxis. *FASEB J* **29**, 4497-4511

192. Tarnowski, M., Grymula, K., Liu, R., Tarnowska, J., Drukala, J., Ratajczak, J., Mitchell, R. A., Ratajczak, M. Z., and Kucia, M. (2010) Macrophage migration inhibitory factor is secreted by rhabdomyosarcoma cells, modulates tumor metastasis by binding to CXCR4 and CXCR7 receptors and inhibits recruitment of cancer-associated fibroblasts. *Mol Cancer Res* **8**, 1328-1343

193. Wang, L., Zheng, J. N., and Pei, D. S. (2016) The emerging roles of Jab1/CSN5 in cancer. *Med Oncol* **33**, 90

194. Cope, G. A., and Deshaies, R. J. (2003) COP9 signalosome: a multifunctional regulator of SCF and other cullin-based ubiquitin ligases. *Cell* **114**, 663-671

195. Claret, F. X., Hibi, M., Dhut, S., Toda, T., and Karin, M. (1996) A new group of conserved coactivators that increase the specificity of AP-1 transcription factors. *Nature* **383**, 453-457

196. Kleemann, R., Hausser, A., Geiger, G., Mischke, R., Burger-Kentischer, A., Flieger, O., Johannes, F. J., Roger, T., Calandra, T., Kapurniotu, A., Grell, M., Finkelmeier, D., Brunner, H., and Bernhagen, J. (2000) Intracellular action of the cytokine MIF to modulate AP-1 activity and the cell cycle through Jab1. *Nature* **408**, 211-216

197. Burger-Kentischer, A., Finkelmeier, D., Thiele, M., Schmucker, J., Geiger, G., Tovar, G. E., and Bernhagen, J. (2005) Binding of JAB1/CSN5 to MIF is mediated by the MPN domain but is independent of the JAMM motif. *FEBS Lett* **579**, 1693-1701

198. Hannemann, N., Jordan, J., Paul, S., Reid, S., Baenkler, H. W., Sonnewald, S., Bauerle, T., Vera, J., Schett, G., and Bozec, A. (2017) The AP-1 Transcription Factor c-Jun Promotes Arthritis by Regulating Cyclooxygenase-2 and Arginase-1 Expression in Macrophages. *J Immunol* **198**, 3605-3614

199. Carr, T. M., Wheaton, J. D., Houtz, G. M., and Ciofani, M. (2017) JunB promotes Th17 cell identity and restrains alternative CD4(+) T-cell programs during inflammation. *Nat Commun* **8**, 301

200. Lue, H., Dewor, M., Leng, L., Bucala, R., and Bernhagen, J. (2011) Activation of the JNK signalling pathway by macrophage migration inhibitory

factor (MIF) and dependence on CXCR4 and CD74. *Cell Signal* **23**, 135-144

201. Coleman, A. M., Rendon, B. E., Zhao, M., Qian, M. W., Bucala, R., Xin, D., and Mitchell, R. A. (2008) Cooperative regulation of non-small cell lung carcinoma angiogenic potential by macrophage migration inhibitory factor and its homolog, D-dopachrome tautomerase. *J Immunol* **181**, 2330-2337

202. Xin, D., Rendon, B. E., Zhao, M., Winner, M., McGhee Coleman, A., and Mitchell, R. A. (2010) The MIF homologue D-dopachrome tautomerase promotes COX-2 expression through beta-catenin-dependent and -independent mechanisms. *Mol Cancer Res* **8**, 1601-1609

203. Nemajerova, A., Mena, P., Fingerle-Rowson, G., Moll, U. M., and Petrenko, O. (2007) Impaired DNA damage checkpoint response in MIF-deficient mice. *EMBO J* **26**, 987-997

204. Winner, M., Koong, A. C., Rendon, B. E., Zundel, W., and Mitchell, R. A. (2007) Amplification of tumor hypoxic responses by macrophage migration inhibitory factor-dependent hypoxia-inducible factor stabilization. *Cancer Res* **67**, 186-193

205. Winner, M., Leng, L., Zundel, W., and Mitchell, R. A. (2007) Macrophage migration inhibitory factor manipulation and evaluation in tumoral hypoxic adaptation. *Methods Enzymol* **435**, 355-369

206. Baugh, J. A., Gantier, M., Li, L., Byrne, A., Buckley, A., and Donnelly, S. C. (2006) Dual regulation of macrophage migration inhibitory factor (MIF) expression in hypoxia by CREB and HIF-1. *Biochem Biophys Res Commun* **347**, 895-903

207. Palazon, A., Goldrath, A. W., Nizet, V., and Johnson, R. S. (2014) HIF transcription factors, inflammation, and immunity. *Immunity* **41**, 518-528

208. De, R., Sarkar, S., Mazumder, S., Debsharma, S., Siddiqui, A. A., Saha, S. J., Banerjee, C., Nag, S., Saha, D., Pramanik, S., and Bandyopadhyay, U. (2018) Macrophage migration inhibitory factor regulates mitochondrial dynamics and cell growth of human cancer cell lines through CD74-NF-kappaB signaling. *J Biol Chem* **293**, 19740-19760

209. Lapuente-Brun, E., Moreno-Loshuertos, R., Acin-Perez, R., Latorre-Pellicer, A., Colas, C., Balsa, E., Perales-Clemente, E., Quiros, P. M., Calvo, E., Rodriguez-Hernandez, M. A., Navas, P., Cruz, R., Carracedo, A., Lopez-Otin, C., Perez-Martos, A., Fernandez-Silva, P., Fernandez-Vizarra, E., and Enriquez, J. A. (2013) Supercomplex assembly determines electron flux in the mitochondrial electron transport chain. *Science* **340**, 1567-1570

210. Letts, J. A., and Sazanov, L. A. (2017) Clarifying the supercomplex: the higher-order organization of the mitochondrial electron transport chain. *Nat Struct Mol Biol* **24**, 800-808

211. Rutter, J., Winge, D. R., and Schiffman, J. D. (2010) Succinate dehydrogenase - Assembly, regulation and role in human disease. *Mitochondrion* **10**, 393-401

212. Mills, E. L., Kelly, B., Logan, A., Costa, A. S. H., Varma, M., Bryant, C. E., Tourlomousis, P., Dabritz, J. H. M., Gottlieb, E., Latorre, I., Corr, S. C., McManus, G., Ryan, D., Jacobs, H. T., Szibor, M., Xavier, R. J., Braun, T., Frezza, C., Murphy, M. P., and O'Neill, L. A. (2016) Succinate Dehydrogenase Supports Metabolic Repurposing of Mitochondria to Drive Inflammatory Macrophages. *Cell* **167**, 457-470 e413

213. Losman, J. A., Koivunen, P., and Kaelin, W. G., Jr. (2020) 2-Oxoglutarate-dependent dioxygenases in cancer. *Nat Rev Cancer* **20**, 710-726

214. Islam, M. S., Leissing, T. M., Chowdhury, R., Hopkinson, R. J., and Schofield, C. J. (2018) 2-Oxoglutarate-Dependent Oxygenases. *Annu Rev Biochem* **87**, 585-620

215. Satoh, T., Takeuchi, O., Vandenbon, A., Yasuda, K., Tanaka, Y., Kumagai, Y., Miyake, T., Matsushita, K., Okazaki, T., Saitoh, T., Honma, K., Matsuyama, T., Yui, K., Tsujimura, T., Standley, D. M., Nakanishi, K., Nakai, K., and Akira, S. (2010) The Jmjd3-Irf4 axis regulates M2 macrophage polarization and host responses against helminth infection. *Nat Immunol* **11**, 936-944

216. Dinkova-Kostova, A. T., and Abramov, A. Y. (2015) The emerging role of Nrf2 in mitochondrial function. *Free Radic Biol Med* **88**, 179-188

217. Deng, Z., Pardi, R., Cheadle, W., Xiang, X., Zhang, S., Shah, S. V., Grizzle, W., Miller, D., Mountz, J., and Zhang, H. G. (2011) Plant homologue constitutive photomorphogenesis 9 (COP9) signalosome subunit CSN5 regulates innate immune responses in macrophages. *Blood* **117**, 4796-4804

218. Mathew, B., Jacobson, J. R., Siegler, J. H., Moitra, J., Blasco, M., Xie, L., Unzueta, C., Zhou, T., Evenoski, C., Al-Sakka, M., Sharma, R., Huey, B., Bulent, A., Smith, B., Jayaraman, S., Reddy, N. M., Reddy, S. P., Fingerle-Rowson, G., Bucala, R., Dudek, S. M., Natarajan, V., Weichselbaum, R. R., and Garcia, J. G. (2013) Role of migratory inhibition factor in age-related susceptibility to radiation lung injury via NF-E2-related factor-2 and antioxidant regulation. *Am J Respir Cell Mol Biol* **49**, 269-278

219. Zhang, D. D., Lo, S. C., Cross, J. V., Templeton, D. J., and Hannink, M. (2004) Keap1 is a redox-regulated substrate adaptor protein for a Cul3-dependent ubiquitin ligase complex. *Mol Cell Biol* **24**, 10941-10953

220. Watanabe, S., Alexander, M., Misharin, A. V., and Budinger, G. R. S. (2019) The role of macrophages in the resolution of inflammation. *J Clin Invest* **129**, 2619-2628

221. Langston, P. K., Nambu, A., Jung, J., Shibata, M., Aksoylar, H. I., Lei, J., Xu, P., Doan, M. T., Jiang, H., MacArthur, M. R., Gao, X., Kong, Y., Chouchani, E. T., Locasale, J. W., Snyder, N. W., and Horng, T. (2019) Glycerol phosphate shuttle enzyme GPD2 regulates macrophage inflammatory responses. *Nat Immunol* **20**, 1186-1195

222. Zhao, S., Torres, A., Henry, R. A., Trefely, S., Wallace, M., Lee, J. V., Carrer, A., Sengupta, A., Campbell, S. L., Kuo, Y. M., Frey, A. J., Meurs, N., Viola, J. M., Blair, I. A., Weljie, A. M., Metallo, C. M., Snyder, N. W., Andrews, A. J., and Wellen, K. E. (2016) ATP-Citrate Lyase Controls a Glucose-to-Acetate Metabolic Switch. *Cell Rep* **17**, 1037-1052

223. Sun, R. C., Dukhande, V. V., Zhou, Z., Young, L. E. A., Emanuelle, S., Brainson, C. F., and Gentry, M. S. (2019) Nuclear Glycogenolysis Modulates Histone Acetylation in Human Non-Small Cell Lung Cancers. *Cell Metab* **30**, 903-916 e907

224. Andres, D. A., Young, L. E. A., Veeranki, S., Hawkinson, T. R., Levitan, B. M., He, D., Wang, C., Satin, J., and Sun, R. C. (2020) Improved workflow for mass spectrometry-based metabolomics analysis of the heart. *J Biol Chem* **295**, 2676-2686

225. Liu, M., Tong, Z., Ding, C., Luo, F., Wu, S., Wu, C., Albeituni, S., He, L., Hu, X., Tieri, D., Rouchka, E. C., Hamada, M., Takahashi, S., Gibb, A. A., Kloecker, G., Zhang, H. G., Bousamra, M., 2nd, Hill, B. G., Zhang, X., and Yan, J. (2020) Transcription factor c-Maf is a checkpoint that programs macrophages in lung cancer. *J Clin Invest* **130**, 2081-2096

226. Halestrap, A. P. (1975) The mitochondrial pyruvate carrier. Kinetics and specificity for substrates and inhibitors. *Biochem J* **148**, 85-96

227. Divakaruni, A. S., Wiley, S. E., Rogers, G. W., Andreyev, A. Y., Petrosyan, S., Loviscach, M., Wall, E. A., Yadava, N., Heuck, A. P., Ferrick, D. A., Henry, R. R., McDonald, W. G., Colca, J. R., Simon, M. I., Ciaraldi, T. P., and Murphy, A. N. (2013) Thiazolidinediones are acute, specific inhibitors of the mitochondrial pyruvate carrier. *Proc Natl Acad Sci U S A* **110**, 5422-5427

228. Kluckova, K., Sticha, M., Cerny, J., Mracek, T., Dong, L., Drahota, Z., Gottlieb, E., Neuzil, J., and Rohlena, J. (2015) Ubiquinone-binding site mutagenesis reveals the role of mitochondrial complex II in cell death initiation. *Cell Death Dis* **6**, e1749

229. Granchi, C. (2018) ATP citrate lyase (ACLY) inhibitors: An anti-cancer strategy at the crossroads of glucose and lipid metabolism. *Eur J Med Chem* **157**, 1276-1291

230. Noe, J. T., and Mitchell, R. A. (2020) MIF-Dependent Control of Tumor Immunity. *Front Immunol* **11**, 609948

231. Simpson, K. D., Templeton, D. J., and Cross, J. V. (2012) Macrophage migration inhibitory factor promotes tumor growth and metastasis by inducing myeloid-derived suppressor cells in the tumor microenvironment. *J Immunol* **189**, 5533-5540

232. Yaddanapudi, K., Rendon, B. E., Lamont, G., Kim, E. J., Al Rayyan, N., Richie, J., Albeituni, S., Waigel, S., Wise, A., and Mitchell, R. A. (2016) MIF Is Necessary for Late-Stage Melanoma Patient MDSC Immune Suppression and Differentiation. *Cancer Immunol Res* **4**, 101-112

233. Zhang, H., Ye, Y. L., Li, M. X., Ye, S. B., Huang, W. R., Cai, T. T., He, J., Peng, J. Y., Duan, T. H., Cui, J., Zhang, X. S., Zhou, F. J., Wang, R. F., and Li, J. (2017) CXCL2/MIF-CXCR2 signaling promotes the recruitment of myeloid-derived suppressor cells and is correlated with prognosis in bladder cancer. *Oncogene* **36**, 2095-2104

234. Winner, M., Meier, J., Zierow, S., Rendon, B. E., Crichlow, G. V., Riggs, R., Bucala, R., Leng, L., Smith, N., Lolis, E., Trent, J. O., and Mitchell, R. A. (2008) A novel, macrophage migration inhibitory factor suicide substrate inhibits motility and growth of lung cancer cells. *Cancer Res* **68**, 7253-7257

235. Weinberg, S. E., Sena, L. A., and Chandel, N. S. (2015) Mitochondria in the regulation of innate and adaptive immunity. *Immunity* **42**, 406-417

236. Asare, Y., Ommer, M., Azombo, F. A., Alampour-Rajabi, S., Sternkopf, M., Sanati, M., Gijbels, M. J., Schmitz, C., Sinitski, D., Tilstam, P. V., Lue, H., Gessner, A., Lange, D., Schmid, J. A., Weber, C., Dichgans, M., Jankowski, J., Pardi, R., de Winther, M. P., Noels, H., and Bernhagen, J. (2017) Inhibition of atherogenesis by the COP9 signalosome subunit 5 in vivo. *Proc Natl Acad Sci U S A* **114**, E2766-E2775

237. Atsumi, T., Cho, Y. R., Leng, L., McDonald, C., Yu, T., Danton, C., Hong, E. G., Mitchell, R. A., Metz, C., Niwa, H., Takeuchi, J., Onodera, S., Umino, T., Yoshioka, N., Koike, T., Kim, J. K., and Bucala, R. (2007) The proinflammatory cytokine macrophage migration inhibitory factor regulates glucose metabolism during systemic inflammation. *J Immunol* **179**, 5399-5406

238. Galluzzi, L., Kepp, O., Vander Heiden, M. G., and Kroemer, G. (2013) Metabolic targets for cancer therapy. *Nat Rev Drug Discov* **12**, 829-846

239. Li, X., Li, Y., Han, G., Li, X., Ji, Y., Fan, Z., Zhong, Y., Cao, J., Zhao, J., Mariusz, G., Zhang, M., Wen, J., Nesland, J. M., and Suo, Z. (2016) Establishment of mitochondrial pyruvate carrier 1 (MPC1) gene knockout mice with preliminary gene function analyses. *Oncotarget* **7**, 79981-79994

240. Vigueira, P. A., McCommis, K. S., Schweitzer, G. G., Remedi, M. S., Chambers, K. T., Fu, X., McDonald, W. G., Cole, S. L., Colca, J. R., Kletzien, R. F., Burgess, S. C., and Finck, B. N. (2014) Mitochondrial

pyruvate carrier 2 hypomorphism in mice leads to defects in glucose-stimulated insulin secretion. *Cell Rep* **7**, 2042-2053

241. Tumanov, S., Bulusu, V., Gottlieb, E., and Kamphorst, J. J. (2016) A rapid method for quantifying free and bound acetate based on alkylation and GC-MS analysis. *Cancer Metab* **4**, 17

242. Alban, T. J., Bayik, D., Otvos, B., Rabljenovic, A., Leng, L., Jia-Shiun, L., Roversi, G., Lauko, A., Momin, A. A., Mohammadi, A. M., Peereboom, D. M., Ahluwalia, M. S., Matsuda, K., Yun, K., Bucala, R., Vogelbaum, M. A., and Lathia, J. D. (2020) Glioblastoma Myeloid-Derived Suppressor Cell Subsets Express Differential Macrophage Migration Inhibitory Factor Receptor Profiles That Can Be Targeted to Reduce Immune Suppression. *Front Immunol* **11**, 1191

243. Waigel, S., Rendon, B. E., Lamont, G., Richie, J., Mitchell, R. A., and Yaddanapudi, K. (2016) MIF inhibition reverts the gene expression profile of human melanoma cell line-induced MDSCs to normal monocytes. *Genom Data* **7**, 240-242

244. Cho, Y., Crichlow, G. V., Vermeire, J. J., Leng, L., Du, X., Hodsdon, M. E., Bucala, R., Cappello, M., Gross, M., Gaeta, F., Johnson, K., and Lolis, E. J. (2010) Allosteric inhibition of macrophage migration inhibitory factor revealed by ibudilast. *Proc Natl Acad Sci U S A* **107**, 11313-11318

CURRICULUM VITAE

Jordan Taylor Noe

University of Louisville – School of Medicine
Clinical and Translational Research
Building 505 S. Hancock St. Louisville, KY
40202
(801) 458-3951 | jordan.noe@louisville.edu

SUMMARY

8th year MD/PhD student at the University of Louisville School of Medicine (ULSOM) with a Ph.D. in Biochemistry and Molecular Genetics under mentor Dr. Robert "Bob" Mitchell. Jordan's research interests focus on understanding how changes in the tumor microenvironment regulate tumor-associated immunosuppression and subsequent cancer progression.

EDUCATION

M.D. (School of Medicine) May 2023 (*Anticipated)*
University of Louisville. Louisville, KY

Ph.D. (Biochemistry and Molecular Genetics) May 2021
University of Louisville. Louisville, KY
Mentor: Dr. Robert "Bob" Mitchell
Thesis: Metabolic-epigenetic regulation of macrophage polarization

M.S. (Biochemistry and Molecular Genetics) May 2017
University of Louisville. Louisville, KY

B.S. (Cellular and Molecular Biology) May 2013
University of Utah. Salt Lake City, UT

RESEARCH SUPPORT

Ruth L. Kirsch stein Individual NRSA Predoctoral Fellowship for MD/PhD Degree
Agency: **NIH NCI F30** CA232550 (**PI**)
Period: 03/01/2019 – 02/28/2023
Title: "The Role of MIF in Mitochondrial Metabolism and M2-TAM Polarization"
Description: The goal of this project is to identify the underlying molecular mechanism(s) by which mitochondrial lactate metabolism contributes to the immunosuppressive capacity of tumor-associated macrophages (TAMs) and the role of MIF in mitochondrial lactate metabolism.

NOTABLE PUBLICATIONS

Noe J.T., Rendon B.E., Geller A.E., Morrissey S.M., Conroy L.R., Kim E.J., Young L.E., Bruntz R.C, Affronti H.A., Baby B.V, Clem B.F., Wellen K.E., Sun R.C., Yan J., McMasters K.M., Mitchell R.A. "Lactate Supports a Metabolic-Epigenetic Link in Macrophage Polarization." *Science Advances*. Submitted (In peer-review). June 2021

Noe, J.T. & Mitchell, R.A. "MIF-dependent control of tumor immunity." *Frontiers in Immunology*. 2020 Nov 25;11:609948.

Noe, J.T. & Mitchell, R.A. "Tricarboxylic acid cycle metabolites in the control of macrophage activation and effector phenotypes." *Journal of Leukocyte Biology*. 2019 Aug;106(2):359-367.

Barbosa de Souza Rizzo, M., **Noe, J.T.** *et al.* Oral squamous carcinoma cells promote macrophage polarization in an MIF-dependent manner. *QJM.* 2018 Nov;111:769-778.

NOTABLE PRESENTATIONS (*within past 12 mo*)

AACR Special Conference on Epigenetics and Metabolism**. "**Mitochondrial lactate metabolism in M2 macrophage polarization and ACLY-dependent histone acetylation." **Noe, J.T.**, Mitchell, R.A. *et al*. Virtual. October 2020.
  ***Top abstract selected by Meeting Organizers for proffered presentation**
  *Plenary Session: Cancer Immunometabolism**

National AAP/ASCI/APSA Joint Meeting. "Mitochondrial lactate metabolism in M2 macrophage polarization and ACLY-dependent histone acetylation." **Noe, J.T.**, Mitchell, R.A. *et al* Virtual. April 2021.

RESEARCH EXPERIENCE

2010-2013 Undergraduate Research Assistant: Don Ayer's Lab – Huntsman Cancer Center

2015-2016 Summer Research Scholar: Jason Chesney's Lab – Brown Cancer Center

2016-present Graduate Student Researcher: Robert Mitchell's Lab –Brown Cancer Center

ACADEMIC/OTHER MEMBERSHIPS

2014-present: Member of the American Medical Association (AMA)

2014-present: Member of the American College of Physicians (ACP)

2014-present: Member of the American Physician-Scientist Association (APSA)

2015-present: Member of the American Association for the Advancement of Science (AAAS)

2019-present: Member of the Society for Leukocyte Biology (SLB)

2020-present: Associate Member of the American Association for Cancer Research (AACR)

ACADEMIC HONORS/AWARDS

2010: New Century Scholarship (State of Utah - Board of Regents)

2014: Summer Research Scholarship (University of Louisville - School of Medicine)

2015: Summer Research Scholarship (University of Louisville - School of Medicine)

2015: Medical Student Poster Award (Norton Healthcare)

2016: Fellowship Award (University of Louisville – Integrated Program in Biomedical Science)

2017: Graduate Student Poster Award (University of Louisville – Biochemistry and Molecular Genetics)

2019: Graduate Student Presentation Award (University of Louisville – Dept of BMG)

Other Presentations (>12 months)

Noe, J.T., Chesney, J., *et al. "Characterization of a novel small molecule antagonists of cytosolic aspartate aminotransferase in pancreatic carcinoma cells."* Research!Louisville. Louisville, KY. September 2014.

Noe, J.T., Mitchell, R., *et al. "Altered bioenergetics during alternative activation of MIF-deficient macrophages."* Research!Louisville. Louisville, KY. September 2015.

Noe, J.T., Mitchell, R., *et al. "Altered bioenergetics during alternative activation of MIF-deficient macrophages."* Southeastern Medical Scientist Symposium (SEMSS). Vanderbilt University. Nashville, TN. September 2015.

Noe, J.T., Mitchell, R., *et al. "The role of MIF in mitochondrial metabolism and macrophage polarization."* Southeastern Medical Scientist Symposium (SEMSS). University of Alabama. Birmingham, AL. September 2016.

Noe, J.T., Mitchell, R., *et al. "The role of MIF in mitochondrial metabolism and macrophage polarization."* BMG Dept. Retreat. University of Louisville. Louisville, KY. August 2017.

Morrisey, S., **Noe, J.T**., Yan, J., et al. *"The Role of Tumor-Derived Exosomes in the Formation of a Pre-Metastatic Niche in Cancer."* Southeastern Medical Scientist Symposium (SEMSS). Emory University. Atlanta, GA. November 2017.

Noe, J.T., Mitchell, R., *et al. "MIF regulates mitochondrial lactate metabolism and phenotypic polarization in tumor-associated macrophages."* Southeastern Medical Scientist Symposium (SEMSS). Emory University. Atlanta, GA. November 2017.

Morrisey, S., **Noe, J.T.,** Yan, J., *et al. "The Role of Tumor-Derived Exosomes in the Formation of a Pre-Metastatic Niche in Cancer."* National American Physician-Scientist Association (APSA) conference. Chicago, IL. April 2018.

Morrisey, S., **Noe, J.T.,** Yan, J., *et al. "The Role of Tumor-Derived Exosomes in the Formation of a Pre-Metastatic Niche in Cancer."* National American Association of Immunologists (AAI) conference. Austin, TX. May 2018.

Noe, J.T., Mitchell, R., *et al. "Mitochondrial metabolism in tumor-associated macrophages: The role of MIF and tumor-derived lactate."* National MD/PhD Student Conference. Keystone, CO. July 2018.

Morrisey, S., **Noe, J.T.,** Yan, J., *et al. "The Role of Tumor-Derived Exosomes in the Formation of a Pre-Metastatic Niche in Cancer."* National MD/PhD Student Conference. Keystone, CO. July 2018.

Noe, J.T., Mitchell, R., *et al. "Mitochondrial Metabolism in Tumor-Associated Macrophages: The Role of MIF and Tumor-Derived Lactate."* National American Association for Cancer Research (AACR) conference. Chicago, IL. April 2018.